New Methods for Analysis of Nonlinear Systems in the Frequency Domain with Applications in Condition Monitoring and Engineering Systems

Rafael Suzuki Bayma

Department of Automatic Control and Systems Engineering

The University of Sheffield

Thesis submitted for the degree of

PhilosophiæDoctor (PhD)

2014 August

Abstract

The study of nonlinear systems has received great attention in recent years because of the necessity of dealing with practical problems that cannot be modelled by linear representations. Although the availability of greater computational power and advances in the field of system identification have allowed significant progresses towards modelling real world processes, a systematic method for understanding the systems characteristics is still an open problem. In this context, as has been demonstrated in many studies, the extension of the well-known concept of linear Frequency Response Function (FRF) to nonlinear systems are a significant potential solution. The condition monitoring problem is closely associated with the analysis of systems characteristics and can therefore be considered as part of this scenario.

Modern industrial processes have grown significantly in both size and complexity, creating the demand for automatic systems that can aid human operators in the important task of recognising when the process is experiencing malfunctions. Although this problem has been studied from the perspective of a wide scope of disciplines, such as modelling, signal processing, intelligent systems and statistical analysis, in many cases, data oriented methods or generic problem solvers (such as neural networks) often have to be applied. This is because complicated system behaviours are often difficult to interpret so as to associate them with possible faulty conditions.

In order to address these challenges, this thesis proposes new methods for

nonlinear system analysis in the frequency domain, and studies the application of these new methods for solving condition monitoring problems. The principle is based on the idea that a nonlinear system formulation can be used to deal with situations of practical interest where nonlinear behaviour cannot be neglected and that the frequency domain analysis approach can be applied to conduct an in-depth study of the system properties for the purpose of characterising systems faulty behaviours. In order to apply this principle, several issues need to be addressed, including the evaluation of the frequency characteristics of nonlinear systems and the generation of useful features that allow an effective characterisation of faulty system conditions. Motivated by these needs, the following research studies are conducted in this thesis:

1. Development of new methods that allow an efficient extraction of the frequency domain representations of nonlinear systems, namely, Generalised Frequency Response Functions (GFRFs) and Nonlinear Output Frequency Response Functions (NOFRFs). The thesis first derives a comprehensive methodology that allows an efficient and systematic extraction of GFRFs from a polynomial NARX (Nonlinear Auto-Regressive with eXogenous inputs) model. Then the same idea is used for addressing issues regarding the computation of NOFRFs, providing efficient algorithms that allow an effective determination of the NORRFs in both numerical and analytical forms.

2. Establishment of a condition monitoring framework based on the new GFRFs/NOFRFs evaluation methods. This framework is constructed over a practical background where physical knowledge about the system is scarce, although process history data

is available. In this context, black-box models can be built and the system properties can be extracted by computing the system's GFRFs/NOFRFs via the newly proposed methods. These functions provide fundamental information for deriving useful features that can be used for characterising faults and building effective diagnosis systems. The effectiveness of the proposed methods has been verified by both simulation studies and real data analysis tests, demonstrating the advantage of the new condition monitoring framework for engineering applications.

These studies significantly improve current frequency analysis methods for nonlinear systems and, at the same time, provide effective condition monitoring approaches for a wide range of engineering systems.

To Giselle

Acknowledgements

Contents

List of Figures

Glossary

ALE   Associated Linear Equations

ANN   Artificial Neural Network

CM   Condition Monitoring

CT   Continuous-Time

DFT   Discrete Fourier Transform

DT   Discrete-Time

DTFT   Discrete Time Fourier Transform

ERR   Error Reduction Ratio

FD   Fault Diagnosis

FDI   Fault Detection and Isolation

FFT   Fast Fourier Transform

FRF   Frequency Response Function

GFRF   Generalised Frequency Response Function

NARMAX   Nonlinear AutoRegressive Moving Average with eXogenous inputs (model)

NARX   Nonlinear AutoRegressive with eXogenous inputs model

GLOSSARY

NOFRF   Nonlinear Output Frequency Response Function

PC   Principal Component

PCA   Principal Component Analysis

PF   Partial Fraction

PLS   Partial Least Squares

PRESS   Predicted Residual Sums of Squares

1

Introduction

1.1 Frequency domain analysis of nonlinear systems

In recent years, the field of nonlinear systems identification (Billings, 2013) experienced great advances, providing a more attractive background for the design of engineering systems that can either better remove nonlinear distortions or even benefit from nonlinear behaviours.

However, the analysis and consequent extraction of useful information from these models still remain a great challenge. This is mainly due to the presence of nonlinearities, which brings difficulties to explicitly expressing the model output in terms of the input and can also produce, in many situations, complex behaviours that usually enforce the analysis to be carried out for particular situations, instead of a more general framework. In the context of single input, single output systems, a particular class of nonlinear systems that is relatively important for practical applications is the one for which the output can be represented by a series of Volterra functionals, also known as a Volterra series.

The Volterra series comprises an explicit description of the system output in terms of input operators(Schetzen, 1980). This representation can be applied to nonlinear sys-

1. INTRODUCTION

tems where moderate nonlinear behaviour, such as harmonics and intermodulations, can be observed (Weiner and Spina, 1980). These systems are more formally described as *fading memory* systems (Boyd and Chua, 1985), which in practice means that they are stable around the equilibrium under which the series is expanded (usually a zero equilibrium). The array of practical systems that can be represented in this way is relatively wide and has been reported in the literature for a broad range of disciplines, *e.g.* communications (Benedetto and Biglieri, 1983; Biglieri et al., 1988), image processing (Ramponi, 1986), biological systems (Marmarelis and Naka, 1974), neuroscience (Joseph and Ghosh, 2003) and circuit modelling (Chen and Huang, 2009; Sakian et al., 2011).

The components of the Volterra series (also known as *functionals*) are often seen as direct extensions of the convolution operator (Schetzen, 1980), which constitutes one of the fundamental basis for studying linear systems, both for continuous-time (CT) and discrete-time (DT) representations. This is justified by the possibility of conducting the analysis via a frequency domain formulation, based on the Fourier and Laplace operators (for CT systems), for instance, where the system input-output description is converted into an algebraic product framework, and under which the concept of *Transfer Function*, also known as *Frequency Response Function* - FRF, is built upon. This is a fundamental principle of many successful applications of linear systems theory, such as automatic control, signal processing and communications. For this reason, there is great interest in studying the Volterra series approach, as it offers the perspective of extending this well established frequency domain framework to the nonlinear systems scenario.

However, the main difficulty encountered in this task is that, the equivalent Volterra series description in the frequency domain consists of a non-algebraic formulation (Lang and Billings, 1996) that is relatively more complicated than the algebraic framework found in linear systems. The fundamental difference is that the traditional nonlinear

systems frequency formulation is expressed in terms of multidimensional operations whose core components are multidimensional functions, the so called *Generalised Frequency Response Functions* - GFRFs (George, 1959). GFRFs are usually considered as direct extensions of the FRF concept (George, 1959; Weiner and Spina, 1980) and can provide great insight about nonlinear systems properties, as they can highlight physical properties via unique system representations (Li and Billings, 2001; Billings and Li, 2000). However, unlike the linear case, conducting nonlinear system analysis via these functions is a much more laborious task. This is mainly due to two reasons: (i) computation of GFRFs is not as trivial as in the linear case; and (ii) interpreting system properties in terms of GFRFs is not simple because of their multidimensional nature.

Considerable work has been done regarding the computation of the GFRFs; the method based on orthogonal functionals (Lee and Schetzen, 1965), the variational approach (Rugh, 1981) and the probing method (Peyton Jones and Billings, 1989) are some of the most widely used algorithms. These methods basically differ in the resulting representation, in which the GFRFs can be obtained in explicit nonparametric form (Lee and Schetzen, 1965; Schetzen, 1981) or through recursive relationships, *i.e.* higher order GFRFs are expressed in terms of their lower order counterparts (Marmarelis and Naka, 1974; Peyton Jones and Billings, 1989; Jing et al., 2008). Although these procedures have been well established, it is worth mentioning that they require considerable more efforts than the usual way linear FRFs are obtained, *e.g.* by Fourier transforming the model difference equation and finding the input-output ratio.

A more difficult problem though, is the systematic analysis of the system behaviours in terms of GFRFs properties, which is mainly caused by their multidimensional characteristics. Graphical approaches are difficult to apply, except for second order cases, where the GFRFs can be displayed as surface plots. Third order cases have been studied to some extent (Yue et al., 2005a), but require large computational efforts and are

difficult to interpret. Higher order cases are simply infeasible, since it is not possible to graphically display such multivariate functions. Similarly, analytical approaches, *i.e.* where the algebraic structure of GFRFs are analysed are also very difficult to conduct. This is due to complexity of the GFRFs explicit algebraic form, which is usually described as multivariate rational functions (George, 1959; Weiner and Spina, 1980), although some efforts have also been dedicated to this problem, by exploring symbolic computations and the recursive relationships between different order GFRFs (Yue et al., 2005b). However, as with the graphical approaches, these analytical results are limited to low order cases, as the analysis become infeasibly complex at higher order problems.

For this reason, researchers have proposed alternative formulations in the attempt of studying the system properties using nonlinear FRFs which can be studied in low-dimensional frequency spaces. In this context, significant work has been developed in the Department of Automatic Control and Systems Engineering at the University of Sheffield, where concepts such as *Nonlinear Output Frequency Response Functions* (NOFRFs) (Lang and Billings, 2005), energy transfer filters (Billings and Lang, 2002) and *Output Frequency Response Functions* (OFRFs) (Lang et al., 2007) have been proposed.

In this research the focus will be on the NOFRFs concept. This approach has been the object of several research studies (Lang and Peng, 2008; Peng et al., 2007a, 2011) and can be considered as a potential tool for building a comprehensive methodology for nonlinear system analysis in the frequency domain. One of the attractive features of NOFRFs is their unidimensional nature, which circumvents many of the problems observed in GFRF based analysis. However, there are several issues that remain to be solved, in order to systematically apply NOFRFs to the analysis of practical engineering problems. More specifically, the algorithm developed for computing NOFRFs from a polynomial NARX model (Lang and Billings, 2005) need to be improved, so that

problems regarding numerical conditioning and truncation order specification can be overcome. In addition, it is still not clear how NOFRFs can be used for more particular goals, *e.g.* for distinguishing between different system conditions, a problem of great relevance for engineering systems. Though this scenario has been studied to some extent - see, for example (Peng et al., 2007b, 2011, 2007), it only has been done by considering a small number of operating conditions (*i.e.* faults), so that a more in-depth analysis need to be carried out in order to extend and validate the principles of the NOFRF based approach to this kind of problem.

1.2 Condition monitoring of engineering systems

A problem of great relevance in modern engineering is the design of systems that automatically detect and respond to abnormal events, such as component break, degradation or failure. The automatic management of these situations is relatively different from the well established task of feedback control; it consists of efficiently detecting the malfunctions and performing additional complex tasks that attempt to obtain the maximum amount of information about the event, while also providing evidences about how these conclusions were drawn. This problem can be generally referred as *fault diagnosis* (Isermann, 2006) - FD - or *condition monitoring* Barron (1996) - CM - where the main focus is to determine information about the system state from measurements taken over the period the anomalous behaviour occurred. This problem has been widely studied in recent years due to the great impact these circumstances can have over industrial processes, ranging from loss of plant performance to human contingencies.

FD/CM strategies have been greatly improved over the last decades, although they need persistent improvements for being on par with the demands of large scale complex processes of modern industry. In the context of model-based approaches, *i.e.* methods that explicitly use a mathematical model for designing the diagnosis strategy, several different methods have been proposed: parity equations, observers and system identifi-

1. INTRODUCTION

cation strategies (Isermann, 2006; Patton et al., 1989) are among the most popular and have been successfully used for solving practical problems. However, in most cases, the models used for developing the FD/CM strategies are a linear system representation. As nonlinear behaviour is present in most of the practical situations (although it can sometimes be safely neglected), the extension of linear FD/CM approaches to cases in which nonlinearities (whether caused by the presence of faults or inherent from the system own nature) cannot be neglected is a relatively difficult task Venkatasubramanian et al. (2003c). For this reason, special techniques have been proposed, such as: statistical analysis, data mining, expert systems or neural networks (Venkatasubramanian et al., 2003a,b). However, a common issue with these approaches is that they tend to avoid the interpretation of the system physical behaviour, ignoring features that could be potentially used for obtaining additional insight about the fault characteristics.

In this context, a combined approach based on system identification principles and GFRFs/NOFRFs-based analysis can be considered as a potential new FD/CM methodology. The principles of system identification based diagnosis (also referred as parameter estimation techniques) consist of postulating faults as disturbances in parameters of a physical model. Although the physical model formulation can be used for devising a diagnosis strategy, this research focused on investigating representative features generated directly from black-box polynomial models, which can be useful for situations where phenomenological modelling is difficult. In this scenario, GFRFs/NOFRFs possess considerable potential for revealing system properties, as they are founded in the frequency domain which provides an important physical background, *e.g.* resonance and harmonic response. Therefore, the construction of a solid framework that allows effective computation and systematic analysis of GFRFs/NOFRFs not only offers a useful framework for nonlinear systems analysis, but also offers a potentially useful approach for developing FD/CM systems for circumstances where input-output data is abundant while process physical knowledge may be absent.

1.3 Aim and objectives

The aim of this research is to develop a new methodology for conducting in-depth studies of nonlinear systems properties, based on the concepts of GFRFs and NOFRFs, while also investigating means of applying this methodology for solving practical CM problems. In order to achieve this, the following objectives will be pursued:

1. To conduct a short survey about nonlinear systems identification methods, in particular, for obtaining polynomial NARX models. This is important because it will be assumed that physical knowledge about the system is scarce, so that a black-box modelling approach is more adequate.

2. To review the Volterra series representation of nonlinear systems, which is the main tool for conducting frequency domain analysis of nonlinear systems. This approach constitutes the main background for the NOFRFs formulation, which will be the main focus of this research. .

3. To investigate the concept of NOFRFs, identify current gaps and address these issues so that NOFRFs can be applied in practice for analysing models obtained from real data. The most relevant issue about this problem is the computation of NOFRFs from polynomial models, and therefore, will be of a greater concern.

4. To develop MATLAB programs that can implement the new NOFRFs computation methods.

5. To develop a systematic approach for using NOFRFs in CM problems. In this case, it is necessary to identify key NOFRFs based features that can provide evidences about system condition changes. This will be investigated using both simple approaches, *e.g.* monitoring NOFRFs maxima, and more advanced methods that are usually considered in CM problems, *e.g.* classification and

statistical tools.

6. To test the condition monitoring methods in problems of practical interest

Therefore, it is expected that, at the end of the research, a set of new useful tools and methodologies become available for integration of well-established nonlinear system modelling approaches with a new GFRFs/NOFRFs based frequency analysis framework, so that better studies of nonlinear systems can be achieved, with potential practical applications in many areas, especially in engineering systems condition monitoring and fault diagnosis.

1.4   Contributions and thesis layout

The objectives of this thesis were fulfilled satisfactorily and some significant results were obtained. In this context, the main contributions to the fields of nonlinear systems analysis and condition monitoring can be listed as follows:

- A new methodology for extracting the recursive representation of the GFRFs of a nonlinear system has been developed. This is presented in Chapter 3, where useful systematic procedures based on order and kernel extraction operators are presented. This result is important due to two reasons: (i) it provides a more efficient manner of obtaining the recursive descriptions of the GFRFs, in comparison to the probing method (Peyton Jones and Billings, 1989), which is currently the usual choice for this task; (ii) some steps of the method can be directly applied for obtaining the so called Associated Linear Equations - ALEs (Feijoo et al., 2005), providing an important basis for addressing the issues related to NOFRFs computation.

- In addition, the GFRF extraction procedures were implemented in MATLAB scripts, which, together with system identification functions, constitute an important set of tools for automated nonlinear systems analysis.

8

- Based on ALEs extraction, two new methods for computation of NOFRFs are presented in Chapter 4. The first one is an efficient numerical procedure designed for dealing with very general polynomial NARX models and arbitrary input signals. Based on linear filtering and FFT (Fast Fourier Transform) algorithms, the new method is capable of circumventing problems observed in the algorithm from (Lang and Billings, 2005) related to truncation order and ill conditioned regression, providing accurate NOFRFs computations up to any order.

- The second algorithm for NOFRF computation, also presented in Chapter 4, is an analytical approach where NOFRFs can be obtained in rational form and, if so desired, in terms of variable parameters, such as the driving frequency of a sinusoidal input. Such representations have not been considered in previous studies and constitute a useful result, as they can be used for describing the NOFRFs in algebraic form for a wide range of frequencies and for better understanding the influence of unknown parameters over the system behaviour. In order to achieve this, a new frequency convolution framework is proposed. Based on the Residue Theorem and partial fraction expansions, this methodology is adopted because it was verified that severe accuracy errors and computational problems can arise in the analytical calculations, especially if the procedures are carried out via symbolic processing. The proposed method overcomes these difficulties, allowing a practical use of the analytical representation of NOFRFs.

- MATLAB scripts were also produced for automating the NOFRFs extraction processes, both in numerical and analytical formats, expanding the set of tools for dealing with practical problems.

- Two condition monitoring algorithms based on the new system analysis tools

are presented in Chapter 5. The algorithms were designed after carrying out study cases related to nonlinear mechanical systems. The first one can be applied to systems when noise levels are small and fault parameters (*e.g.* stiffness, damping, impedance) are clearly defined. The approach consists of using process history for modelling the behaviour of NOFRFs based features (*e.g.* NOFRFs resonance peaks or indices based on NOFRFs energy) under different faulty conditions, so that the fault parameters can be recovered, via function inversion, for characterising the system condition.

- The second CM strategy can be applied to scenarios where the noise levels are more significant and fault parameters are not clearly defined. In this circumstance, a classification approach can be used, in which faults are characterised by clusters and their geometric distribution in the feature space. Features are directly generated from NOFRFs measurements, by using dimensionality reduction techniques such as *Principal Component Analysis* - PCA - or *Partial Least Squares* - PLS, so that only a small number of representative variables is used for better interpretation of results and efficient training of automatic classifiers.

As part of these achievements, the following research papers have been elaborated: (Bayma and Lang, 2012) "A new method for determining the generalised frequency response functions of nonlinear systems" was published in the IEEE Transactions on Circuits and Systems I: Regular Papers, where the new GFRF extraction algorithm is presented. The article (Bayma and Lang, 2014) "Fault diagnosis methodology based on nonlinear system modelling and frequency analysis" is to be published at the 19th IFAC World Congress, where the basic principles of the methodology described in Chapter 5 are presented with an application. The contents of Chapter 4 are currently being considered for a future new publication.

The remaining of this thesis consists of four chapters covering literature review, development of new methods for the frequency domain analysis of nonlinear systems, the application of these new methods to construct a new framework for engineering systems CM/FD, as well as simulation and experimental studies. The contents of each chapter are summarised as follows:

Chapter 2 offers a review of the state of the art of the Volterra series approach. It consists of some basic ideas about how functionals are formed and a more formal treatment about how they can be used for representing nonlinear systems. The core of Chapter 2, though, is the frequency domain formulation in which GFRFs and NOFRFs are introduced, with an in-depth discussion about how they can be obtained in practice.

Chapter 3 presents a fundamental result that was used throughout this research for the development of new methods for the frequency analysis of nonlinear systems. It consists of a new algorithm that allows obtaining the system's GFRFs directly from a polynomial NARX model. The result is provided in recursive form, which is similar to other available algorithms; however, the proposed method is capable of performing this task in a much more efficient manner, where symbolic calculations and recursive procedures are avoided. In addition to these, the results presented in this chapter provide a very important basis for the development of the NOFRF-based nonlinear systems frequency domain analysis in later chapters.

In Chapter 4, a new NOFRF based approach for the frequency domain analysis of nonlinear systems is proposed. The approach consists of building (using the results of Chapter 3) and systematically solving the system Associated Linear Equations. Algorithms are developed for obtaining these equations from a polynomial nonlinear difference equation model up to arbitrary order. Both numerical and analytical approaches are derived for obtaining the solutions, which provide a new and efficient way of obtaining NOFRFs and establishing an effective new method for analysing nonlinear systems in the frequency domain;

In Chapter 5, a new framework for engineering system condition monitoring/fault diagnosis is first established. This is a framework based on the idea of time-domain modelling and frequency domain analysis where the new methods for determining GFRFs/NOFRFs derived in chapters 3 and 4 are the very basis. The new framework is then used for developing two new CM strategies, which are used for dealing with problems where fault parameters are either well or poorly defined. The strategies are then verified using both simulation studies and practical data analysis. After that, a generalised CM procedure is established; the basic ideas potentially have a wide range of practical applications

Finally, in Chapter 6, the main results are summarised and the contributions of this research are presented. Emphasis is also given to some topics that can become future research using the results of this thesis as a starting point.

2

Frequency domain approach to nonlinear systems

2.1 Introduction

Nonlinear systems modelling and analysis received great attention in recent years due to an increasing demand in dealing with practical phenomena of complex nature. However, because of the variety of nonlinear problems that exists and the difficulties of establishing universal procedures for analysing general situations, nonlinear systems are usually divided into classes for which particular strategies are developed for the tasks of analysis and design.

The Volterra series is a classical approach to a particular, although broad class of nonlinear systems. It can be used for describing moderate nonlinear behaviour that is commonly observed in many practical situations, *e.g.* intermodulations and generation of harmonics. The main feature of this approach is the explicit description of the system output in terms of polynomial based representations of the input signal, which allows some of the well established frequency domain techniques from linear systems analysis to be extended to the nonlinear case. This can be very useful in FD/CM

problems, as monitoring typical nonlinear phenomenon, such as output harmonics, is already recognised as a consolidated technique, although it is commonly used from a pure data-analysis perspective. In this context, a system analysis approach can reveal further details about the situation and, therefore, constitutes a potential tool for designing fault diagnosis systems.

This chapter is dedicated to introducing the basic aspects of this approach and reviewing recent advances in the area, in order to present the theoretical foundation over which the results of this research have been built.

2.2 The functional series approach

The term functional generally refers to a map between functions. However, the focus of this work shall be narrowed to a more particular description in which functionals can be described as natural extensions of polynomial functions, a notion originally proposed by the Italian mathematician Vito Volterra (1959). This idea is useful in engineering and applied mathematics because it allows developing a formal theory for approximating operators between vectors spaces, which is important for better understanding relationships between input and output signals.

To illustrate the basic idea, consider a multivariate polynomial function of degree n in variables u_i, $i \in \{1, \ldots, k\}$, described as:

$$y_n\left(u_1, \ldots, u_k\right) = \sum_{i_1=1}^{k} \ldots \sum_{i_n=1}^{k} h_{i_1, \ldots, i_n}\, u_{i_1} \ldots u_{i_n} \tag{2.1}$$

where the n-dimensional coefficients $h_{i_1 \ldots i_n}$ are known as the kernel coefficients.

The notion of functional arises when $k \to \infty$. In this case, the extrapolation of (2.1) consists of replacing summations by integrals, the variables u_1, ..., u_k by a single function and the summation indices i_1, ..., i_n by integration variables, yielding:

$$y_n = \int_{a_1}^{b_1} \ldots \int_{a_n}^{b_n} h_n(\tau_1, \ldots, \tau_n) \prod_{i=1}^{n} u(\tau_i) d\tau_i \tag{2.2}$$

where the intervals $[a_i, b_i]$ are analogous, although more general, to the integer ranges $i_p = \{1, \ldots, k\}$, where $p = \{1, \ldots, n\}$. Also notice that the kernel coefficients were replaced by a n-dimensional function $h_n(\tau_1, \ldots, \tau_n)$, which is called the n-th order kernel.

In order to model memory effects and dynamical behaviour, formulation (2.2) is usually written in a different form, where the time t is introduced and an explicit dependence of $y_n(t)$ in terms of the past values of the input is assumed. This is described as:

$$y_n(t) = \int_{-\infty}^{+\infty} \ldots \int_{-\infty}^{+\infty} h_n(\tau_1, \ldots, \tau_n) \prod_{i=1}^{n} u(t - \tau_i) d\tau_i \tag{2.3}$$

which can also be written as:

$$y_n(t) = \int_{-\infty}^{+\infty} \ldots \int_{-\infty}^{+\infty} h_n(t - \tau_1, \ldots, t - \tau_n) \prod_{i=1}^{n} u(\tau_i) d\tau_i \tag{2.4}$$

by using a simple change of variables. Expression (2.3) can be understood as a polynomial function of the past values of the input, weighted by the kernel function for each group of delays $\tau_1, \ldots, \tau_n$; but since the delays can assume any value on a continuous range, this polynomial function need to be described in terms of continuous summations (*i.e.* integrals), instead of discrete ones. Functional (2.3) is said to be *homogeneous* with respect to $u(t)$, because it is only formed by terms of degree n.

It is also important to notice that for $n = 1$, (2.3) reduces to the well known convolution integral:

$$y_1(t) = \int_{-\infty}^{+\infty} h(\tau) u(t - \tau) \tag{2.5}$$

so that (2.3) can be viewed as a generalisation of the convolution operator.

Another interesting aspect regarding the analogy between functionals and polynomials is that, according to the Stone-Weirstrass Theorem (Rudin, 1976), any single variable continuous function $f(u)$ can be approximated by a polynomial series:

$$f(u) \approx c_0 + \sum_{n=1}^{N} c_n u^n \tag{2.6}$$

2. FREQUENCY DOMAIN APPROACH TO NONLINEAR SYSTEMS

where $\{c_0, c_1, \ldots\}$ represent appropriate constants. Therefore, it is natural to conjecture that any system operator:

$$y(t) = H[u(t)] \tag{2.7}$$

can also be approximated by a functional series:

$$y(t) \approx y_0 + \sum_{n=1}^{N} y_n(t) \tag{2.8}$$

where y_0 is a constant and $y_n(t)$ is described as (2.3). Usually, y_0 is set to 0 for simplifying the formulation. For this reason, the Volterra series is sometimes referred as a "Taylor series with memory" (Schetzen, 1980).

This is indeed the case, as demonstrated in (Boyd and Chua, 1985), when H represents a fading memory system. This is equivalent to saying that the system is stable around an equilibrium point and the output does not depend on the remote past of the input, which is the case of many practical situations. Moreover, notice that (2.3) is nonlinear with respect to $u(t)$ for $n \geq 2$, which suggests that (2.8) can be used for describing nonlinear systems.

The application of functionals for describing nonlinear systems received increased attention through the works of Wiener (1958), where a theory for studying nonlinear circuits and modelling the spectra of electroencephalograms was elaborated. Several other studies followed Wiener's work, including the theory of orthogonal functionals (Lee and Schetzen, 1965) and inverse operators (Schetzen, 1976).

Functionals (2.3) and functional series (2.8) can also be defined for discrete-time systems, which is useful for carrying out functional calculations in digital computers. In this case, $y(t)$ and $u(t)$ respectively denote output and input samples, where $t \in \mathbb{Z}$. When H in (2.7) is fading memory, the output can be described as the series (2.8), where functionals $y_n(t)$ are now described as:

$$y_n(t) = \sum_{\tau_1=-\infty}^{+\infty} \cdots \sum_{\tau_n=-\infty}^{+\infty} h_n(\tau_1, \ldots, \tau_n) \prod_{i=1}^{n} u(t - \tau_i) \tag{2.9}$$

The Volterra series have found many applications in a wide variety of fields, including: nonlinear filtering and image processing (Mathews and Sicuranza, 2000; Ramponi, 1986); nonlinear circuits (Weiner and Spina, 1980), echo cancelling (Casar-Corredera et al., 1985; Zhao et al., 2005), biological systems (Marmarelis and Naka, 1974), channel equalisation (Karam and Sari, 1989; Carini et al., 1998), modelling of recording devices (Hermann, 1990), among others.

2.3 Analysis in the frequency domain

System analysis based on integral transforms, *e.g.* the Laplace, Fourier and $\mathcal{Z}$ transforms, is the theoretical foundation of many areas such as Control Engineering and Signal Processing. The successful application of this theory to practical problems is due to the possibility of transforming linear problems described in the time-domain by the convolution integral, into an algebraic formulation in the frequency domain. Because polynomial functionals are an extension of the convolution operator, the Volterra series approach provides the fundamental basis for extending these results for a class of nonlinear systems.

Although similar results can be derived for other transforms, the Fourier transform is more commonly used for formulating the frequency domain analysis of functional series. The Fourier transform of a square integrable function $x(t)$ is denoted as $X(j\xi) = \mathcal{F}\{x(t)\}$ and is defined as:

$$X(j\xi) = \int_{-\infty}^{+\infty} x(t)\, e^{-j\xi t} dt \tag{2.10}$$

where $\xi \in \mathbb{R}$ is the angular frequency and $j = \sqrt{-1}$ is the imaginary unit. The time domain function $x(t)$ can always be recovered from its unique transform via the inverse Fourier transform:

$$x(t) = \frac{1}{2\pi} \int_{-\infty}^{+\infty} X(j\xi)\, e^{j\xi t} d\omega \tag{2.11}$$

2. FREQUENCY DOMAIN APPROACH TO NONLINEAR SYSTEMS

Consider the continuous-time case. Let $Y_n(j\xi)$ denote the Fourier transform of n-th order functional (2.3) and $U(j\xi)$ denote the Fourier transform of $u(t)$, i.e.:

$$y_n(t) = \frac{1}{2\pi} \int_{-\infty}^{+\infty} Y_n(j\xi)\, e^{j\xi t} d\xi \tag{2.12}$$

$$u(t) = \frac{1}{2\pi} \int_{-\infty}^{+\infty} U(j\xi)\, e^{j\xi t} d\xi \tag{2.13}$$

Expressions (2.12) and (2.13) can be substituted into (2.3) for obtaining a relationship between the n-th order output spectrum $Y_n(j\xi)$ and the input spectrum $U(j\xi)$. The result is found as (Lang and Billings, 1996).

$$Y_n(j\xi) = \int_{\xi=\xi_1+\ldots+\xi_n} H_n(j\xi_1,\ldots,j\xi_n) \prod_{i=1}^{n} U(j\xi_i) d\sigma_{n,\xi} \tag{2.14}$$

where the integration is computed over the hyperplane $\xi = \xi_1 + \ldots + \xi_n$. The function $H_n(j\xi_1,\ldots,j\xi_n)$ denotes the n-dimensional Fourier transform of the n-th order kernel:

$$H_n(j\xi_1,\ldots,j\xi_n) = \int_{-\infty}^{+\infty} \ldots \int_{-\infty}^{+\infty} h_n(\tau_1,\ldots,\tau_n) \prod_{i=1}^{n} e^{-j\xi_i \tau_i} d\tau_i \tag{2.15}$$

Expression (2.14) is of little practical use, though, as it is relatively complicated to compute it either numerically or in closed form, especially for large n. For this reason, the system properties are usually studied via the analysis of functions $H_n(j\xi_1,\ldots,j\xi_n)$ or concepts derived from formulation (2.14).

2.3.1 Generalised Frequency Response Functions

Functions (2.15) are commonly known as Generalised Frequency Response Functions (GFRFs). The term was introduced in (George, 1959) as it represents a natural extension of the well known concept of Frequency Response Function (FRF) from linear systems theory. This can be readily seen since, for $n = 1$, (2.14) reduces to:

$$Y_1(j\xi) = H_1(j\xi)U(j\xi) \tag{2.16}$$

However, in contrast to the linear case, the role that the GFRFs play in the composition of the output spectrum for nonlinear systems is very complicated, as it requires analysing multidimensional frequency spaces. For example, for the linear case

$Y(j\xi) = H(j\xi)U(j\xi)$ and the support of the output spectrum $Y(j\xi)$, *i.e.* the frequencies ξ for which $|Y(j\xi)| \neq 0$, is the same support of the input spectrum. This is generally not true for the nonlinear case, which admits a much richer support, usually larger than the input bandwidth. This has been more deeply studied in (Lang and Billings, 1997; Wu et al., 2007), where complex algorithms for composing the output spectrum, given an arbitrary input support, was presented.

For a time-invariant nonlinear system, the GFRFs can be used for describing system characteristics in the frequency domain. This has been widely used in applications, *e.g.* : Palumbo and Piroddi (2000) used a GFRF based procedure for studying a dam buttress. Tang et al. (2010) used GFRFs for characterising three kinds of faults in a rotor-bearing system. However, there are several issues with this approach, which are due to the GFRFs multidimensional nature. For example, the realization of (2.14) is not unique; usually, $H_n(j\xi_1, \ldots, j\xi_n)$ is an asymmetric function and a permutation of variables in (2.14) can usually be carried out without necessarily altering the value of $Y_n(j\xi)$. This basically means that the system can admit more than one asymmetric n-th order GFRF. These ambiguities can be avoided by symmetrising the GFRFs, which consists of replacing $H_n(j\xi_1, \ldots, j\xi_n)$ in (2.14) by the symmetrical GFRF computed from the original function as:

$$H_n^s(j\xi_1, \ldots, j\xi_n) = \frac{1}{n!} \sum_{\Omega_n} H_n(j\xi_1, \ldots, j\xi_n) \qquad (2.17)$$

where Ω_n represents the set of all permutations of $(\xi_1, \ldots, \xi_n)$. Obviously, this becomes infeasible when n is large, as the time required for computing $H_n(j\xi_1, \ldots, j\xi_n)$ for every possible permutation of arguments becomes prohibitive.

Another notable issue with GFRF-based analysis is that graphical analysis is seldom possible. In the linear case, FRF analysis via classical tools such as Bode and Nyquist plots is useful because typical system properties such as bandwidth, resonance frequencies and phase margin can be easily understood from graphical displays of the FRF, which are always plane figures. For 2-nd order cases, this is still possible, as

2. FREQUENCY DOMAIN APPROACH TO NONLINEAR SYSTEMS

$H_2(j\xi_1, j\xi_2)$ can be studied via surface plots against ξ_1 and ξ_2, for example, although the analysis is not as simple as in the linear case, since the composition of the output spectrum has to be analysed from plane slices of the form $\xi_1 + \xi_2 = \xi$. For cases of order 3, graphical displays become much more difficult, although some attempts of establishing more rigorous analysis procedures have been made (Yue et al., 2005a,b). This requires special computational procedures, but the complexity of the algorithms make these approaches infeasible.

2.3.2 Nonlinear Output Frequency Response Functions

Because of the difficulties with the analysis of multidimensional characteristics of GFRFs, alternative FRF concepts have been proposed. The main idea behind them is to study the system frequency behaviours while maintaining the dimensionality of the features low. The concept of *Nonlinear Output Frequency Response Functions* - NOFRFs (Lang and Billings, 2005) was defined in this context and has been established as a potential alternative, as it has been successfully used in several studies of both theoretical and practical natures.

The concept of NOFRFs was initially proposed by Lang and Billings (2005) for explaining how nonlinear systems transfer the input energy between different frequency bands and how this phenomenon can be translated into comprehensive properties that allow a better understanding of nonlinear systems. Based on a simple reasoning about linear operators with input polynomial nonlinearities, the authors proposed that the n-th order NOFRFs for continuous-time systems can be defined as:

$$G_n(j\xi) = \frac{\mathcal{F}\{y_n(t)\}}{\mathcal{F}\{u(t)^n\}} = \frac{Y_n(j\xi)}{U_n(j\xi)} \tag{2.18}$$

where $Y_n(j\xi)$ is defined as (2.14) and $U_n(j\xi)$ represents the n-th order generalised spectrum of the input and is defined as:

$$U_n(j\xi) = \mathcal{F}\{u(t)^n\} \tag{2.19}$$

In this context, the output spectrum can be written as:

$$Y(j\xi) = \sum_{n=1}^{\infty} G_n(j\xi)U_n(j\xi) \tag{2.20}$$

For discrete-time systems, a similar formulation can also be obtained, where the output is described as:

$$Y(e^{j\omega}) = \sum_{n=1}^{\infty} G_n(e^{j\omega})U_n(e^{j\omega}) \tag{2.21}$$

and $G_n(e^{j\omega})$ is now defined as:

$$G_n(e^{j\omega}) = \frac{\text{DTFT}\{y_n(t)\}}{\text{DTFT}\{u(t)^n\}} \tag{2.22}$$

where DTFT{ } denotes the Discrete Time Fourier Transform, and ω denotes normalised frequency.

The basic advantage of the NOFRF formulation is that the system can be studied via a series of one dimensional FRFs, for any order of interest. This greatly simplifies the analysis in comparison to GFRF-based analysis, which becomes more difficult to carry out as n increases. In addition, NOFRFs possess useful properties that can be directly derived from definitions (2.18) and (2.22). These properties are described as follows (Lang and Billings, 2005)

(i) The output components $Y_n(j\xi)$ are described in a manner similar to linear systems

(ii) The frequency support of $U_n(j\xi)$ is the same as of $Y_n(j\xi)$

(iii) $G_n(j\xi)$ is invariant to an input constant gain

Property (i) is useful for carrying out analysis in which nonlinear components are studied separately. The algebraic product formulation allows studying properties such as resonance and bandwidth for these higher order components in a more convenient way.

2. FREQUENCY DOMAIN APPROACH TO NONLINEAR SYSTEMS

It is important to mention that NOFRFs are, in general, input dependent. This can be understood as a reflection of the system nonlinear characteristics, which can be revealed in more or less details, depending on the input used for probing the system. This is mainly due to NOFRFs being extracted from low dimensional slices of the GFRFs that are directly affected by the excitation. However, certain changes in input characteristics do not produce any changes in the NOFRFs, which is the basic idea of property (iii) above. Property (iii) shows that if the NOFRFs computed with $U(j\xi) = U_0(j\xi)$ produce the NOFRFs $G_n(j\xi)$, then the NOFRFs obtained with $U(j\xi) = k U_0(j\xi)$ are described as $G_n(j\xi)$ as well, for any nonzero constant k.

This is the basis of an algorithm developed for estimating the NOFRFs (Lang and Billings, 2005) from a pre-established model. The procedure consists of a linear regression scheme that is constructed from several excitations of the form $k_i u(t)$, $i \in \{1, \ldots, s\}$. In this circumstance, the output spectrum produced by input $k_i u(t)$ can be described as:

$$Y_i(j\xi) = \sum_{n=1}^{p} G_n(j\xi) k_i^n U_n(j\xi) \tag{2.23}$$

Let:

$$G_n(j\xi) = G_n^R(j\xi) + jG_n^I(j\xi) \tag{2.24}$$

$$U_n(j\xi) = U_n^R(j\xi) + jU_n^I(j\xi) \tag{2.25}$$

$$Y_i(j\xi) = Y_i^R(j\xi) + jY_i^I(j\xi) \tag{2.26}$$

where $G_n^R(j\xi)$, $U_n^R(j\xi)$ and $Y_i^R(j\xi)$ respectively denote the real parts of $G_n(j\xi)$, $U_n(j\xi)$ and $Y_i(j\xi)$, while $G_n^I(j\xi)$, $U_n^I(j\xi)$ and $Y_n^I(j\xi)$ respectively denote the imaginary parts of $G_n(j\xi)$, $U_n(j\xi)$ and $Y_n(j\xi)$.

Then, (2.23) can be rewritten as:

$$Y_i(j\xi) = \sum_{n=1}^{p} \left(G_n^R(j\xi) + jG_n^I(j\xi) \right) k_i^n \left(U_n^R(j\xi) + jU_n^I(j\xi) \right) \tag{2.27}$$

yielding:

$$Y_i^R(j\xi) = \sum_{n=1}^{p} k_i^n \left(G_n^R(j\xi) U_n^R(j\xi) - G_n^I(j\xi) U_n^I(j\xi) \right) \tag{2.28}$$

$$Y_i^I(j\xi) = \sum_{n=1}^{p} k_i^n \left(G_n^R(j\xi) U_n^I(j\xi) + G_n^I(j\xi) U_n^R(j\xi) \right) \tag{2.29}$$

Equations (2.28)-(2.29) can be written in matrix format, which is more convenient for the estimation scheme. To this end, let:

$$\boldsymbol{\theta} = \left[\begin{array}{ccccccc} G_1^R(j\xi) & \ldots & G_p^R(j\xi) & G_1^I(j\xi) & \ldots & G_p^R(j\xi) \end{array} \right]^T \tag{2.30}$$

$$\boldsymbol{Y}^R = \left[\begin{array}{ccc} Y_1^R(j\xi) & \ldots & Y_s^R(j\xi) \end{array} \right]^T \tag{2.31}$$

$$\boldsymbol{Y}^I = \left[\begin{array}{ccc} Y_1^I(j\xi) & \ldots & Y_s^I(j\xi) \end{array} \right]^T \tag{2.32}$$

and:

$$\boldsymbol{U}^R = \begin{bmatrix} k_1 U_1^R(j\xi) & k_1^2 U_2^R(j\xi) & \ldots & k_1^p U_p^R(j\xi) \\ k_2 U_1^R(j\xi) & k_2^2 U_2^R(j\xi) & \ldots & k_2^p U_p^R(j\xi) \\ \vdots & \vdots & \vdots & \vdots \\ k_s U_1^R(j\xi) & k_s^2 U_2^R(j\xi) & \ldots & k_s^p U_p^R(j\xi) \end{bmatrix} \tag{2.33}$$

$$\boldsymbol{U}^I = \begin{bmatrix} k_1 U_1^I(j\xi) & k_1^2 U_2^I(j\xi) & \ldots & k_1^p U_p^I(j\xi) \\ k_2 U_1^I(j\xi) & k_2^2 U_2^I(j\xi) & \ldots & k_2^p U_p^I(j\xi) \\ \vdots & \vdots & \vdots & \vdots \\ k_s U_1^I(j\xi) & k_s^2 U_2^I(j\xi) & \ldots & k_s^p U_p^I(j\xi) \end{bmatrix} \tag{2.34}$$

Therefore, the following linear relationships can be built:

$$\left[\begin{array}{c} \boldsymbol{Y}^R \\ \boldsymbol{Y}^I \end{array} \right] = \left[\begin{array}{cc} \boldsymbol{U}^R & -\boldsymbol{U}^I \\ \boldsymbol{U}^I & \boldsymbol{U}^R \end{array} \right] \boldsymbol{\theta} \tag{2.35}$$

Usually, the system should be excited for a large number of gains k_i, so that the NOFRFs can be estimated via a least squares approach.

In practice, this algorithm can be applied after a model has been identified for the system under study. The procedure has some issues, however, as formulation (2.23) requires specifying the maximum order of the NOFRFs in advance. This is relatively

problematic since it is inconsistent with other Volterra series based approaches where the lower order functional components are not affected by their higher order counterparts. In addition the construction of the regression matrices requires probing the system different times with different inputs, demanding additional computational efforts, since the system needs to be simulated for each excitation level. The most critical issue, though, is that the gain parameters k_i need to be carefully chosen. Due to the polynomial nature of the regression terms, a poor choice of these gains can easily produce ill conditioning of the regression matrix.

There are exceptions to this rule, though. The NOFRFs become input independent when the input is either sinusoidal, or when the kernels possess a special structure. When the input is sinusoidal of frequency ω_h, all functional components are described by harmonic components located at $k\omega_h$, $k \in \{0, \pm 1, \ldots, \pm n\}$. In this case, the NOFRFs only need to be evaluated at these frequencies. The continuous-time NOFRFs are found as (Peng et al., 2007b):

$$G_n(j(-n + 2k)\omega_h) = H_n(\underbrace{j\omega_h, \ldots, j\omega_h}_{k}, \underbrace{-j\omega_h, \ldots, -j\omega_h}_{n-k}) \qquad (2.36)$$

where H_n denotes the n-th order GFRF. Several applications have explored this form for studying properties of particular nonlinear systems. For example: a comparison between harmonic balance and NOFRF approaches was investigated in (Peng et al., 2008), in terms of computation of harmonic responses in Duffing type oscillators. It was shown that the NOFRF formulation provides a considerably simpler way of understanding higher order harmonics, even when the oscillator exhibits highly nonlinear damping terms, although it cannot be used for describing more complicated behaviours such as frequency jumps.

In addition, previous studies based on bilinear oscillators (Peng et al., 2007) reinforced the idea that the sinusoidal characteristics of nonlinear systems can be explained by NOFRF-based representations. This study was able to provide a more systematic understanding of sub-resonances, which is a widely used phenomenon for characterising

cracked structures. A more in-depth study of nonlinear resonance phenomena based on NOFRFs can also be found in (Peng et al., 2007b), in which a deep investigation about the influence of linear damping over the nonlinear resonance characteristics was conducted.

Sinusoidal analysis based on NOFRFs have also been used for identifying nonlinear behaviour as source of potential system anomaly. A comprehensive general approach was reported in (Lang and Peng, 2008), based on simplified multi degree of freedom simulation model, in which the nonlinear stiffness component can be effectively localised. The philosophy of this approach was also tested in real applications (Peng et al., 2007a, 2011). These results suggest that the NOFRF formulation provides a suitable extension of the FRF concept to the nonlinear case and is, therefore, a potential tool towards the development of frequency domain techniques for addressing problems of practical interest.

2.4 Methods for GFRF extraction

As previously shown, one important step for Volterra series based analysis is to obtain the time-domain kernels or GFRFs. However, in most applications, the system is usually not explicitly represented as a functional series, which means that the kernels/GFRFs must be derived from other types of representation. This section is dedicated to present and briefly discuss some common methods for deriving the system GFRFs from input-output data and difference/differential equation models, since these are the most common forms of *a priori* information about the system.

Throughout this discussion, two types of GFRF representation will be considered: parametric and non-parametric. A non-parametric representation is characterised by a finite number of complex values of $H_n(j\xi_1, \ldots, j\xi_n)$ computed at specific points of the n-dimensional frequency space. The parametric representation, is characterised by the description of $H_n(j\xi_1, \ldots, j\xi_n)$ in terms of explicit algebraic expressions, such

as a n-variable rational function or a recursive implicit representation, *i.e.* when $H_n(j\xi_1,\ldots,j\xi_n)$ is written in terms of $H_k(j\xi_1,\ldots,j\xi_k)$, with $k < n$.

2.4.1 The variational approach

The variational method (Schetzen, 1980; Rugh, 1981) is a very simple approach that can be applied when an input-output model is available, which can be either continuous-time or discrete-time. It consists of algebraic steps that can be primarily implemented as symbolical calculations, although it has been demonstrated that a purely numeric procedure is also possible (Bayma and Lang, 2012).

The general steps can be described as follows. A continuous-time formulation will be considered, without loss of generality. Let $y'(t)$ be the system output when the input is described as $u(t)$, so that:

$$y'(t) = \sum_{n=1}^{p} y_n(t) \tag{2.37}$$

where p is the truncation order and:

$$y_n(t) = \int_{-\infty}^{+\infty} \ldots \int_{-\infty}^{+\infty} h_n(\tau_1,\ldots,\tau_n) \prod_{i=1}^{n} u(t-\tau_i) d\tau_i \tag{2.38}$$

In these circumstances, if the input is replaced by $\Gamma u(t)$, where $\Gamma > 0$ is a constant, the corresponding output can be described as

$$y(t) = \sum_{n=1}^{p} \Gamma^n y_n(t) \tag{2.39}$$

Assume the system is described by the input-output differential equation:

$$F(\phi_y(t), \phi_u(t)) = 0 \tag{2.40}$$

where

$$\phi_y(t) = \left[\begin{array}{cccc} y(t) & \dfrac{dy(t)}{dt} & \ldots & \dfrac{d^m y(t)}{dt^m} \end{array} \right] \tag{2.41}$$

$$\phi_u(t) = \left[\begin{array}{cccc} u(t) & \dfrac{du(t)}{dt} & \ldots & \dfrac{d^m u(t)}{dt^m} \end{array} \right] \tag{2.42}$$

and F is a polynomial function. The variational approach consists of the following steps:

1. Replace $u(t)$ by $\Gamma u(t)$ and $y(t)$ by (2.39) in (2.40).

2. Expand all multinomial terms that arise from the nonlinearities

3. Reorganise the left-hand side as a polynomial in Γ

4. Equate to zero all coefficients of the resulting polynomial, up to order p

5. Solve the resulting equations for components $y_n(t)$, $n \in \{1, 2, \ldots, p\}$ in terms of $u(t)$ and determine the kernels by inspection.

It is important to notice that the artificial parameter Γ was merely introduced to simplify the process of identifying the terms of a particular order, and the final result should not depend on it. In practice, the introduction of this parameter is not required, as the order of any functional can be determined directly by the number of terms in $u(t)$ that appear in the functional formula.

The result of step 4 above is a series of linear differential (difference, in the discrete-time case) equations of the form (Feijoo et al., 2004):

$$A\,y_n(t) = F_n\left(\phi_y(t), \phi_u(t)\right) \qquad\qquad 1 \leq n \leq p \qquad\qquad (2.43)$$

where A is a linear differential operator and F_n represents an algebraic function, both depending on the characteristics of F in (2.40). These equations are called Associated Linear Equations (ALEs) (Feijoo et al., 2004, 2005, 2006) and play a very important role in Volterra series based system analysis. They possess two important features that imply in important properties about their solutions:

- The right-hand side of the n-th order ALE depends only on the input and solutions of order less than n, *i.e.* they are recursive

2. FREQUENCY DOMAIN APPROACH TO NONLINEAR SYSTEMS

- The n-th order ALE is linear with respect to $y_n(t)$

The first feature shows that ALEs can be solved in a recursive manner, *i.e.* by starting from the 1-st order equation and progressively using previous solutions as n is increased. This is similar to solving a triangular system of linear algebraic equations. Moreover, due to linear characteristics of the ALEs, the solutions can be analytically found using classical linear methods or in numerical format, via linear filtering techniques.

In order to find the n-th order time-domain kernels, the n-th order ALE need to be solved in terms of convolutions with the input $u(t)$, from which the kernels are determined via inspection. This last part is highly dependent on the circumstances and cannot be written explicitly, unless a particular form for function $F(\phi_y(t), \phi_u(t))$ in (2.40) is used.

In order to illustrate how to use the variational approach, consider the Duffing equation:

$$\ddot{y}(t) + a\,\dot{y}(t) + b\,y(t) + c\,y(t)^3 = u(t) \tag{2.44}$$

Introducing the artificial gain and using $p = 3$ yields:

$$\sum_{n=1}^{3} \Gamma^n \ddot{y}_n(t) + a \sum_{n=1}^{3} \Gamma^n \dot{y}_n(t) + b \sum_{n=1}^{3} \Gamma^n y_n(t) + c \left(\sum_{n=1}^{3} \Gamma^n y_n(t) \right)^3 = u(t) \tag{2.45}$$

The cubic term can be easily expanded, yielding terms of several different orders between 3 to 9 with respect to Γ. Most of these terms are discarded, however, as the the analysis is only carried out up to order 3. After identifying the coefficients of Γ, Γ^2 and Γ^3, the following ALEs are found:

$$\ddot{y}_1(t) + a\,\dot{y}_1(t) + b\,y_1(t) = u(t) \tag{2.46}$$

$$\ddot{y}_2(t) + a\,\dot{y}_2(t) + b\,y_2(t) = 0 \tag{2.47}$$

$$\ddot{y}_3(t) + a\,\dot{y}_3(t) + b\,y_3(t) = -c\,y_1(t)^3 \tag{2.48}$$

The solution to (2.46) can be described as:

$$y_1(t) = \int_{-\infty}^{+\infty} h_1(t-\tau)u(\tau)d\tau \qquad (2.49)$$

where

$$h_1(\tau) = \mathcal{L}^{-1}\left\{\frac{1}{s^2 + a\,s + b}\right\} \qquad (2.50)$$

and $\mathcal{L}^{-1}$ denotes the inverse Laplace transform. Equation (2.49) is in the standard functional form, therefore, (2.50) denotes the first order kernel.

Equation (2.47) implies that the second component will be always zero, since the right-hand side terms vanishes. Because this is true for any input, the only possible conclusion is:

$$h_2(\tau_1, \tau_2) = 0 \qquad (2.51)$$

The solution to (2.48) can be described as:

$$y_3(t) = -c \int_{-\infty}^{+\infty} h_1(\tau)y_1(t-\tau)^3 d\tau \qquad (2.52)$$

which must be written in the standard form (2.3) so that the order 3 kernel can be identified. This can be done through the following transformations:

$$y_3(t) = -c \int_{-\infty}^{+\infty} h_1(\tau)\left(\int_{-\infty}^{+\infty} h_1(\sigma)u(t-\tau-\sigma)d\sigma\right)^3 d\tau \qquad (2.53)$$

$$= -c \int_{-\infty}^{+\infty} h_1(\tau) \int_{-\infty}^{+\infty} \int_{-\infty}^{+\infty} \int_{-\infty}^{+\infty} \prod_{i=1}^{3} h_1(\sigma_i)u(t-\tau-\sigma_i)d\sigma_i\, d\tau \qquad (2.54)$$

Applying the change of variables $\tau_i = \tau + \sigma_i$, $i = 1, 2, 3$ into (2.54), yields:

$$y_3(t) = -c \int_{-\infty}^{+\infty} h_1(\tau) \int_{-\infty}^{+\infty} \int_{-\infty}^{+\infty} \int_{-\infty}^{+\infty} \prod_{i=1}^{3} h_1(\tau_i-\tau)u(t-\tau_i)d\tau_i\, d\tau \qquad (2.55)$$

Rearranging the order of the integrations yields:

$$y_3(t) = \int_{-\infty}^{+\infty} \int_{-\infty}^{+\infty} \int_{-\infty}^{+\infty} \left(-c \int_{-\infty}^{+\infty} h_1(\tau)\prod_{i=1}^{3} h_1(\tau_i-\tau)d\tau\right)\prod_{i=1}^{3} u(t-\tau_i)d\tau_i \qquad (2.56)$$

Therefore, by comparing with the standard 3-rd order form, we can obtain the third order kernel in an implicit form:

$$h_3(\tau_1, \tau_2, \tau_3) = -c \int_{-\infty}^{+\infty} h_1(\tau) \prod_{i=1}^{3} h_1(\tau_i - \tau) d\tau \qquad (2.57)$$

Notice that the result is only partially complete, since obtaining the kernels in explicit form requires expressing h_1 in terms of elementary functions. In addition, obtaining the GFRFs, if desired is only a matter of applying the Fourier transform to (2.57).

Obviously the variational approach is a very laborious procedure and is not feasible for practical purposes in this form. One way of simplifying the process is to work out all calculations in the frequency domain, as all operations become algebraic. This can be done using different approaches, for example the probing method (Peyton Jones and Billings, 1989; Peyton Jones, 2007) or the Diophantine equations approach (Bayma and Lang, 2012). Notice, however, that in both situations the GFRFs are obtained in recursive form and extracting them in full explicit form requires additional efforts, although simpler than those in the time-domain.

2.4.2 Orthogonal functionals

The orthogonal functionals representation (Lee and Schetzen, 1965; Schetzen, 1981; Wiener, 1958) was introduced for dealing with two problems associated with the conventional Volterra series: convergence and identification (Schetzen, 1981).

The convergence problem is related to the difficulties of finding a convergent Volterra series representation for a given operator. This is similar to the problem that occurs when approximating a function by conventional polynomials, as the convergence of the series is based on conservative criteria. It is well known that this is partly alleviated by using a basis of orthogonal functions (*e.g.* complex exponentials, orthogonal polynomials, etc.), since series of this form converge by the mean, which is a less conservative requirement. The orthogonal functional series plays a similar role, as the terms of the

series are constructed to be orthogonal to each other, providing more relaxed conditions for the convergence problem.

An orthogonal functional series is described as:

$$y(t) = \sum_{n=0}^{\infty} g_n(t) \tag{2.58}$$

where $g_n(t)$ are functionals with respect to the input $u(t)$ that possess zero mean and are orthogonal to each other with respect to the conventional inner product, $i.e.$

$$\langle g_m(t), g_n(t) \rangle = \int_{-\infty}^{+\infty} g_m(t) g_n(t) dt = 0 \qquad m \neq n \tag{2.59}$$

and when $u(t)$ is a Gaussian white process. The functionals $g_n(t)$ are usually called the n-th order Wiener functionals or G-functionals. The kernels associated with each functional are called the n-th order Wiener kernel.

The G-functionals possess a structure that is similar to the ordinary Volterra functionals, except that they are not homogeneous, $i.e.$ the n-th order G-functional is formed from Volterra functionals of order n and smaller. The basic principle for constructing the G-functionals is the orthogonality principle (2.59). The derivations are relatively laborious (Schetzen, 1980) and therefore will be omitted. The G-functionals of order up to 4 are described as:

$$g_0(t) = k_0 \tag{2.60}$$

$$g_1(t) = K_1[u(t)] \tag{2.61}$$

$$g_2(t) = K_2[u(t)] + k_{20} \tag{2.62}$$

$$g_3(t) = K_3[u(t)] + K_{31}[u(t)] \tag{2.63}$$

$$g_4(t) = K_4[u(t)] + K_{42}[u(t)] + k_{40} \tag{2.64}$$

where

$$K_n[u(t)] = \int_{-\infty}^{+\infty} \ldots \int_{-\infty}^{+\infty} k_n(\tau_1, \ldots, \tau_n) \prod_{i=1}^{n} u(t - \tau_i) d\tau_i \tag{2.65}$$

$$K_{np}[u(t)] = \int_{-\infty}^{+\infty} \ldots \int_{-\infty}^{+\infty} k_{np}(\tau_1, \ldots, \tau_p) \prod_{i=1}^{p} u(t - \tau_i) d\tau_i \tag{2.66}$$

and $k_n(\tau_1, \ldots, \tau_n)$ denotes the n-th order principal kernel. The secondary kernels k_{np} are directly derived from the corresponding principal as:

$$k_{20} = -A \int_{-\infty}^{+\infty} k_2(\tau_1, \tau_1) d\tau_1 \tag{2.67}$$

$$k_{31}(\tau_1) = -3A \int_{-\infty}^{+\infty} k_3(\tau_1, \tau_2, \tau_2) d\tau_2 \tag{2.68}$$

$$k_{40} = 3A^2 \int_{-\infty}^{+\infty} \int_{-\infty}^{+\infty} k_4(\tau_1, \tau_1, \tau_2, \tau_2) d\tau_1 d\tau_2 \tag{2.69}$$

$$k_{42}(\tau_1, \tau_2) = -6A \int_{-\infty}^{+\infty} k_4(\tau_1, \tau_2, \tau_3, \tau_3) d\tau_3 \tag{2.70}$$

where A is the power of the Gaussian white input $u(t)$.

The orthogonality between G-functionals of different order is also useful for dealing with the identification problem, *i.e.* the process of finding the Wiener kernels k_n from input-output data. Orthogonal functionals make this process very systematic, similarly to its algebraic counterpart, where series coefficients can be found in a decoupled manner, using correlations between function observations and the basis functions of the orthogonal expansion. The procedure consists of applying a Gaussian white signal and correlate the response with the G-functionals in increasing order for obtaining the kernels (Lee and Schetzen, 1965; Schetzen, 1981). More specifically, for determining the n-th order kernel, the following steps can be applied:

1. Define the point $(\tau_1, \ldots, \tau_n)$ over which the kernel will be computed

2. Compute:

$$d_n(t) = \prod_{i=1}^{n} u(t - \tau_i) \tag{2.71}$$

3. Use any previously determined kernels for computing:

$$\bar{y}(t) = y(t) - \sum_{m=0}^{n-1} g_m(t) \tag{2.72}$$

4. Compute the n-order Wiener kernel as

$$k_n(\tau_1, \ldots, \tau_n) = \frac{1}{n!\, A^n} \, \langle\, \bar{y}(t), d_n(t)\, \rangle \tag{2.73}$$

A great advantage of this system identification procedure is that its correlation based foundation provides some filtering features that can be useful for dealing with noisy measurements. However, the resulting kernel representation is still multidimensional, therefore, it suffers from the same fundamental problems previously discussed in the context of Volterra kernels and their analysis. In addition, the nonparametric form of the results is an aggravating matter, as the storage of the multidimensional points becomes a serious issue, especially because a large number of points is required for a reasonable kernel representation. This can be partly alleviated by using multidimensional interpolation schemes in which the kernels are represented by orthogonal decompositions, such as gate functions (Schetzen, 1980) and Laguerre polynomials (Campello et al., 2004; Schetzen, 1981), leading to a nonlinear system representation known as the Wiener model, in which the system is decomposed as connections of linear dynamical networks in series with no-memory polynomial nonlinearities.

The decomposition of kernels into orthogonal series is efficient because the series coefficients rapidly decay to zero, producing a more condensed representation. However, the multidimensional problem still exists, as the resulting orthogonal coefficients are also multidimensional. In addition, this approach introduces a new problem, which is the tuning of additional parameters, such as the poles of Laguerre functions, which can only be achieved, in an optimal way, via special algorithms (Campello et al., 2004).

2.4.3 Harmonic probing

Harmonic probing refers to a group of methods in which the GFRFs are obtained from a pre-established model. The main objective is to obtain a set of algebraic expressions that allow computing one or more GFRFs in terms of their lower order counterparts,

i.e. G_k as a function of G_{k-1}, G_{k-2}, ..., G_1. This yields a moderately compact representation of the GFRFs while still allowing to compute them in explicit form, if required.

One of the first versions of the probing algorithm for practical polynomial models was proposed in (Peyton Jones and Billings, 1989, 1988), which was later improved in (Peyton Jones, 2007). The GFRFs are extracted from a Nonlinear AutoRegressive with eXogenous inputs (NARX) model, proposed in (Leontaritis and Billings, 1985) as:

$$y(t) = \sum_{m=1}^{M} \sum_{p=0}^{m} \sum_{k_1, k_{p+q}=1}^{K} c_{p,q}(k_1, \ldots, k_{p+q}) \prod_{i=1}^{p} y(t-k_i) \prod_{i=p+1}^{p+q} u(t-k_i) \tag{2.74}$$

The method can be derived by considering a multi-tone sinusoidal input

$$u(t) = \sum_{r=1}^{R} e^{j\omega_k t} \tag{2.75}$$

for which:

$$y(t) = \sum_{n=1}^{N} \sum_{r_1, r_n=1}^{R} H_n(e^{j\omega_1}, \ldots, e^{j\omega_n}) e^{j(\omega_1 + \ldots + \omega_n)t} \tag{2.76}$$

Formulation (2.76) can be substituted into model (2.74), and the GFRFs can be found by matching terms of corresponding order. The n-th order GFRF can be found as (Peyton Jones, 2007):

$$H_n(e^{j\omega_1}, \ldots, e^{j\omega_n}) = \frac{H_{n_u}(\ldots) + H_{n_{uy}}(\ldots) + H_{n_y}(\ldots)}{1 - \sum_{k_1=1}^{K} c_{1,0}(k_1) \exp(-j\omega_1 k_1 - \ldots - j\omega_n k_1)} \tag{2.77}$$

where:

$$H_{n_u}(e^{j\omega_1}, \ldots, e^{j\omega_n}) = \sum_{k_1, k_n=1}^{K} c_{0,n}(k_1, \ldots, k_n) \exp(-j\omega_1 k_1 - \ldots - j\omega_n k_n) \tag{2.78}$$

$$H_{n_{uy}}(e^{j\omega_1}, \ldots, e^{j\omega_n}) = \sum_{q=1}^{n-1} \sum_{p=1}^{n-q} \sum_{k_1, k_{p+q}=1}^{K} c_{p,q}(k_1, \ldots, k_{p+q}) H_{n-q,p}(e^{j\omega_1}, \ldots, e^{j\omega_{n-q}})$$

$$\times \exp(-j\omega_{n-q+1} k_{n-q+1} - \ldots - j\omega_{p+q} k_{p+q}) \tag{2.79}$$

$$H_{n_y}(e^{j\omega_1}, \ldots, e^{j\omega_n}) = \sum_{p=2}^{n} \sum_{k_1, k_n=1}^{K} c_{p,0}(k_1, \ldots, k_n) H_{n,p}(e^{j\omega_1}, \ldots, e^{j\omega_n}) \tag{2.80}$$

$$H_{n,p}(e^{j\omega_1}, \ldots, e^{j\omega_n}) = \sum_\Omega H_{\gamma_1}(\boldsymbol{w}_{\gamma_1}) \ldots H_{\gamma_p}(\boldsymbol{w}_{\gamma_p}) f_y(\boldsymbol{w}_{\gamma_1}, \ldots, \boldsymbol{w}_{\gamma_p}) \tag{2.81}$$

$$f_y(\boldsymbol{w}_{\gamma_1}, \ldots, \boldsymbol{w}_{\gamma_p}) = \sum_\sigma \prod_{i=1}^p \exp\left(-jk_i \sum \boldsymbol{w}_{\gamma_i}\right) \tag{2.82}$$

and Ω represents all combinations $(\gamma_1, \ldots, \gamma_p)$ taken from $(1, \ldots, N)$ with repetition and $\sum \gamma_i = n$; and σ represents all permutations of $(\gamma_1, \ldots, \gamma_p)$. An alternative formulation, although yielding the same results, can be found in (Jing et al., 2008).

The main disadvantage of this method is its complexity: the computation of $H_{n,p}$ is recursive and lacks an intuitive interpretation; in addition, the implementation requires listing combinations and permutations of variables, which demands large computational power for large n or when the number of model terms is considerable. This happens because of how the NARX model was formulated, a problem that can be avoided by adopting a slightly different formulation, as demonstrated in (Bayma and Lang, 2012).

2.5   Notes about nonlinear systems identification

This section is dedicated to briefly review some nonlinear systems identification basic concepts. Although the main focus of this thesis is not about this subject, it is important to recognise that it does play a very important role to this research, as all analysis methods under investigation assume that a nonlinear polynomial model is available.

The general purpose of system identification is to build mathematical relationships between measurable quantities, without necessarily using any physical insight about how they are related. For this reason, these methods are usually called *black box* modelling.

This work is mainly concerned with modelling of single input single output, discrete-time dynamical systems, *i.e.* where one input and one output are related by a temporal relationship. This can be generally described as:

$$y(t) = F\left(\boldsymbol{\phi}_y(t), \boldsymbol{\phi}_u(t)\right) \tag{2.83}$$

where $t \in \mathbb{Z}$ denotes the t-th sample, $u(t)$ and $y(t)$ respectively represent the input and output sequences, F is an arbitrary (usually nonlinear) function and:

$$\phi_y(t) = \begin{bmatrix} y(t-1) & \ldots & y(t-L) \end{bmatrix} \tag{2.84}$$

$$\phi_u(t) = \begin{bmatrix} u(t-1) & \ldots & u(t-L) \end{bmatrix} \tag{2.85}$$

$$\tag{2.86}$$

where L is the model maximum delay. Due to its recursive nature, *i.e.* the t-th output sample depends on past samples, this model is usually known as *Nonlinear AutoRegressive with eXogenous inputs* - NARX. In some situations, for the purpose of improving the model prediction capabilities, it is common to include a noise signal $e(t)$, so that *Moving Average* - MA terms appear and the model is simply renamed as NARMAX.

For the purpose of representing F, many different mathematical structures can be used, *e.g.* neural networks (Haykin, 1999), wavelets (Billings and Wei, 2005; Coca and Billings, 1999) and polynomials (Leontaritis and Billings, 1985). The polynomial formulation is particularly useful for carrying out Volterra series analysis, while estimation methods for this specific approach have been widely studied Chen and Billings (1989); Korenberg et al. (1988); Li et al. (2013).

In this work, the general polynomial formulation will be described as:

$$y(t) = \sum_{m=1}^{M} \theta_m \psi_m(t) + e(t) \tag{2.87}$$

where $e(t)$ denotes the modelling error and:

$$\psi_m(t) = \prod_{l=1}^{L} y(t-l)^{p(m,l)} u(t-l)^{q(m,l)} \tag{2.88}$$

This formulation is different from the original and usual notation adopted in other works, for example (Chen and Billings, 1989; Billings, 2013). Though the model is still described as a linear function of the parameters θ_m to be estimated, the main difference with respect to the traditional polynomial NARX representation is that repeated terms,

such as $y(t-1)^2$, are explicitly described in terms of the integer parameters $p(m, l)$ and $q(m, l)$. This has no particular impact for modelling purposes, but offers significant advantages to Volterra series analysis of the model, as demonstrated in Chapters 3 and 4.

Equation (2.87) can also be written in a matrix format as:

$$y(t) = \boldsymbol{\psi}^T(t)\,\boldsymbol{\theta} + e(t) \tag{2.89}$$

where

$$\boldsymbol{\psi}^T(t) = \left[\begin{array}{ccc} \psi_1(t) & \dots & \psi_M(t) \end{array}\right] \tag{2.90}$$

$$\boldsymbol{\theta}^T = \left[\begin{array}{ccc} \theta_1 & \dots & \theta_M \end{array}\right] \tag{2.91}$$

where entries of $\boldsymbol{\psi}(t)$ contain all terms described in (). The order in which these are organised in vector $\boldsymbol{\psi}(t)$ is usually arbitrary, although it can exhibit some influences over the estimation procedure (Korenberg, 1987).

Assuming N samples have been gathered, the observed data can be written as follows:

$$\boldsymbol{y} = \boldsymbol{\Psi}\,\boldsymbol{\theta} + \boldsymbol{e} \tag{2.92}$$

where

$$\boldsymbol{y}^T = \left[\begin{array}{ccc} y(1) & \dots & y(N) \end{array}\right] \tag{2.93}$$

$$\boldsymbol{e}^T = \left[\begin{array}{ccc} e(1) & \dots & e(N) \end{array}\right] \tag{2.94}$$

$$\boldsymbol{\Psi} = \left[\begin{array}{ccc} \psi_1(1) & \dots & \psi_M(1) \\ \vdots & \vdots & \vdots \\ \psi_1(N) & \dots & \psi_M(N) \end{array}\right] \tag{2.95}$$

The basic identification problem consists of estimating a parameter vector $\hat{\boldsymbol{\theta}}$ so that the sum of squared errors $J = \boldsymbol{e}^T\boldsymbol{e}$ is minimised. This classical least squares solution is described as (Billings, 2013)

$$\hat{\boldsymbol{\theta}} = (\boldsymbol{\Psi}^T\boldsymbol{\Psi})^{-1}\boldsymbol{\Psi}^T\boldsymbol{y} \tag{2.96}$$

However, this solution is usually not suitable for identifying nonlinear models such as (2.87)-(2.88), because the number of candidate terms (*i.e.* columns of $\mathbf{\Psi}$) is usually large, which brings ill conditioning problems. In this context, it has been demonstrated that it is usually of great advantage to work with (2.92) in an orthogonalised form (Korenberg et al., 1988; Chen et al., 1988), *i.e.*

$$\boldsymbol{y} = \boldsymbol{W}\,\boldsymbol{g} + \boldsymbol{e} \tag{2.97}$$

where

$$\boldsymbol{g}^T = \left[\begin{array}{ccc} g_1 & \ldots & g_M \end{array} \right] \tag{2.98}$$

$$\boldsymbol{W} = \left[\begin{array}{ccc} w_1(1) & \ldots & w_M(1) \\ \vdots & \vdots & \vdots \\ w_1(N) & \ldots & w_M(N) \end{array} \right] \tag{2.99}$$

This formulation can be obtained in different ways, for example, via singular value decomposition (Weisstein, 2014e), the Gram-Schimdt algorithm (Weisstein, 2014d) or a more specialised approach (Korenberg, 1987). Orthogonality implies that:

$$\boldsymbol{W}^T\boldsymbol{W} = \boldsymbol{D} = \left[\begin{array}{ccc} d_1 & & \\ & \ddots & \\ & & d_M \end{array} \right] \tag{2.100}$$

so that parameters $\boldsymbol{g}$ can be easily estimated as $\hat{\boldsymbol{g}} = \boldsymbol{D}^{-1}\boldsymbol{W}^T\boldsymbol{y}$. Usually, the original parameters $\boldsymbol{\theta}$ can be recovered from $\boldsymbol{g}$ by a simple linear transformation. However, the advantages of the orthogonal formulation go further beyond, as it allows the development of valuable mechanisms that provide a way of quantifying the relevance of each candidate term of the model, which is a useful for optimising the model structure.

In this work, two structure selection criteria were used. The *Error Reduction Ratio* formulation - ERR, which was introduced in (Korenberg, 1987; Chen et al., 1988), where it was noticed that the following relationship can be derived between the orthogonal model and the estimation error:

$$\frac{1}{N}\sum_{t=1}^{N} y^2(t) = \frac{1}{N}\sum_{t=1}^{N}\sum_{m=1}^{M} g_m^2\, w_m^2(t) + \frac{1}{N}\sum_{t=1}^{N} e^2(t) \tag{2.101}$$

In (2.101), all terms are positive, so that the first term on the right-hand side reduces the term on the left-hand side. The left-hand side term can be interpreted as the maximum value of the squared error, since it is the value achieved by it when no model terms are used. Based on this observation, the ERR for the i-th candidate term can be defined as:

$$\text{ERR}_{(i)} = \frac{\sum\limits_{t=1}^{N} g_i^2\, w_i^2(t)}{\sum\limits_{t=1}^{N} y^2(t) - \frac{1}{N}\left(\sum\limits_{t=1}^{N} y(t)\right)^2} \tag{2.102}$$

Equation (2.102) describes the relative reduction in the modelling error when the i-th term is included, providing a metric for adding or removing new terms into the model, and constitutes an important tool for constructing polynomial NARX models.

Another metric that can be used for selecting terms is the *Predicted Residuals Sum of Squares* statistic - PRESS (Wang and Cluett, 1996). A predicted residual is the modelling error obtained by trying to predict an output sample that was not used for estimating the model structure and parameters. This is usually written as:

$$e_{-t}(t) = y(t) - \hat{y}_{-t}(t) \tag{2.103}$$

where the subscript "$-t$" means that the t-th sample was not considered for model construction and parameter estimation. This is considerably different from the ordinary residuals computed as:

$$e(t) = y(t) - \hat{y}(t) \tag{2.104}$$

where $\hat{y}(t)$ is the prediction of the t-th sample computed from a model that was estimated from a data set that included this same sample.

The PRESS statistic is obtained by computing the predicted residuals for many samples, typically one at a time ("leave one out" strategy) and adding the squares:

$$\text{PRESS} = \sum_{t=t_1}^{t_N} e_{-t}^2(t) \tag{2.105}$$

2. FREQUENCY DOMAIN APPROACH TO NONLINEAR SYSTEMS

PRESS can also be used as a metric for selecting model terms. It works similar to ERR, where a term is added or excluded, depending if the associated PRESS is smaller than a pre-specified maximum limit, although it is usually difficult to compute it. However, it was demonstrated in (Myers, 1990) that for a linear in the parameters model, the predicted residuals can be obtained from the ordinary residuals in a orthogonal forward regression scheme. The strategy is based on the orthogonal formulation (2.97) and is called forward regression because the PRESS statistic is computed as the model progressively increases in size. In this context, the efficient calculation of the associated PRESS when the model contains k terms is described as:

$$\text{PRESS}_{(k)} = \sum_{t=1}^{N} e_{k,-t}^2(t) \tag{2.106}$$

$$e_{k,-t}^2(t) = \frac{e_k(t)}{\beta_k(t)} \tag{2.107}$$

where the ordinary residual $e_k(t)$ is described as:

$$e_k(t) = y(t) - \sum_{m=1}^{k} g_m w_m(t) \tag{2.108}$$

and $\beta_k(t)$ is computed recursively as:

$$\beta_k(t) = \beta_{k-1}(t) - \frac{w_k(t)}{\sum_{t=1}^{N} w_k^2(t)} \tag{2.109}$$

with $\beta_0(t) = 1$.

This procedure greatly simplifies the adoption of PRESS as a model selection criterion, allowing identification of nonlinear representations that possess, in principle, better prediction capabilities than those constructed from ERR, since ERR is based on ordinary residuals.

Throughout this work, both identification methods were employed for obtaining polynomial NARX models. It is often difficult to predict which method can provide the "best" model for a given data set, since the mechanisms yield different results depending on the candidate terms used and the noise levels present in the measurements.

Experience has shown that it is more effective to simply apply both methodologies and analyse the resulting models performance using simulation, while also balancing model complexity for further analysis purposes.

2.6   Conclusions

The Volterra series is a consolidated tool for nonlinear system analysis, as demonstrated by the fundamental concepts introduced in this chapter and various published works. The homogeneous polynomial functionals generalise the convolution integral and allow the functional components to be studied in the frequency domain, providing a description about how phenomena such as harmonics and intermodulations arise. Both continuous-time and discrete-time formulations are available, which allow the development of important applications in various fields.

The usual route for conducting frequency analysis of nonlinear systems is based on the so called Generalised Frequency Response Functions. However, despite notable work based on GFRFs has been developed, many issues need to be resolved. The first problem is how the GFRFs can be obtained from a given problem scenario. It has been shown that this is can be done by directly using input-output data or by fitting a model and a posterior extraction of the GFRFs from the model equations. Various methods exist for accomplishing this task, and the main ones have been reviewed in this chapter. This list, however, is by no means exhaustive, and several others can be found in literature, for example: Carleman Linearization method; the variational approach for state space models; the growing exponential approach. (Rugh, 1981), among others. The reason why these methods were not explored in this chapter is because some of them were not designed for dealing with discrete-time input-output representations, while others are less efficient than the ones that were presented.

The second, and perhaps the most problematic issue with the GFRF based nonlinear system analysis is how to extract their multidimensional features and how to use them

for understanding system properties. However, the large computational efforts that are required for dealing with these problems suggest that alternative FRF formulations are more attractive.

The concept of NOFRFs was proposed in this context and can be considered as a potential tool towards practical nonlinear systems analysis. The properties of NOFRFs provide a convenient background for studying nonlinear systems in the frequency domain, which have been attested by several application studies recently published. However, issues regarding the computation of NOFRFs from a NARX model still need to be solved, as the currently available algorithm can present numerical conditioning problems and therefore, cannot be applied to fundamentally resolve the problems.

3

A new algorithm for determination of GFRFs of nonlinear systems

3.1 Introduction

One fundamental step in classical Volterra series based system analysis is the extraction of the time-domain kernels or, equivalently, the GFRFs. Although there are difficulties regarding the study of these multidimensional functions, GFRF based analysis is still very useful and commonly used in several practical problems involving analysis and design of nonlinear systems.

This chapter presents a new result that permits the GFRFs extraction from nonlinear systems models, which were originally introduced in (Bayma and Lang, 2012). The main result is an efficient algorithm that allows obtaining the recursive equations for generating the GFRFs. Although the basic idea is similar to the well known probing method (Peyton Jones, 2007; Peyton Jones and Billings, 1989), the calculations involved in the new algorithm are carried out in a different way that avoids symbolic

processing and many other unnecessary computations. The main advantage of the new method is that it can be used to determine the GFRFs up to any arbitrary order from a relatively general nonlinear model in a very efficient approach. In addition, the new method also provides an important basis for the derivation of a more effective approach to the computation of NOFRFs of nonlinear systems in the next chapter.

3.2 Notation and basic considerations

3.2.1 Notation and definitions

The new algorithm has been designed to deal with discrete-time (DT) models and functionals. The frequency domain transform used for representing the GFRFs in this context is the multidimensional $\mathcal{Z}$ transform, which is defined, for a n-dimensional function $h_n(t_1, \ldots, t_n)$, as:

$$
\begin{aligned}
H_n(z_1, \ldots, z_n) &= \mathcal{Z}\{h_n(t_1, \ldots, t_n)\} \\
&= \sum_{t_1=0}^{+\infty} \cdots \sum_{t_n=0}^{+\infty} h_n(t_1, \ldots, t_n) \prod_{i=1}^{n} z_i^{-t_i}
\end{aligned}
\tag{3.1}
$$

For simplicity, a compact notation will be used throughout the chapter for denoting the arguments of multidimensional functions. To this end, let $h_n(t_1, \ldots, t_n)$ be the n-th order kernel of a DT functional $y_n(t)$, *i.e.*

$$
y_n(t) = \sum_{\tau_1=-\infty}^{+\infty} \cdots \sum_{\tau_n=-\infty}^{+\infty} h_n(\tau_1, \ldots, \tau_n) \prod_{i=1}^{n} u(t - \tau_i)
\tag{3.2}
$$

Then, the kernel and its corresponding $\mathcal{Z}$ transform will be denoted as:

$$
h_n(\boldsymbol{t}_{1,n}) = h_n(t_1, \ldots, t_n)
\tag{3.3}
$$

$$
H_n(\boldsymbol{z}_{1,n}) = H_n(z_1, \ldots, z_n)
\tag{3.4}
$$

Moreover, in many situations below, expressions involving a multidimensional term delayed by l samples in all variables will be encountered, *e.g.* $h_n(t_1 - l, \ldots, t_n - l)$. A

compact notation will also be used in these cases, which is described as:

$$h_n(\boldsymbol{t}_{1,n} - l) = h_n\left(t_1 - l, \ldots, t_n - l\right) \tag{3.5}$$

In addition, the $\mathcal{Z}$ transform of (3.5) can be found as:

$$\mathcal{Z}\{h_n(\boldsymbol{t}_{1,n} - l)\} = z_1^{-l} \ldots z_n^{-l} H_n\left(\boldsymbol{z}_{1,n}\right) \tag{3.6}$$

3.2.2 Considerations about functional orders

The determination of the order of functionals formed from algebraic expressions is also of great importance, because it allows avoiding computations involving terms of higher order. This can be done using some basic principles for finding the order of functional terms. To this end, let $\mathcal{D}$ be an order extraction operator, so that, for a n-th order functional $y_n(t)$, $\mathcal{D}[y_n(t)] = n$.

$\mathcal{D}$-**Property 1.** Shifting a functional $y_n(t)$ by any delay l does not alter the functional order, *i.e.*

$$\mathcal{D}[y_n(t - l)] = n \tag{3.7}$$

$\mathcal{D}$-**Property 2.** Let $y_k(t)$ and $y_m(t)$ be functionals of order k and m, respectively. Then:

$$\mathcal{D}[y_k(t)y_m(t)] = k + m \tag{3.8}$$

$\mathcal{D}$-**Property 3.** Let $p \geq 0$ and $l \geq 0$ be integers and $y_n(t)$ be a functional of order n. Then:

$$\mathcal{D}\left[y_n(t)^p\right] = n\,p \tag{3.9}$$

$$\mathcal{D}\left[y_n(t - l)^p\right] = n\,p \tag{3.10}$$

This follows directly from properties 1 and 2.

$\mathcal{D}$-**Property 4.** Let:

$$\alpha_1(t) = \prod_{k=1}^{n} y_k(t-l)^{p(k)} \tag{3.11}$$

$$\alpha_2(t) = \prod_{l=1}^{L} \prod_{k=1}^{n} y_k(t-l)^{p(k,l)} \tag{3.12}$$

Then:

$$\mathcal{D}\left[\alpha_1(t)\right] = \sum_{k=1}^{n} k\, p(k) \tag{3.13}$$

$$\mathcal{D}\left[\alpha_2(t)\right] = \sum_{l=1}^{L} \sum_{k=1}^{n} k\, p(k,l) \tag{3.14}$$

This follows directly from $\mathcal{D}$-property 3. Determining the order of functionals $\alpha_1(t)$ and $\alpha_2(t)$ is important because they arise in the analysis of model (3.22) in Section 3.3, where the output is replaced by the Volterra series formulation.

3.2.3 Kernel extraction operator

In order to make the GFRF extraction procedure more systematic, we shall also consider a kernel extraction operator $\mathcal{K}$. To this end, consider an arbitrary n-th order functional $y_n(t)$ described as:

$$y_n(t) = \sum_{t_1=-\infty}^{+\infty} \cdots \sum_{t_n=-\infty}^{+\infty} h_n(\boldsymbol{t}_{1,n}) \prod_{i=1}^{n} u(t-t_i) \tag{3.15}$$

The $\mathcal{K}$-operator is defined as the operator that returns the kernel of a given functional, *i.e.*

$$\mathcal{K} y_n(t) = h_n(\boldsymbol{t}_{1,n}) \tag{3.16}$$

The $\mathcal{K}$-operator has some interesting properties that are useful for the kernel/GFRF extraction process. The derivations are relatively simple and can be carried out directly from inspection of the functional forms (3.15).

$\mathcal{K}$-**Property 1.** Let $y_n(t)$ and $z_n(t)$ be functionals of the same order with kernels respectively described as $h_n(\boldsymbol{t}_{1,n})$ and $g_n(\boldsymbol{t}_{1,n})$. Then, for any constants c_1 and c_2:

$$\mathcal{K}\left(c_1\, y_n(t) + c_2\, z_n(t)\right) = c_1\, h_n(\boldsymbol{t}_{1,n}) + c_2\, g_n(\boldsymbol{t}_{1,n}) \tag{3.17}$$

$\mathcal{K}$**-Property 2.** Let $y_n(t)$ and $z_m(t)$ be functionals of order n and m, respectively, with kernels respectively described as $h_n(\boldsymbol{t}_{1,n})$ and $g_m(\boldsymbol{t}_{1,m})$, then

$$\mathcal{K}\left(y_n(t)\,z_m(t)\right) = h_n(\boldsymbol{t}_{1,n})g_m(\boldsymbol{t}_{n+1,n+m}) \tag{3.18}$$

This is proven from the functional definition and rearrangement of variables. Notice that the order with which the arguments $\boldsymbol{t}_{1,n+m}$ are organized is arbitrary. Therefore, it is also acceptable to write (3.18) as:

$$\mathcal{K}\left(y_n(t)\,z_m(t)\right) = h_n(\boldsymbol{t}_{m+1,n+m})g_m(\boldsymbol{t}_{1,m}) \tag{3.19}$$

$\mathcal{K}$**-Property 3.** Let A be a linear time-shifting operator. Then:

$$\mathcal{K}\left(A\,y_n(t)\right) = A\,h_n(\boldsymbol{t}_{1,n}) = \sum_{l=1}^{L} a_l\,h_n(\boldsymbol{t}_{1,n}-l) \tag{3.20}$$

In addition:

$$\mathcal{Z}\{\mathcal{K}\left(A\,y_n(t)\right)\} = A\left(\prod_{i=1}^{n} z_i\right) H_n(\boldsymbol{z}_{1,n}) \tag{3.21}$$

which follows directly from (3.6).

3.3   A new algorithm for the determination of the GFRFs

The properties of operators $\mathcal{D}$ and $\mathcal{K}$ from Sections 3.2.2 and 3.2.3 form the fundamental basis for obtaining the GFRFs from an arbitrary polynomial NARX model. The polynomial formulation is important to this context, because it is closely related to the polynomial nature of the functional series approach. Moreover, it is also important to mention that the new GFRF extraction algorithm can be applied to different NARX models (*e.g.* neural networks), but, in this case, the model needs to be reduced to the polynomial form via, for example, Taylor series approximation of its nonlinearities, in order to apply the methodology proposed in this chapter.

The principles of the procedure consist of two fundamental steps:

3. A NEW ALGORITHM FOR DETERMINATION OF GFRFS OF NONLINEAR SYSTEMS

1. The Volterra series formulation is substituted into the model equation and the terms of the same order in the right and left-hand side of the model equation are identified using the $\mathcal{D}$-operator and equated for obtaining the Associated Linear Equations;

2. The GFRFs are extracted directly from the ALEs, using the $\mathcal{K}$-operator and $\mathcal{K}$-Properties 1-3

Consider the polynomial NARX model (Leontaritis and Billings, 1985):

$$A\,y(t) = B\,u(t) + \sum_{m=1}^{M} c_m \prod_{l=1}^{L} y(t-l)^{p(m,l)} u(t-l)^{q(m,l)} \tag{3.22}$$

where A and B are linear time-shifting operators so that:

$$A\,y(t) = y(t) + \sum_{l=1}^{L} a_l\,y(t-l) \tag{3.23}$$

$$B\,u(t) = \sum_{l=1}^{L} b_l\,u(t-l) \tag{3.24}$$

and $p(m,l)$ and $q(m,l)$ are nonnegative integers such that

$$\sum_{l=1}^{L} p(m,l) + q(m,l) \geq 2 \tag{3.25}$$

It is worth mentioning that model (3.22) is slightly different from the usual formulation found in (Leontaritis and Billings, 1985) and other references. The main differences are that the linear part of model (3.22) is isolated from the nonlinear terms, and nonlinearities are described in terms of parameters $p(m,l)$ and $q(m,l)$, which makes the notation of terms containing powers more explicit.

3.3.1   Determination of the ALEs

Proceeding with step 1 above requires dealing with several multinomial terms that need to be expanded before identifying terms of a specific order, for example n. One issue, however, is that these expansions generate terms of many different orders, including

some that will not be used in any circumstances, constituting time-consuming and unnecessary calculations. In order to avoid that, a more efficient procedure for finding the ALEs is introduced as Proposition 1.

Proposition 1. *The n-th order ALE of system* (3.22) *is described as*

$$A\,y_n(t) = B\,u(t) \qquad\qquad n = 1 \qquad\qquad (3.26)$$

$$A\,y_n(t) = \sum_{m=1}^{M} c_m\,\psi_m(t) \sum_{S_m} \rho_m\,\phi_m(t) \qquad\qquad n \geq 2 \qquad\qquad (3.27)$$

where

$$\rho_m = \frac{\prod_{l=1}^{L} p(m,l)\,!}{\prod_{l=1}^{L} \prod_{k=1}^{N_m} r(m,l,k)\,!} \qquad\qquad (3.28)$$

$$\psi_m(t) = \prod_{l=1}^{L} u(t-l)^{q(m,l)} \qquad\qquad (3.29)$$

$$\phi_m(t) = \prod_{l=1}^{L} \prod_{k=1}^{N_m} y_k(t-l)^{r(m,l,k)} \qquad\qquad (3.30)$$

$$N_m = n - \sum_{l=1}^{L} q(m,l) + p(m,l) + 1 \qquad\qquad (3.31)$$

and S_m is the set of all nonnegative integer solutions of the linear Diophantine system

$$\sum_{k=1}^{N_m} r(m,l,k) = p(m,l) \qquad\qquad 1 \leq l \leq L \qquad\qquad (3.32)$$

$$\sum_{l=1}^{L} \sum_{k=1}^{N_m} (k-1)\,r(m,l,k) = N_m - 1 \qquad\qquad (3.33)$$

Proof. Rewrite system (3.22) as

$$A\,y(t) = B\,u(t) + \sum_{m=1}^{M} c_m F_m(t) \qquad\qquad (3.34)$$

$$F_m(t) = \prod_{l=1}^{L} y(t-l)^{p(m,l)}\,u(t-l)^{q(m,l)} \qquad\qquad (3.35)$$

The output can be described as a Volterra series:

$$y(t) = \sum_{k=1}^{\infty} y_k(t) \qquad\qquad (3.36)$$

3. A NEW ALGORITHM FOR DETERMINATION OF GFRFS OF NONLINEAR SYSTEMS

Substituting (3.36) into (3.34)-(3.35), yields:

$$\sum_{k=1}^{\infty} A\, y_k(t) = B\, u(t) + \sum_{m=1}^{M} c_m\, F_m(t) \tag{3.37}$$

where

$$F_m(t) = \psi_m(t)\, \alpha_m(t) \tag{3.38}$$

$$\psi_m(t) = \prod_{l=1}^{L} u(t-l)^{q(m,l)} \tag{3.39}$$

$$\alpha_m(t) = \prod_{l=1}^{L} \left(\sum_{k=1}^{\infty} y_k(t) \right)^{p(m,l)} \tag{3.40}$$

In order to determine the n-th order ALE, it is necessary to expand (3.38), identify all n-th order terms and equate them to those of the same order on the left-hand side of (3.37). The n-th order terms on the left-hand side can be found by noticing that the linear operator A does not change the order of any functional component. Therefore, the n-th order component on the left-hand side of (3.37) is $A\, y_n(t)$.

On the other hand, the products in (3.38) produce an expansion in terms of each $y_k(t)$, spanning functionals of many different orders. The order of the first term, $\psi_m(t)$ can be found using the $\mathcal{D}$-operator and its properties, yielding:

$$\mathcal{D}\left[\psi_m(t)\right] = \sum_{l=1}^{L} q(m,l) \tag{3.41}$$

Therefore, the n-th order terms in (3.38) can be found by identifying terms of $\alpha_m(t)$ of order

$$n - \sum_{l=1}^{L} q(m,l) \tag{3.42}$$

For computing these terms, consider the multinomial expansion with respect to $y_k(t)$, $k \geq 1$:

$$\left(\sum_{k=1}^{\infty} y_k(t-l) \right)^{p(m,l)} = \sum \beta(m,l) \prod_{k=1}^{\infty} y_k(t-l)^{r(m,l,k)} \tag{3.43}$$

where

$$\beta(m,l) = \frac{p(m,l)!}{\prod_{k=1}^{\infty} r(m,l,k)!} \tag{3.44}$$

The sum (3.43) is computed over all nonnegative integers $r(m,l,k)$ that satisfy

$$\sum_{k=1}^{\infty} r(m,l,k) = p(m,l)$$

Using (3.43), $\alpha_m(t)$ can be expanded as:

$$\alpha_m(t) = \sum \prod_{l=1}^{L} \beta(m,l) \prod_{k=1}^{\infty} y_k(t)^{r(m,l,k)} \tag{3.45}$$

The order of any term in (3.45) can be described as:

$$\mathcal{D}\left[\prod_{l=1}^{L} \beta(m,l) \prod_{k=1}^{\infty} y_k(t)^{r(m,l,k)}\right] = \sum_{l=1}^{L} \sum_{k=1}^{\infty} k\, r(m,l,k) \tag{3.46}$$

Therefore, for finding terms of the target order (3.42), it is necessary to find all integers $r(m,l,k)$ that satisfy:

$$\sum_{k=1}^{\infty} r(m,l,k) = p(m,l) \qquad\qquad 1 \le l \le L \tag{3.47}$$

$$\sum_{l=1}^{L} \sum_{k=1}^{\infty} k\, r(m,l,k) = n - \sum_{l=1}^{L} q(m,l) \tag{3.48}$$

System (3.47)-(3.48) is known as a system of Diophantine equations (Weisstein, 2014a), because all unknowns are integers. The particular form of these equations allow them to be further simplified by subtracting (3.48) from (3.47), for every possible l, yielding:

$$\sum_{l=1}^{L} \sum_{k=2}^{\infty} (k-1)\, r(m,l,k) = n - \sum_{l=1}^{L} q(m,l) + p(m,l) \tag{3.49}$$

Notice that, since all $r(m,l,k)$ are nonnegative, the main index k must satisfy:

$$k - 1 \le n - \sum_{l=1}^{L} q(m,l) + p(m,l)$$

otherwise, it would not be possible to balance (3.49). Therefore,

$$N_m = n - \sum_{l=1}^{L} q(m,l) + p(m,l) + 1 \tag{3.50}$$

can be used as an upper limit to all summations and products in k and system (3.47)-(3.48) can be rewritten as (3.32)-(3.33).

Let S_m denote the set of all nonnegative solutions of (3.32)-(3.33). By taking only the n-th order terms from the expansion of (3.38), the n-th order ALE can be written as:

$$A\, y_n(t) = \sum_{m=1}^{M} c_m\, \psi_m(t) \sum_{S_m} \prod_{l=1}^{L} \beta(m,l) \prod_{k=1}^{N_m} y_k(t-l)^{r(m,l,k)}$$

Finally, by splitting the product with respect to l and defining

$$\rho_m = \prod_{l=1}^{L} \beta(m,l) = \frac{\prod_{l=1}^{L} p(m,l)!}{\prod_{l=1}^{L} \prod_{k=1}^{N_m} r(m,l,k)!}$$

$$\phi_m(t) = \prod_{l=1}^{L} \prod_{k=1}^{N_m} y_k(t-l)^{r(m,l,k)}$$

we obtain the final result, Equation (3.27). $\qquad\qquad\square$

3.3.2 Derivation of the GFRFs from the ALEs

It is now possible to continue with step 2 of the procedure, where the properties of the $\mathcal{K}$-operator can be applied to the determined ALEs for effectively obtaining the recursive expressions for the GFRFs. This is summarized in Proposition 2

Proposition 2. *The n-th order GFRF of model* (3.22) *is described as:*

$$H_n(z_1) = \frac{B(z_1)}{A(z_1)} \qquad\qquad n = 1 \qquad (3.51)$$

$$H_n(\boldsymbol{z}_{1,n}) = \frac{1}{A\left(\prod_{i=1}^{n} z_i\right)} \sum_{m=1}^{M} c_m\, \mathcal{Z}\{\mathcal{K}\psi_m(t)\} \sum_{S_m} \rho_m\, \mathcal{Z}\{\mathcal{K}\phi_m(t)\} \qquad n \geq 2 \qquad (3.52)$$

where

$$\mathcal{Z}\{\mathcal{K}\psi_m(t)\} = \prod_{l=1}^{L} \prod_{i=w}^{q(m,l)+w-1} z_i^{-l} \tag{3.53}$$

$$\mathcal{Z}\{\mathcal{K}\phi_m(t)\} = \prod_{l=1}^{L} \prod_{k=1}^{N_m} \prod_{i=1}^{r(m,l,k)} H_k(\boldsymbol{z}_{s,s+k-1}) \prod_{\alpha=s}^{s+k-1} z_\alpha^{-l} \tag{3.54}$$

$$w = 1 + \sum_{i_1=1}^{l-1} q(m,i_1) \tag{3.55}$$

$$s = 1 + \sum_{l=1}^{L} q(m,l) + \sum_{i_1=1}^{l} \sum_{i_2=1}^{k-1} i_2\, r(m,i_1,i_2) \tag{3.56}$$

and ρ_m and N_m are respectively described as (3.28) and (3.31), and S_m is the set of all nonnegative integer solutions of the linear Diophantine system described as (3.32)-(3.33).

Proof. The GFRFs can be found directly from the determined ALEs (3.26)-(3.27) by using the properties described in Section 3.2.3 for obtaining the kernels and their corresponding transforms.

The case $n = 1$ is relatively simple, since only linear operators are involved. The result is the system linear transfer function, which is derived from (3.26) as:

$$H_1(z_1) = \frac{B(z_1)}{A(z_1)} \tag{3.57}$$

Applying $\mathcal{K}$ to (3.27) and using $\mathcal{K}$-properties 1 and 2 yields:

$$\mathcal{K}\left(A\, y_n(t)\right) = \sum_{m=1}^{M} c_m\, \mathcal{K}\{\psi_m(t)\} \sum_{S_m} \rho_m \mathcal{K}\phi_m(t) \tag{3.58}$$

Moreover, taking the $\mathcal{Z}$ transform of (3.58) and using property 3, yields:

$$A\left(\prod_{i=1}^{n} z_i\right) H_n(\boldsymbol{z}_{1,n}) = \sum_{m=1}^{M} c_m\, \mathcal{Z}\{\mathcal{K}\psi_m(t)\} \sum_{S_m} \rho_m \mathcal{Z}\{\mathcal{K}\phi_m(t)\} \tag{3.59}$$

In order to proceed, the kernel of $\psi_m(t)$ will be computed first. For an arbitrary input $u(t)$, it is possible to write:

$$u(t) = \sum_{v} \delta(t-v)u(v) \tag{3.60}$$

where $\delta(t)$ is the unit impulse sequence:

$$\delta(t) = \begin{cases} 1 & t = 0 \\ 0 & t \neq 0 \end{cases} \tag{3.61}$$

In this case:

$$\mathcal{K}u(t) = \delta(t_1) \tag{3.62}$$

Since the term $\psi_m(t)$, equation (3.29), can be written as:

$$\psi_m(t) = \prod_{l=1}^{L} u(t-l)^{q(m,l)} \tag{3.63}$$

$$= \prod_{l=1}^{L} \prod_{i=1}^{q(m,l)} u(t-l) \tag{3.64}$$

using $\mathcal{K}$-property 2 and (3.60), yields:

$$\mathcal{K}\psi_m(t) = \prod_{l=1}^{L} \prod_{i=w}^{q(m,l)+w-1} \delta(t_i - l) \tag{3.65}$$

where

$$w = 1 + \sum_{i_1=1}^{l-1} q(m, i_1) \tag{3.66}$$

Notice that w depends on l and i, which is not explicitly shown for simplifying the notation. This auxiliary index was introduced for better organising the arguments t_i. Finally, taking the $\mathcal{Z}$ transform of (3.65) yields:

$$\mathcal{Z}\{\mathcal{K}\psi_m(t)\} = \prod_{l=1}^{L} \prod_{i=w}^{q(m,l)+w-1} z_i^{-l} \tag{3.67}$$

Using the same procedure for $\phi_m(t)$ (3.30) yields:

$$\phi_m(t) = \prod_{l=1}^{L} \prod_{k=1}^{N_m} y_k(t-l)^{r(m,l,k)} \tag{3.68}$$

$$= \prod_{l=1}^{L} \prod_{k=1}^{N_m} \prod_{i=1}^{r(m,l,k)} y_k(t-l) \tag{3.69}$$

$$\mathcal{K}\phi_m(t) = \prod_{l=1}^{L} \prod_{k=1}^{N_m} \prod_{i=1}^{r(m,l,k)} h_k(\boldsymbol{t}_{s,s+k-1} - l) \tag{3.70}$$

where:

$$s = 1 + \sum_{l=1}^{L} q(m,l) + \sum_{i_1=1}^{l} \sum_{i_2=1}^{k-1} i_2\, r(m,i_1,i_2) \tag{3.71}$$

which, again, is an auxiliary index that has been introduced for better organising the arguments. The $\mathcal{Z}$ transform of (3.70) can be obtained as:

$$\mathcal{Z}\{\mathcal{K}\phi_m(t)\} = \prod_{l=1}^{L} \prod_{k=1}^{N_m} \prod_{i=1}^{r(m,l,k)} H_k(\boldsymbol{z}_{s,s+k-1}) \prod_{\alpha=s}^{s+k-1} z_\alpha^{-l} \tag{3.72}$$

Therefore, the n-th order GFRF can be obtained as:

$$H_n(\boldsymbol{z}_{1,n}) = \frac{1}{A\left(\prod_{i=1}^{n} z_i\right)} \sum_{m=1}^{M} c_m\, \mathcal{Z}\{\mathcal{K}\psi_m(t)\} \sum_{S_m} \rho_m\, \mathcal{Z}\{\mathcal{K}\phi_m(t)\} \tag{3.73}$$

where $\mathcal{Z}\{\mathcal{K}\psi_m(t)\}$ and $\mathcal{Z}\{\mathcal{K}\phi_m(t)\}$ are respectively described as (3.67) and (3.72).

$\square$

Expression (3.73) is relatively complex, but provides a straightforward way for recursively computing the n-th order GFRF. Notice that the formulation in terms of the Fourier transform can be easily obtained by letting $z_i = e^{j\omega_i}$, $i \in \{1,\dots,n\}$. In addition, results for continuous-time systems can also be obtained using basically the same procedure, as this formulation does not change the properties of the $\mathcal{D}$-operator.

In comparison to the traditional probing method described in section 2.4.3, the new GFRF extraction algorithm presents some significant advantages. In the probing method, the recursive expression for the n-th order GFRF is obtained via recursive symbolic calculations described by (2.81)-(2.82), which are usually slow and provide the results in a form that often requires additional algebraic simplifications. The new algorithm, however, carries out the same task by converting the solutions of the Diophantine system (3.32)-(3.33) directly into algebraic expressions. This is more efficient because the solutions can be obtained via a numerical procedure (discussed in section 3.3.4) or a simple table look-up scheme, which are usually faster than symbolic processing. In addition, the rules used for converting the solutions into expressions provide

algebraic forms which are already simplified, therefore, avoiding further unnecessary computations.

3.3.3 Implementation algorithm

Propositions 1 and 2 form the basis of a new algorithm for determining the GFRFs from a nonlinear system NARX representation. The new method is presented as Algorithm 1 in the following.

Algorithm 1 Computation of n-th order GFRF

---

1. For each nonlinear term ($1 \leq m \leq M$):

   1.1. Solve the corresponding Diophantine system (3.32)-(3.33)

   1.2. Convert each solution found in step 1.1 into an algebraic term as follows:

       1.2.1. Compute ρ_m using (3.28)

       1.2.2. Compute $\mathcal{Z}\{\mathcal{K}\psi_m(t)\}$ using (3.53), (3.55)

       1.2.3. Compute $\mathcal{Z}\{\mathcal{K}\phi_m(t)\}$ using (3.54), (3.56)

       1.2.4. Compute the product of all terms found in steps 1.2.1 to 1.2.3 and multiply the result by c_m

   1.3. Sum up all terms found in step 1.2

2. Sum up all terms found in step 1

3. Divide the result of step 2 by $A(\prod_{i=1}^{n} z_i)$

Notice that this implementation does not require any symbolical calculations, although the algorithm can be adapted for Computer Algebra Systems for obtaining the result in this format.

3.3.4 Solution of the Diophantine system

The most important step for obtaining the system ALEs is to solve the Diophantine systems associated with each nonlinear term. The core of each Diophantine system is the linear Diophantine equation (3.33), from which variables $r(m, l, 1)$ have been eliminated. Solutions need to be found from this single equation, as it is not possible to eliminate any further variables.

The solution of (3.33) can be found using the Euclidean algorithm (Weisstein, 2014b) for computing the greatest common divisor (GCD), which is an important method for solving linear Diophantine equations in general. However, its implementation is usually found for a reduced number of positive variables, which requires some modifications for the current context. On the other hand, the number of solutions of (3.33) is always finite, which can be explored for a more computationally efficient procedure.

The main idea is based on a more fundamental problem described as:

$$x + y = p \tag{3.74}$$

where $x \geq 0$, $y \geq 0$ and p are integers. Equation (3.74) is commonly known as a partition equation (Weisstein, 2014c). Suppose that solutions of (3.74) are represented as a two column matrix $\boldsymbol{S}$, where the first column represents all solution values for x and the second column represents all solution values for y. Let $\varnothing$ denote an empty matrix, $\boldsymbol{0} = \begin{bmatrix} 0 & 0 \end{bmatrix}$ and:

$$\boldsymbol{Q}_p = \begin{bmatrix} 0 & p \\ 1 & p-1 \\ 2 & p-2 \\ \vdots & \vdots \\ p & 0 \end{bmatrix} \tag{3.75}$$

Then, the solution matrix $\boldsymbol{S}$ of (3.74) can be found as follows:

- If $p < 0$, then $\boldsymbol{S} = \varnothing$

- If $p = 0$, then $\boldsymbol{S} = \boldsymbol{0}$

- If $p > 0$, then $\boldsymbol{S} = \boldsymbol{Q}_p$

Now, consider a more general partition equation:

$$\sum_{k=1}^{n} x_k = p \tag{3.76}$$

where both $x_k \geq 0$ and p are integers. The solution of this problem can be found by breaking (3.76) into smaller basic partitions of form (3.74) and performing an appropriate combination of the solutions. To illustrate this, consider the following partition problem:

$$x_1 + x_2 + x_3 = 2 \tag{3.77}$$

which can be rewritten as:

$$x_1 + y = 2 \tag{3.78}$$

$$x_2 + x_3 = y \tag{3.79}$$

The solutions of (3.78) are found as:

$$\boldsymbol{S}_1 = \boldsymbol{Q}_2 \tag{3.80}$$

Each element of the second column of (3.80) produces a different partition equation derived from (3.79), which are described as:

$$x_2 + x_3 = 2 \tag{3.81}$$

$$x_2 + x_3 = 1 \tag{3.82}$$

$$x_2 + x_3 = 0 \tag{3.83}$$

The solution matrices of (3.81), (3.82) and (3.83) are respectively found as:

$$\boldsymbol{S}_{21} = \boldsymbol{Q}_2 \qquad\qquad (x_1 = 0) \qquad\qquad (3.84)$$

$$\boldsymbol{S}_{22} = \boldsymbol{Q}_1 \qquad\qquad (x_1 = 1) \qquad\qquad (3.85)$$

$$\boldsymbol{S}_{23} = \boldsymbol{0} \qquad\qquad (x_1 = 2) \qquad\qquad (3.86)$$

Combining the solutions yield:

$$\boldsymbol{S} = \begin{bmatrix} 0 & 0 & 2 \\ 0 & 1 & 1 \\ 0 & 2 & 0 \\ 1 & 0 & 1 \\ 1 & 1 & 0 \\ 2 & 0 & 0 \end{bmatrix} \qquad\qquad (3.87)$$

Notice that the general partition problem (3.76) is completely characterised by p and n, therefore, solutions can be pre-computed and stored for future reference, using a table look-up scheme.

In order to apply these results for solving the Diophantine system (3.32)-(3.33), rewrite (3.33) as:

$$\sum_{l=1}^{L} X_l = N_m - 1 \qquad\qquad (3.88)$$

where

$$\sum_{k=2}^{N_m} (k-1)\, r(m,l,k) = X_l \qquad\qquad (3.89)$$

The left-hand side of (3.89) can also be written as partition equations, using the following steps:

$$\sum_{k=2}^{N_m} (k-1)\, r(m,l,k) = r(m,l,2) + 2r(m,l,3) + \ldots + (N_m - 1)r(m,l,N_m) \qquad (3.90)$$

$$= \sum_{k=2}^{N_m} r(m,l,k) + \sum_{k=3}^{N_m} r(m,l,k) + \ldots + r(m,l,N_m) \qquad (3.91)$$

$$= \sum_{i=2}^{N_m} Y_{l,i} \qquad\qquad (3.92)$$

where

$$Y_{l,i} = \sum_{k=i}^{N_m} r(m,l,k) \tag{3.93}$$

Equation (3.93) defines a linear system with respect to $r(m,l,k)$, described as:

$$\begin{bmatrix} 1 & 1 & \dots & 1 \\ 0 & 1 & \dots & 1 \\ \vdots & \vdots & \dots & \vdots \\ 0 & 0 & \dots & 1 \end{bmatrix} \begin{bmatrix} r(m,l,2) \\ r(m,l,3) \\ \vdots \\ r(m,l,N_m) \end{bmatrix} = \begin{bmatrix} Y_{l,2} \\ Y_{l,3} \\ \vdots \\ Y_{l,N_m} \end{bmatrix} \tag{3.94}$$

whose solution is described as:

$$r(m,l,k) = Y_{l,k-1} - Y_{l,k} \qquad\qquad 2 \le k \le N_m \tag{3.95}$$

This allows obtaining the values of $r(m,l,k)$ by first solving the partition equations (3.89)-(3.93) and using (3.95) for recovering the main variables. The remaining original unknowns $r(m,l,1)$ are found from (3.32) as:

$$r(m,l,1) = p(m,l) - \sum_{k=2}^{N_m} r(m,l,k) \qquad\qquad 1 \le l \le L \tag{3.96}$$

Therefore, for a fixed m, $1 \le m \le M$, the procedure can summarised as Algorithm 2 below:

This procedure is very efficient as the computations only require logical and matrix operations. For this reason, obtaining the ALEs for lower order cases ($n \le 5$) is relatively fast, while higher order cases ($n > 5$) can demand a larger computational load, but mainly because the number of solutions of the partition equations tend to increase at combinatorial rates.

This result is important because it allows writing down the n-th order ALE using the solutions of the Diophantine system instead of computing the symbolical operations involved in the variational approach. Moreover, the Diophantine system approach allows finding only terms of order n, avoiding unnecessary calculations that arise if the symbolical approach is used.

Algorithm 2 Determination of the solutions of (3.32)-(3.33)

---

1. Solve the partition equation with respect to X_l:

$$\sum_{l=1}^{L} X_l = N_m - 1 \tag{3.97}$$

2. For each X_l found in step 1, solve the partition equation with respect to $Y_{l,i}$:

$$\sum_{i=2}^{N_m} Y_{l,i} = X_l \tag{3.98}$$

3. For each $Y_{l,i}$ obtained in step 2, find $r(m,l,k)$ as:

$$r(m,l,k) = Y_{l,k-1} - Y_{l,k} \qquad 2 \le k \le N_m,\ 1 \le l \le L \tag{3.99}$$

4. Find $r(m,l,1)$ as:

$$r(m,l,1) = p(m,l) - \sum_{k=2}^{N_m} r(m,l,k) \qquad 1 \le l \le L \tag{3.100}$$

3.4   Example

For illustrating Algorithm 1, an example using a simple polynomial NARX model with a few nonlinear terms will be used. The objective is to extract the GFRFs of order up to three.

Consider model (3.34)-(3.35) with $L = 2$, $M = 3$, arbitrary c_1, c_2, c_3 and:

$$A(z) = 1 - a_2\, z^{-2} \tag{3.101}$$

$$B(z) = b_1\, z^{-1} \tag{3.102}$$

$$F_1(t) = u(t-2)^2 \tag{3.103}$$

$$F_2(t) = y(t-1)u(t-2) \tag{3.104}$$

$$F_3(t) = y(t-1)^3 \tag{3.105}$$

3. A NEW ALGORITHM FOR DETERMINATION OF GFRFS OF NONLINEAR SYSTEMS

The nonlinear terms $F_1(t)$, $F_2(t)$ and $F_3(t)$ are described by the parameters:

$$p(1,1) = 0 \qquad p(1,2) = 0 \qquad q(1,1) = 0 \qquad q(1,2) = 2 \qquad (3.106)$$

$$p(2,1) = 1 \qquad p(2,2) = 0 \qquad q(2,1) = 1 \qquad q(2,2) = 0 \qquad (3.107)$$

$$p(3,1) = 3 \qquad p(3,2) = 0 \qquad q(3,1) = 0 \qquad q(3,2) = 0 \qquad (3.108)$$

for which:

$$\sum_{l=1}^{L} p(1,l) + q(1,l) = 2 \qquad (3.109)$$

$$\sum_{l=1}^{L} p(2,l) + q(2,l) = 2 \qquad (3.110)$$

$$\sum_{l=1}^{L} p(3,l) + q(3,l) = 3 \qquad (3.111)$$

The first order GFRF is formed only by the linear part of the model, which is readily found as:

$$H_1(z_1) = \frac{B(z_1)}{A(z_1)} = \frac{b_1 \, z_1^{-1}}{1 - a_2 \, z_1^{-2}} \qquad (3.112)$$

For $n = 2$:

$$N_1 = 2 - 2 + 1 = 1 \qquad (3.113)$$

$$N_2 = 2 - 2 + 1 = 1 \qquad (3.114)$$

$$N_3 = 2 - 3 + 1 = 0 \qquad (3.115)$$

Therefore, only the first and second nonlinear terms contribute for the second order GFRF. The Diophantine systems associated to these nonlinear terms are respectively

described as:

$$
\begin{cases}
r(1,1,1) & = 0 \\
r(1,1,2) & = 0 \\
\quad\quad 0 & = 0
\end{cases}
\tag{3.116}
$$

$$
\begin{cases}
r(2,1,1) & = 1 \\
r(2,1,2) & = 0 \\
\quad\quad 0 & = 0
\end{cases}
\tag{3.117}
$$

whose solutions are already explicitly described. Using (3.53)-(3.56), these solutions are converted as follows:

$$
\mathcal{Z}\{\mathcal{K}\psi_1(t)\} = z_1^{-2} z_2^{-2}
\tag{3.118}
$$

$$
\mathcal{Z}\{\mathcal{K}\phi_1(t)\} = 1
\tag{3.119}
$$

$$
\mathcal{Z}\{\mathcal{K}\psi_2(t)\} = z_1^{-2}
\tag{3.120}
$$

$$
\mathcal{Z}\{\mathcal{K}\phi_2(t)\} = H_1(z_2)\, z_2^{-1}
\tag{3.121}
$$

Therefore:

$$
H_2(z_1, z_2) = \frac{c_1\, z_1^{-2} z_2^{-2} + c_2\, z_1^{-2}\, H_1(z_2)\, z_2^{-1}}{A(z_1 z_2)}
\tag{3.122}
$$

For $n = 3$:

$$
N_1 = 3 - 2 + 1 = 2
\tag{3.123}
$$

$$
N_2 = 3 - 2 + 1 = 2
\tag{3.124}
$$

$$
N_3 = 3 - 3 + 1 = 1
\tag{3.125}
$$

3. A NEW ALGORITHM FOR DETERMINATION OF GFRFS OF NONLINEAR SYSTEMS

The Diophantine systems associated to the nonlinear terms are:

$$\begin{cases} r(1,1,1) + r(1,1,2) & = 0 \\ r(1,2,1) + r(1,2,2) & = 0 \\ r(1,1,2) + r(1,2,2) & = 1 \end{cases} \tag{3.126}$$

$$\begin{cases} r(2,1,1) + r(2,1,2) & = 1 \\ r(2,2,1) + r(2,2,2) & = 0 \\ r(2,1,2) + r(2,2,2) & = 1 \end{cases} \tag{3.127}$$

$$\begin{cases} r(3,1,1) & = 3 \\ r(3,1,1) & = 0 \\ 0 & = 0 \end{cases} \tag{3.128}$$

These systems contain a small number of variables and can be solved by inspection. System (3.126) is clearly inconsistent, as the first two equations imply that all variables should be zero, while the third equation suggests that at least one of them should be 1. This means that the first nonlinear term does not contribute to the third order GFRF. This is reasonable, as $F_1(t)$ is a pure input nonlinearity of degree 2, therefore, the only GFRF that can be affected by it is the second order one.

System (3.127) admits only one solution, which is described as:

$$r(2,1,1) = 0, \qquad r(2,1,2) = 1, \qquad r(2,2,1) = 0, \qquad r(2,2,2) = 0 \tag{3.129}$$

Lastly, system (3.128) does not need to be solved, as the equations are consistent and explicitly describe the solutions.

The final step is converting the available solutions into algebraic terms. Solution (3.129) is converted as:

$$\mathcal{Z}\{\mathcal{K}\psi_1(t)\} = z_1^{-2} \tag{3.130}$$

$$\mathcal{Z}\{\mathcal{K}\phi_1(t)\} = H_2(z_2, z_3) \tag{3.131}$$

while the term associated to system (3.128) is described as:

$$\mathcal{Z}\{\mathcal{K}\psi_1(t)\} = 1 \tag{3.132}$$

$$\mathcal{Z}\{\mathcal{K}\phi_1(t)\} = H_1(z_1)\, z_1^{-1}\, H_1(z_2)\, z_2^{-1}\, H_1(z_3)\, z_3^{-1} \tag{3.133}$$

Therefore, the 3-rd order GFRF can be obtained as:

$$H_3(z_1, z_2, z_3) = \frac{c_2\, z_1^{-2}\, H_2(z_2, z_3) + c_3\, H_1(z_1)\, z_1^{-1}\, H_1(z_2)\, z_2^{-1}\, H_1(z_3)\, z_3^{-1}}{A(z_1\, z_2\, z_3)} \tag{3.134}$$

Although the example was restricted to the 3-rd order case, the philosophy for higher order cases is the same, where Diophantine systems are built and solved and their solutions are converted into algebraic expressions. Notice that this systematic procedure is very important for more realistic models, because practical data usually yields polynomial models with several terms, which can often be more complicated than those explored in the example. The methodology illustrated in this section can be equally applied in these cases, providing an efficient manner of extracting GFRFs in practical situations. For the purposes of this work and future research, the full procedure has been implemented in MATLAB functions, allowing a more automatic extraction of GFRFs of nonlinear systems.

3.5 Conclusions

This chapter is dedicated to report a new result regarding extraction of the GFRFs of nonlinear systems from a NARX model. This is important in practical situations in which a polynomial NARX model is identified from the input-output data of a nonlinear system and system GFRFs are to be determined from the identified NARX model. The new algorithm allows a very systematic way to deal with this situation which is more efficient than other approaches such as the classical probing method and the parametric characteristics approach (Jing et al., 2008). The efficiency is mainly due to the core calculations being based on a numerical procedure, in which the main computational

efforts are on solving a set of linear Diophantine equations. Because the form of these equations depends on the structure of the model nonlinear terms, the solutions, in principle, need only to be computed once for being stored and used in a table look-up scheme. The GFRFs are then constructed via algebraic expressions that directly use the Diophantine solutions for building the relevant algebraic expressions.

These results are useful for the general application of frequency domain methods in nonlinear systems, including fault diagnosis problems in which the fault features are based on the GFRF representation (Tang et al., 2010). In addition, the results also provide an important basis for the development of new numerical and analytical methods for computation of NOFRFs of nonlinear systems. This will be the focus of the studies reported in the next chapter.

4

New methods for computation of NOFRFs of nonlinear systems

4.1 Introduction

Characterising frequency domain behaviour of nonlinear systems via the Volterra series approach is a powerful strategy for applications such as fault diagnosis and system analysis and design. The algorithm presented in Chapter 4 allows a systematic and efficient extraction of the GFRFs, the main frequency domain characteristics of nonlinear systems. However, this does not eliminate the difficulties of analysis and feature extraction from these functions, which are inherent from their multidimensional nature.

As discussed in Chapter 3, the issues with the multidimensional frequency spaces analysis can be avoided by using alternative FRF concepts, such as the NOFRFs. The computation of these functions, however, need to be significantly improved as the currently available algorithm can suffer from numerical problems and requires the maximum order of the functional series to be specified in advance (Lang and Billings, 2005). Moreover, since a fixed probing input must be chosen *a priori* for carrying out the analysis, a natural question that arises is how this signal can be chosen so that

4. NEW METHODS FOR COMPUTATION OF NOFRFS OF NONLINEAR SYSTEMS

the resulting NOFRFs can exhibit appropriate features for achieving a specific goal, for example, clarifying the differences and similarities between a group of faulty conditions.

In this chapter, we propose a new procedure for computing the n-th order NOFRF directly from a polynomial NARX model, which does not suffer from numerical issues and does not require the truncation order to be specified in advance. The basic idea is to decouple the Volterra series components $y_n(t)$ from the output $y(t)$, so that its Fourier transform $Y_n(e^{j\omega})$ can be readily computed. Then, $G_n(e^{j\omega})$ can be obtained as the ratio between $Y_n(e^{j\omega})$, and the n-th order input spectrum $U_n(e^{j\omega})$. The general idea for computing all NOFRFs up to order n can be described as follows:

1. Obtain the system ALEs from the polynomial NARX model up to order n

2. For a fixed input, solve the ALEs for all functional components $y_i(t)$, where $i \in \{1, \ldots, n\}$

3. Obtain the frequency transforms of the functional components $Y_i(z) = \mathcal{Z}\{y_i(t)\}$ and of the generalised input spectrum $U_i(z) = \mathcal{Z}\{u(t)^i\}$, where $i \in \{1, \ldots, n\}$

4. Compute the NOFRFs as the ratios $G_i(z) = Y_i(z)/U_i(z)$, where $z = e^{j\omega}$

The efficiency of this new procedure is due to Proposition 1 from Chapter 3, which allows the extraction of the Associated Linear Equations (ALEs) based from the system NARX model, without requiring specifying the truncation order in advance. Once built, the ALEs can be numerically solved for any probing input for yielding discrete-time sequences $y_i(t)$, which can then be used in conjunction with the DFT computations for obtaining the n-th order NOFRF as the ratio described above.

Throughout this chapter, we shall also demonstrate that the components $Y_i(z)$ can be obtained in analytical form. Although this is a more laborious procedure, the result can offer some potential advantages as the output can be obtained as a function of varying parameters, which can be useful, for example, for tuning the probing input according to diagnosis goals.

The details of each step of the procedure above will be discussed throughout the remaining sections of this chapter.

4.2 Derivation of ALEs from a NARX model

The extraction of the ALEs from a general polynomial NARX model was introduced in Section 3.3.1. The advantages of this result, however, go beyond the purpose of deriving the GFRFs, as the ALEs can also be used for obtaining the functional components. This is the basis of the new frequency analysis framework.

Consider again the NARX model:

$$A\,y(t) = B\,u(t) + \sum_{m=1}^{M} c_m \prod_{l=1}^{L} y(t-l)^{p(m,l)} u(t-l)^{q(m,l)} \tag{4.1}$$

where A and B are linear time-shifting operators so that:

$$A\,y(t) = y(t) + \sum_{l=1}^{L} a_l\,y(t-l) \tag{4.2}$$

$$B\,u(t) = \sum_{l=1}^{L} b_l\,u(t-l) \tag{4.3}$$

and $p(m,l)$ and $q(m,l)$ are nonnegative integers such that

$$\sum_{l=1}^{L} p(m,l) + q(m,l) \geq 2 \tag{4.4}$$

According to the results of Section 3.3.1, the ALEs of model (4.1) are described as:

$$A\,y_n(t) = B\,u(t) \qquad\qquad n = 1 \tag{4.5}$$

$$A\,y_n(t) = \sum_{m=1}^{M} c_m\,\psi_m(t) \sum_{S_m} \rho_m\,\phi_m(t) \qquad\qquad n \geq 2 \tag{4.6}$$

where

$$\rho_m = \frac{\prod_{l=1}^{L} p(m,l)!}{\prod_{l=1}^{L} \prod_{j=k}^{N_m} r(m,l,k)!} \tag{4.7}$$

$$\psi_m(t) = \prod_{l=1}^{L} u(t-l)^{q(m,l)} \tag{4.8}$$

$$\phi_m(t) = \prod_{l=1}^{L} \prod_{k=1}^{N_m} y_k(t-l)^{r(m,l,k)} \tag{4.9}$$

$$N_m = n - \sum_{l=1}^{L} q(m,l) + p(m,l) + 1 \tag{4.10}$$

and S_m is the set of all nonnegative integer solutions of the linear Diophantine system

$$\sum_{k=1}^{N_m} r(m,l,k) = p(m,l) \qquad 1 \le l \le L \tag{4.11}$$

$$\sum_{l=1}^{L} \sum_{k=1}^{N_m} (k-1)\, r(m,l,k) = N_m - 1 \tag{4.12}$$

The most important procedure for writing down the n-th order ALE for $n > 1$ ($n = 1$ is trivial) is to write down the right-hand side, since its exact form depends on the solution of the associated Diophantine system built from the model parameters. In order to write down the right-hand side, Algorithm 3 can be followed, for each nonlinear term of model (4.1), *i.e.* $m \in \{1, \ldots, M\}$

This result is important because it allows writing down the n-th order ALE using the solutions of the Diophantine system instead of computing the symbolical operations involved in the variational approach. Moreover, the Diophantine system approach allows finding only terms of order n, avoiding unnecessary calculations that arise if the symbolical approach is used. Currently, ALEs are obtained via an algorithm based on a variational approach and symbolical calculations (Feijoo et al., 2006, 2005), similar to those carried out in the probing method.

Algorithm 3 Derivation of the n-th order ALE

---

1. For $1 \leq m \leq M$, compute the right-hand side terms as follows:

    1.1. Build and solve the Diophantine system (4.11)-(4.12)

    1.2. Convert each solution found in step 1 into an algebraic term as follows:

       1.2.1. Compute ρ_m using (4.7)

       1.2.2. Compute $\psi_m(t)$ using (4.8)

       1.2.3. Compute $\phi_m(t)$ using (4.9)

       1.2.4. Compute the product: $c_m \, \rho_m \, \psi_m(t) \, \phi_m(t)$

    1.3. Sum up all terms found in step 1.2

2. Sum up all terms found in step 1

4.3   Solution of the ALEs

Once the ALEs have been obtained, they can be solved for obtaining each of the functional components, $y_n(t)$. This is possible because of the recursive and linear nature of the equations, which is similar to that of a triangular system of linear algebraic equations. The first order ALE is very simple and purely linear, so that, for a particular input, $y_1(t)$ can be found by solving (4.5) using well established linear techniques. For the n-th order ALE, where $n > 1$, the procedure is slightly more complicated, but can be generally described as two main steps:

1. Compute the signal that corresponds to the right-hand side

2. Obtain $y_n(t)$ as the output of the filter whose transfer function is described as $1/A(z)$ and whose input is the signal computed in step 1

This general procedure can be carried out in two different ways, namely a numerical or an analytical approach, each with their own advantages and disadvantages, which are discussed in further details below.

4.3.1 Numerical approach

The numerical approach consists of finding the functional components $y_n(t)$ and representing those as a finite sequence of samples, for instance, for $t \in \{0, 1, \ldots, N\}$. Typically, these finite sequences are represented in a vector format, where the first element represents the initial sample $y_n(0)$ and and last entry represents the sample of $y_n(t)$ at the final time, denoted as $y_n(N)$. Therefore, for the numerical approach, an equivalence between the signal $y_n(t)$ and a vector $\boldsymbol{y}_n$ will be established, where

$$\boldsymbol{y}_n = \left[\begin{array}{cccc} y_n(0) & y_n(1) & \ldots & y_n(N) \end{array} \right]^T \tag{4.13}$$

which, in essence, constitutes a nonparametric time-domain representation of $y_n(t)$.

In order to numerically solve the ALEs using the notation adopted above, a general two-step procedure can be followed. The first step consists of computing the right-hand side of each ALE. This is feasible because, the equations are solved for ascending n (the order of the functional component) and the right-hand sides only depend on the input and components of order less than n. When carrying out this computation, four basic operations frequently appear:

- Time delay of a sequence: $x(t - l)$, $l > 0$

- Summation between two sequences: $x(t) + w(t)$

- Multiplication of a sequence by a constant: $c\,x(t)$

- Multiplication between two sequences: $x(t)w(t)$

In terms of the vector notation, these operations can easily be implemented. To this end, let the vector representations of sequences $x(t)$ and $w(t)$ respectively be denoted

as $\boldsymbol{x}$ and $\boldsymbol{w}$, where:

$$\boldsymbol{x} = \left[\begin{array}{cccc} x(0) & x(1) & \ldots & x(N) \end{array}\right]^T \tag{4.14}$$

$$\boldsymbol{w} = \left[\begin{array}{cccc} w(0) & w(1) & \ldots & w(N) \end{array}\right]^T \tag{4.15}$$

The representative vector of a sequence delayed by l samples can be obtained by simply inserting zeros to first l entries and shifting the original $N - l + 1$ samples to the left. In other words, the vector representation of $x(t - l)$ is described as:

$$\boldsymbol{x}_l = \left[\begin{array}{ccccccc} \underbrace{0 \quad \ldots \quad 0}_{l} & x(0) & x(1) & \ldots & x(N - l) \end{array}\right]^T \tag{4.16}$$

The summation between sequences and multiplication by a constant can be done as usual vector operations from Linear Algebra. Therefore, by letting $\boldsymbol{s}$ represent the sequence $s(t) = x(t) + w(t)$ and $\boldsymbol{z}$ represent $z(t) = c\,x(t)$, then:

$$\boldsymbol{s} = \boldsymbol{x} + \boldsymbol{w} = \left[\begin{array}{cccc} x(0) + w(0) & x(1) + w(1) & \ldots & x(N) + w(N) \end{array}\right]^T \tag{4.17}$$

$$\boldsymbol{z} = c\boldsymbol{x} = \left[\begin{array}{cccc} c\,x(0) & c\,x(1) & \ldots & c\,x(N) \end{array}\right]^T \tag{4.18}$$

The last operation, the product between two sequences, can be described in vector terms as the element-wise product, also known as the Hadamard product (Styan, 1973). Therefore, by letting $\boldsymbol{p}$ be the vector notation of $p(t) = x(t)w(t)$:

$$\boldsymbol{p} = \boldsymbol{x} \circ \boldsymbol{w} = \left[\begin{array}{cccc} x(0)w(0) & x(1)w(1) & \ldots & x(N)w(N) \end{array}\right]^T \tag{4.19}$$

The second and final step of the numerical approach consists of obtaining the vector $\boldsymbol{y}_n$ by linear-filtering the right-hand side signal (obtained from the previous step) by a system described by the transfer function $1/A(z)$. This can be easily done via simulation of the filter's difference equation using simple recurrences.

The vector notation allows the computations to run relatively faster, the resulting representation of the functional components is in the time-domain, so that the computation of frequency-domain characteristics requires computing the Discrete Time Fourier

Transform (DTFT) of the sequences using, for example, the Fast Fourier Transform (FFT) algorithm. However, even after this step, the representations are still nonparametric, which prevents a direct inspection of the influence of varying parameters over the components or the overall response. This can be circumvented by computing the responses for some sample values of the parameter and using an interpolation technique for better understanding the effects of these changes, but at the computational cost of solving extracting and solving the ALEs repeatedly. As it will be demonstrated in the next section, these problems can be avoided by using an analytical approach.

4.3.2   Analytical approach

Under some circumstances, it is possible to obtain the exact analytical form of the functional components, both in the time and the frequency domain. This is more restrictive though, as it requires additional computational efforts and can only be carried out for some types of inputs. However, there are advantages for computing the components in this form, as some parameters of interest, such as input poles or model coefficients, can be left as a varying parameter so their influence over the response can be studied for design tasks.

The circumstances in which this is possible are those where the input can be described as a linear combination of basic functions, usually shifted in time. The basic functions are the unit impulse:

$$u(t) = u_0(t) = \begin{cases} 0 & t \neq 0 \\ 1 & t = 0 \end{cases} \tag{4.20}$$

and the generalised damped sinusoidal:

$$u(t) = t^\alpha \, \beta^t \, \cos(\Omega t + \theta) \, u_1(t) \tag{4.21}$$

where $|\beta| < 1$, $\alpha \geq 0$, $\alpha \in \mathbb{Z}$ and $u_1(t)$ is the unit step function:

$$u_1(t) = \begin{cases} 1 & t \geq 0 \\ 0 & t < 0 \end{cases} \tag{4.22}$$

Any linear combination of these basic functions results in frequency domain representation described by a rational function. This is important, as the analytical approach consists of solving frequency convolutions using the residue theorem, which is easier to apply when all functions involved are rational.

The procedure for computing the components in an analytical form is based on the direct application of the $\mathcal{Z}$ transform to the ALEs (4.5)-(4.6). The $\mathcal{Z}$ transform is defined for a causal sequence $x(t)$ as:

$$X(z) = \mathcal{Z}\{x(t)\} = \sum_{t=0}^{\infty} x(t) z^{-t} \tag{4.23}$$

Notice that since only causal sequences are being considered, the specification of a region of convergence is not necessary.

Consider again the ALEs (4.5)-(4.6). Applying $\mathcal{Z}$ and its linearity and modulation properties yields:

$$A(z)Y_1(z) = B(z)U(z) \tag{4.24}$$

$$A(z)Y_n(z) = \sum_{m=1}^{M_n} c_m \sum_{S_m} \rho_m \, \Psi_m(z) \otimes \Phi_m(z) \qquad n \geq 2 \tag{4.25}$$

where:

$$\Psi_m(z) = \mathcal{Z}\left\{\prod_{l=1}^{L} u(t-l)^{q(m,l)}\right\} \tag{4.26}$$

$$= \underbrace{z^{-1}U(z) \otimes \cdots \otimes z^{-1}U(z)}_{q(m,1)} \cdots \underbrace{z^{-L}U(z) \otimes \cdots \otimes z^{-L}U(z)}_{q(m,L)} \tag{4.27}$$

$$= \bigotimes_{l=1}^{L} \bigotimes_{i=1}^{q(m,l)} z^{-l}U(z) \tag{4.28}$$

$$\Phi_m(z) = \mathcal{Z}\left\{\prod_{l=1}^{L}\prod_{k=1}^{N_m} y_k(t-l)^{r(m,l,k)}\right\} \tag{4.29}$$

$$= \underbrace{z^{-1}Y_1(z) \otimes \cdots \otimes z^{-1}Y_1(z)}_{r(m,1,1)} \cdots \underbrace{z^{-L}Y_{N_m}(z) \otimes \cdots \otimes z^{-L}Y_{N_m}(z)}_{r(m,L,N_m)} \tag{4.30}$$

$$= \bigotimes_{l=1}^{L}\bigotimes_{k=1}^{N_m}\bigotimes_{i=1}^{r(m,l,k)} z^{-l}Y_k(z) \tag{4.31}$$

and $\otimes$ denotes frequency convolution. Furthermore, the following notation has been introduced:

$$\bigotimes_{i=1}^{n} X_i(z) = X_1(z) \otimes \ldots \otimes X_n(z) \tag{4.32}$$

Notice that by carrying out the calculations in the frequency domain, the products on the right-hand side of ALEs for $n > 1$ become frequency convolutions. This might seem to introduce unnecessary complications, since it is more intuitive to simply compute the products of the right-hand sides in the time-domain. However, there are benefits in using a full frequency-domain approach, since obtaining $Y_n(z)$ requires transforming the right-hand side back to the $\mathcal{Z}$-domain and dividing it by $1/A(z)$. In other words, the frequency convolution approach avoids alternating between time and frequency domains.

In addition, it is always possible that, in practical computations, impulse or step terms are introduced in lower order components. This requires additional simplifications when evaluating the right-hand sides in the time-domain. For example, the product between two steps or two impulses need to be simplified into a single step or

impulse, before the filtering by $1/A(z)$ is performed. The simplifications are relatively less systematic than computing frequency convolutions, because, in the time-domain, it is necessary to verify the nature of the functions and their respective delays. For example, the product of two impulses can only be converted into a single impulse if their delays are the same, otherwise, the result is always zero. These requirements are not present when computing the right-hand sides using frequency convolutions, because all delayed functions are represented in the same rational format, making the calculations significantly more systematic than their time-domain counterpart.

The computation of $\Psi_m(z)$ and $\Phi_m(z)$, can be carried out via a simple recursive procedure. In order to demonstrate that, consider first the computation of $\psi_m(t)$ in the time-domain. This would require the following steps:

1. Set $\psi_m(t) = 1$, *i.e.* the neutral element of multiplication

2. For $l \in \{1, \ldots, L\}$ and $i \in \{1, \ldots, q(m,l)\}$ compute:

$$\psi_m(t) = \psi_m(t) \cdot u(t - l)$$

The procedure is similar in the frequency domain, except that multiplication is replaced by convolution, and the neutral element used in step 1 is replaced by the equivalent transform of the neutral element in the time-domain, *e.g.* $\mathcal{Z}\{1\} = z/(z-1)$, which is equivalent to the step function. It is worth mentioning that a more natural choice for this would be the impulse function in the frequency domain, whose time-domain representation is a constant function for any $t \in \mathbb{Z}$. However, because only causal sequences are being considered, the step and a constant sequence are essentially equivalent in this context. The step function is chosen as the neutral element because its transform is rational, which is in agreement with the formulation of other signals (input and functional components) considered for the analytical approach.

The procedures for computing $\Psi_m(z)$ and $\Phi_m(z)$ can be summarised as Algorithms 4 and 5.

Algorithm 4 Computation of $\Psi_m(z)$

---

1. Set $\Psi_m(z) = z/(z-1)$

2. For $l = \{1, \ldots, L\}$ and $i = \{1, \ldots, q(m,l)\}$, compute:

$$\Psi_m(z) = \Psi_m(z) \otimes \left(z^{-l} U(z)\right)$$

Algorithm 5 Computation of $\Phi_m(z)$

---

1. Set $\Phi_m(z) = z/(z-1)$

2. For $l = \{1, \ldots, L\}$, $k = \{1, \ldots, N_m\}$ and $i = \{1, \ldots, r(m,l,k)\}$, compute:

$$\Phi_m(z) = \Phi_m(z) \otimes \left(z^{-l} Y_k(z)\right)$$

Algorithms 4 and 5 form the core of the analytical approach, in which $Y_n(z)$ is obtained in a closed form. By gathering together these procedures, we obtain Algorithm 6, which is the main guideline for analytically solving the ALEs in the frequency domain:

Although the background for computing the frequency domain representation of the functionals has been established, there are some particular details regarding the implementation that need to be discussed. This will be discussed in the next section.

4.3.3   Symbolic computational aspects of the analytical approach

The analytical approach presented in section 4.3.2 is a novel tool for analysing the system behaviour, especially when one or more varying parameters are present in the model equations. The main procedure for solving the ALEs requires frequency convolutions, which must, however, be computed with care.

The frequency convolutions are mathematically described as complex integrals com-

---

Algorithm 6 Computation of $Y_n(z)$

---

1. For $m = \{1, \ldots, M\}$, compute $V_m(z)$ as follows:

    1.1. Compute $\Psi_m(z)$ using Algorithm 4

    1.2. Find the solution set S_m of the Diophantine system (4.11)-(4.12)

    1.3. For each solution found in step 1.2:

        1.3.1. Compute ρ_m from (4.7)

        1.3.2. Compute $\Phi_m(z)$ using Algorithm 5

        1.3.3. Compute the product $\rho_m \, \Phi_m(z)$

    1.4. Sum up all terms found in step 1.3.3

    1.5. Using the results of steps 1.1 and 1.4, compute:

    $$V_m(z) = c_m \, \Psi_m(z) \otimes \sum_{S_m} \beta_m \, \Phi_m(z)$$

2. Compute the sum of all terms found in step 1.5

3. Obtain $Y_n(z)$ by dividing the result of step 2 by $A(z)$

---

puted over closed contours. Because all transforms involved in these operations are assumed to be rational functions, the evaluation of convolutions can be greatly simplified via the Residue Theorem (Brown, 2009). However, a direct application of this result can produce significant accuracy errors and large computational times, if the involved transforms are used in their conventional rational form, *i.e.* quotients of polynomials. This is mainly due to the computation of residues requiring symbolic operations that rapidly grow in complexity as the order of denominators of the involved transforms become larger, which is usually the case when dealing with ALEs. In this section, it will be demonstrated how these problems can be avoided by adopting a partial fraction representation of the operands.

4. NEW METHODS FOR COMPUTATION OF NOFRFS OF NONLINEAR SYSTEMS

4.3.3.1 Frequency convolutions

Frequency convolutions are required for computing the right-hand sides of the ALEs, in order to avoid alternating between the time and frequency domains. The main terms that compose the ALEs right-hand sides are formed from recursive convolutions, which are computed between two transformations at a time.

For two discrete-time signals represented as $H(z)$ and $G(z)$, the frequency convolution between them, denoted as $H(z) \otimes G(z)$, is defined as:

$$H(z) \otimes G(z) = \frac{1}{j2\pi} \oint_C v^{-1} H(v) G(z/v) dv \tag{4.33}$$

where C is a closed contour that encloses all poles of $H(z)$ (Poularikas, 2000). When both $H(z)$ and $G(z)$ are rational functions, the evaluation of (4.33) can be greatly simplified using the Residue Theorem (Brown, 2009).

Residue Theorem: Let $F : \mathbb{C} \to \mathbb{C}$ be analytic and C a closed contour in the complex plane. Then:

$$\oint_C F(z) dz = \sum_{i=1}^{N_\alpha} \mathcal{R}_F(\alpha_i) \tag{4.34}$$

where α_i, $i \in \{1, \ldots, N_\alpha\}$, represents poles of $F(z)$ inside C and $\mathcal{R}_F(\alpha_i)$ denotes the residue of F computed at pole α_i. When $F(z)$ is a rational function, the computation of residues is straightforward and can be carried out as:

$$\mathcal{R}_F(\alpha_i) = \frac{1}{(m_i - 1)!} \frac{d^{m_i - 1} F(z)}{dz^{m_i - 1}} \bigg|_{z = \alpha_i} \tag{4.35}$$

where m_i is the multiplicity of pole α_i.

Although the Residue Theorem constitutes a prominent tool for analytically solving the ALEs, it cannot be directly used in most practical situations, because (4.35) is essentially a symbolic operation which requires differentiation and other algebraic calculations that easily become impractical due to computational time, depending on how complex the operands are (*i.e.*, depending on the degrees of numerators and denominators of the rational functions). In addition, severe accuracy errors can occur, if the operands contain elements represented in floating point notation.

This can be avoided by representing $H(z)$ and $G(z)$ in partial fraction (PF) form and exploring the linearity of the convolution operator. To this end, consider:

$$H(z) = \hat{H}_0 + \sum_{i=1}^{I} \frac{\hat{H}_i}{(z - \alpha_i)^{n_i}} \qquad\qquad n_i \in \mathbb{Z},\, n_i \geq 1 \qquad (4.36)$$

$$G(z) = \hat{G}_0 + \sum_{k=1}^{K} \frac{\hat{G}_i}{(z - \beta_i)^{m_k}} \qquad\qquad m_k \in \mathbb{Z},\, m_k \geq 1 \qquad (4.37)$$

where $\hat{H}_i$, $\hat{G}$, α_i and β_k are complex numbers. Notice that a full PF representation is being used, in contrast to the usual PF expansion of the signal divided by z, which is a more traditional choice when dealing with the $\mathcal{Z}$ transform.

Using (4.36)-(4.37), $H(z) \otimes G(z)$, can be written as:

$$H(z) \otimes G(z) = \hat{H}_0 \otimes \hat{G}_0 + M_1(z) + M_2(z) + M_3(z) \qquad (4.38)$$

where

$$M_1(z) = \sum_{k=1}^{K} \hat{H}_0 \otimes \frac{\hat{G}_k}{(z - \beta_k)^{m_k}} \qquad (4.39)$$

$$M_2(z) = \sum_{i=1}^{I} \hat{G}_0 \otimes \frac{\hat{H}_i}{(z - \alpha_i)^{n_i}} \qquad (4.40)$$

$$M_3(z) = \sum_{i=1}^{I} \sum_{k=1}^{K} \hat{H}_i \hat{G}_k \, W_{n_i m_k}(z) \qquad (4.41)$$

$$W_{n_i m_k}(z) = \frac{1}{(z - \alpha_i)^{n_i}} \otimes \frac{1}{(z - \beta_k)^{m_k}} \qquad (4.42)$$

Notice that operations have been reduced to sums of convolutions between much simpler transforms, which is what makes this approach more efficient. Furthermore, the term $\hat{H}_0 \otimes \hat{G}_0$ in (4.38) can be simplified as:

$$\hat{H}_0 \otimes \hat{G}_0 = \frac{1}{j2\pi} \oint_C \hat{H}_0 \hat{G}_0 \, v^{-1} dv = \hat{H}_0 \hat{G}_0 \oint_C v^{-1} dv \qquad (4.43)$$

By letting $F(v) = 1/v$, the result is found as:

$$\hat{H}_0 \otimes \hat{G}_0 = \hat{H}_0 \hat{G}_0 \, \mathcal{R}_F(0) = \hat{H}_0 \hat{G}_0 \qquad (4.44)$$

Similarly, $M_1(z)$ can be simplified by analysing the general term of the sum (4.39).

$$\hat{H}_0 \otimes \frac{\hat{G}_k}{(z - \beta_k)^{m_k}} = \frac{1}{j2\pi} \oint_C \frac{\hat{H}_0 \, \hat{G}_k \, v^{m_k-1} dv}{(z - \beta_k v)^{m_k}} \qquad (4.45)$$

Let:

$$F(v) = \frac{v^{m_k-1}}{(z - \beta_k v)^{m_k}} \qquad (4.46)$$

It is observed that the only term capable of introducing a pole inside C is v^{m_k-1}, which can only happen if $m_k = 0$. Because it was assumed that $m_k > 1$, we can conclude that there are no poles inside C. Then, using the Residue Theorem yields:

$$\hat{H}_0 \otimes \frac{\hat{G}_k}{(z - \beta_k)^{m_k}} = 0 \qquad (4.47)$$

so that $M_1(z) = 0$. Since $M_2(z)$ is essentially similar to $M_1(z)$, the same procedure can be applied yielding a similar result, $i.e.$ $M_2(z) = 0$.

In order to simplify $M_3(z)$, the general term (4.42) is analysed. One issue, however, is that the convolution:

$$W_{n_i m_k}(z) = \frac{1}{j2\pi} \oint_C \frac{v^{m_k-1} dv}{(v - \alpha_i)^{n_i} (z - \beta_k v)^{m_k}} \qquad (4.48)$$

is difficult to solve for general values of n_i and m_k, in contrast to what was done for the previous cases. This is not a serious issue though, as n_i and m_k are integer-valued, so that $W_{n_i m_k}(z)$ can be pre-computed for some common pairs (n_i, m_k) for the purposes

of building an efficient table look-up scheme. A few results are demonstrated below:

$$W_{11}(z) = \frac{1}{z - \alpha_i \beta_k} \tag{4.49}$$

$$W_{12}(z) = \frac{\alpha_i}{(z - \alpha_i \beta_k)^2} \tag{4.50}$$

$$W_{13}(z) = \frac{\alpha_i^2}{(z - \alpha_i \beta_k)^3} \tag{4.51}$$

$$W_{21}(z) = \frac{\beta_k}{(z - \alpha_i \beta_k)^2} \tag{4.52}$$

$$W_{22}(z) = \frac{2\,\alpha_i \beta_k}{(z - \alpha_i \beta_k)^3} + \frac{1}{(z - \alpha_i \beta_k)^2} \tag{4.53}$$

$$W_{23}(z) = \frac{2\,\alpha_i}{(z - \alpha_i \beta_k)^3} + \frac{3\,\alpha_i^2 \beta_k}{(z - \alpha_i \beta_k)^4} \tag{4.54}$$

$$W_{31}(z) = \frac{\beta_k^2}{(z - \alpha_i \beta_k)^3} \tag{4.55}$$

$$W_{32}(z) = \frac{2\,\beta_k}{(z - \alpha_i \beta_k)^3} + \frac{3\,\alpha_i \beta_k^2}{(z - \alpha_i \beta_k)^4} \tag{4.56}$$

$$W_{33}(z) = \frac{1}{(z - \alpha_i \beta_k)^3} + \frac{6\,\alpha_i^2 \beta_k^2}{(z - \alpha_i \beta_k)^5} + \frac{6\,\alpha_i \beta_k}{(z - \alpha_i \beta_k)^4} \tag{4.57}$$

Notice that the results have been converted into PF form. This is important because terms $\Psi_m(z)$ and $\Phi_m(z)$ in (4.25) are recursively computed, and the implementation greatly benefits when returned data is provided in the same format as the received data.

An important remark is that the resulting poles of $W_{n_i m_k}(z)$, in any situation, are described as $\alpha_i \beta_k$, and only differ in terms of their multiplicities. This means that the main effect of the frequency convolution between two signals is the production of a new set of poles that is basically the product between all poles of the two transforms. This phenomenon is similar to the generation of intermodulation and harmonics, which are usually studied in the context of the Volterra series approach. However, the phenomenon identified here is more general, as intermodulations and harmonics are particular cases for which the pole products are of the form $e^{j\omega_r}$, *i.e.* are sinusoidal components. The described phenomenon is capable of generating, not only these steady

state terms, but also new transient forms at the higher components, whenever $|\alpha_i| < 1$ and $|\beta_k| < 1$.

This approach allows computing the convolution between any two transforms, given their partial fraction forms, and, therefore, provide the basic procedure for evaluating the right-hand sides of any ALEs in the frequency domain.

4.3.3.2 Frequency-domain filtering using PF forms

The second step required for obtaining the functional components $Y_n(z)$ is filtering the ALE right-hand side and $1/A(z)$. This can be analytically done by simply computing the algebraic division between the right-hand side by $A(z)$. However, as pointed out before, it is important, from the computational perspective, that these operations receive and return data in the same partial fraction form, as many of the operations involved are performed in a recursive manner. Therefore, it is required to derive a procedure for providing the partial fraction form of the filter output, given a partial fraction form of the input.

This is accomplished by expanding both the filtering signal and the filter transfer function in partial fraction form, and computing the partial fraction form of the output. To this end, let:

$$H(z) = \hat{H}_0 + \sum_{i=1}^{I} \frac{\hat{H}_i}{(z - \alpha_i)^{n_i}} \qquad\qquad n_i \in \mathbb{Z},\, n_i \geq 1 \qquad\qquad (4.58)$$

$$G(z) = \hat{G}_0 + \sum_{k=1}^{K} \frac{\hat{G}_k}{(z - \beta_k)^{m_k}} \qquad\qquad m_k \in \mathbb{Z},\, m_k \geq 1 \qquad\qquad (4.59)$$

and the filtering process be described as:

$$W(z) = H(z)G(z) \qquad\qquad (4.60)$$

Then, the output can be described as:

$$W(z) = H(z)\,G(z) \tag{4.61}$$

$$= \hat{H}_0\,\hat{G}_0 + Q(z) + \sum_{i=1}^{I}\sum_{k=1}^{K} \frac{\hat{H}_i\,\hat{G}_k}{(z-\alpha_i)^{n_i}(z-\beta_k)^{m_k}} \tag{4.62}$$

$$Q(z) = \hat{H}_0 \sum_{k=1}^{K} \frac{\hat{G}_k}{(z-\beta_k)^{m_k}} + \hat{G}_0 \sum_{i=1}^{I} \frac{\hat{H}_i}{(z-\alpha_i)^{n_i}} \tag{4.63}$$

Notice that the term $Q(z)$ is already represented in a partial fraction form. Therefore, for obtaining the desired result it is necessary to find the partial fraction form of the third term. This is done by expanding the general term as follows:

$$\frac{1}{(z-\alpha_i)^{n_i}(z-\beta_k)^{m_k}} = \sum_{p=1}^{n_i} \frac{C_p}{(z-\alpha_i)^p} + \sum_{p=1}^{m_k} \frac{D_p}{(z-\beta_k)^p} \tag{4.64}$$

where coefficients C_p and D_p can be found by induction as:

$$C_p = \binom{m_k + n_i - p - 1}{m_k - 1} \frac{(-1)^{n_i-p}}{(\alpha_i - \beta_k)^{m_k+n_i-p}} \tag{4.65}$$

$$D_p = \binom{m_k + n_i - p - 1}{n_i - 1} \frac{(-1)^{m_k-p}}{(\beta_k - \alpha_i)^{m_k+n_i-p}} \tag{4.66}$$

4.4 Computation of NOFRFs

The last step of the methodology consists of obtaining the target NOFRFs, after the functional components have been found. However, as the calculations are based on the $\mathcal{Z}$-transform but the NOFRFs are computed in terms of the DTFT, care must be taken because the substitution $z = e^{j\omega}$ cannot always be done, *e.g.* when the input is sinusoidal or a step function. This is only problematic when using the analytical approach, so the computations will be discussed separately for the two approaches.

4.4.1 Numerical computation of NOFRFs

When computing the n-th order NOFRF using the numerical approach, the calculations are carried out using numerical sequences and DTFT evaluations via the FFT

4. NEW METHODS FOR COMPUTATION OF NOFRFS OF NONLINEAR SYSTEMS

algorithm. In this case, the NOFRFs can be computed as

$$G_n(e^{j\omega}) = \frac{Y_n(e^{j\omega})}{U_n(e^{j\omega})} \tag{4.67}$$

where

$$U_n(e^{j\omega}) = \text{DTFT}\{u(t)^n\} \tag{4.68}$$

$$Y_n(e^{j\omega}) = \text{DTFT}\{y_n(t)\} \tag{4.69}$$

The resulting numerical representation consists of a set of values of $G_n(e^{j\omega})$ for a finite number of frequency points $\omega_1 < \omega_2 < \ldots < \omega_{s(n)}$ that belong to the frequency support of $U_n(e^{j\omega})$, *i.e.*

$$G_n(e^{j\omega}) \Leftrightarrow \left[\begin{array}{cccc} G_n(e^{j\omega_1}) & G_n(e^{j\omega_2}) & \ldots & G_n(e^{j\omega_{s(n)}}) \end{array} \right]^T \tag{4.70}$$

The procedure can be summarised as Algorithm 7 below.

Algorithm 7 Numerical computation of the n-th order NOFRF

---

1. Obtain $y_n(t)$ by numerically solving the n-th order ALE

2. Compute $Y_n(e^{j\omega})$ as the DTFT of $y_n(t)$

3. Compute $U_n(e^{j\omega})$ as the DTFT of $u(t)^n$

4. Obtain the support samples of $U_n(e^{j\omega})$

5. Compute $G_n(\omega_i) = Y_n(e^{j\omega_i})/U_n(e^{j\omega_i})$ where ω_i belongs to the support of $U_n(e^{j\omega})$.

Generally speaking, numerical issues are not expected from Algorithm 7. However, attention is required because the computations need to be carried out only for the frequency support of $|U_n(e^{j\omega})|$. When FFT is used for evaluating DTFT, a large number of points will usually be outside the frequency support and, therefore, need to be discarded, in order to avoid inconsistent results.

4.4.2 Analytical computation of NOFRFs - general input

When the input signal $U(z)$ is rational, the functional components $Y_n(z)$ obtained through the analytical approach are also rational. This allows obtaining a closed form representation for the NOFRFs, which can be parametrised in terms of numerator and denominator coefficients as follows:

$$G_n(z) = \frac{Y_n(z)}{U_n(z)} = \frac{\sum_{k=0}^{P_n} \alpha_k \, z^k}{\sum_{k=0}^{Q_n} \beta_k \, z^k} \tag{4.71}$$

Notice that determining the coefficients α_k and β_k requires additional symbolic calculations, since the analytical approach provides $Y_n(z)$ and $U_n(z)$ in partial fraction forms only.

The analytical representation may be interesting in some situations, because a rational form can be simplified via pole-zero cancellation, similar to what is done with transfer functions, allowing the NOFRFs to be analysed in terms of minimum order rational functions. The analytical form is also more compact, as the number of numerator and denominator coefficients are usually less than the number of frequency points required for numerically representing the NOFRFs.

However, in applications such as fault diagnosis, it might be more effective to use the actual values of $G_n(e^{j\omega})$ at different ω rather than its parameters, as, sometimes, different parameters may yield NOFRFs that exhibit approximately the same behaviour, which could lead to false alarms. In this case, the procedure for evaluating the NOFRFs based on the analytical approach consists of using the algebraic representation of $G_n(z)$ for obtaining NOFRFs samples, as in (4.70). This can be carried out by using Algorithm 8 below.

It is important to notice that the numerical Algorithm 7 is usually suited for most situations as it can be applied for any input without any concerning issues. One drawback, however, is that if we wish to analyse the influence of varying parameters over the system properties, Algorithm 7 needs to be reapplied for every value of the vary-

---

Algorithm 8 Analytical computation of $G_n(e^{j\omega})$ in nonparametric form

---

1. Obtain $Y_n(z)$ by analytically solving the n-th order ALE

2. Obtain $U_n(z)$ in analytical form

3. Compute:

$$G_n(z) = \frac{Y_n(z)}{U_n(z)} = \frac{\sum_{k=0}^{P_n} \alpha_k\, z^k}{\sum_{k=0}^{Q_n} \beta_k\, z^k}$$

4. Compute the NOFRF by replacing $z = e^{j\omega}$ in $G_n(z)$ obtained in step 3

5. Evaluate $G_n(e^{j\omega})$ for $\omega = \{\omega_1, \dots, \omega_{s(n)}\}$

---

ing parameter under study. In this case Algorithm 8 is more suitable for the task, as the components $Y_n(z)$ can be solved in terms of the varying parameter, yielding an algebraic formula which can be rapidly evaluated for any of the parameter target values.

It is important to mention, however, that Algorithm 8 cannot be applied for some types of inputs, such as sinusoidal functions, because the DTFT of these signals cannot be described in rational form. In these situations, poles over the unit circle will occur and produce division by zero when we substitute $z = e^{j\omega}$ and evaluate the function for several ω. For these situations, a more specific procedure should be applied, which is discussed in the next section.

4.4.3 Analytical computation of NOFRFs - sinusoidal input

When the input $u(t)$ is sinusoidal with normalized frequency ω_h, its transform $U(z)$ has a pole over the unit circle at $e^{j\omega_h}$. As a consequence, the output components $Y_n(z)$ contain rational terms described by poles at $e^{jk\omega_h}$, $k \in \{0, \pm1, \dots, \pm n\}$. In this case, Algorithm 8 cannot be directly applied because the process of substituting $z = e^{j\omega}$

eventually leads to division by zero. This happens due to the non-existence of the DTFT for some signals (*e.g.* sinusoids), although their $\mathcal{Z}$-transform, so that the substitution $z = e^{j\omega}$ cannot be made.

This problem can be efficiently avoided by noticing that, for a sinusoidal input, the NOFRFs can only be computed at multiple integers of the input frequency, $k\omega_h$, $k = \{0, \pm 1, \ldots, \pm n\}$. In other words, the n-th order NOFRF can be computed as the ratio between the harmonics of $y_n(t)$ and the harmonics of $u(t)^n$. The harmonics of any periodic signal $x(t)$ can be easily found from its partial fraction representation as the residue of its transform $X(z)$ at pole $e^{jk\omega_h}$, i.e.: $\mathcal{R}_X(e^{jk\omega_h})$. Therefore, $G_n(e^{jk\omega_h})$ can be found using Algorithm 9 below:

Algorithm 9 Analytical computation of the n-th order NOFRF for a sinusoidal input

---

1. Obtain $Y_n(z)$ by analytically solving the n-th order ALE

2. Obtain $U_n(z)$ in analytical form

3. For $k \in \{0, \ldots, n\}$:

    3.1. Find $\mathcal{R}_{Y_n}(e^{jk\omega_h})$

    3.2. Find $\mathcal{R}_{U_n}(e^{jk\omega_h})$

    3.3. Compute the NOFRF as:

$$G_n(e^{jk\omega_h}) = \frac{\mathcal{R}_{Y_n}(e^{jk\omega_h})}{\mathcal{R}_{U_n}(e^{jk\omega_h})}$$

Notice that Algorithm 9 can be applied with ω_h represented as a numerical value or a symbolic quantity. The second case is more interesting because the NOFRFs can be evaluated for several different frequencies, providing system characteristics under different excitations. This can be considered as source of additional redundancy that can be useful for achieving diagnosis objectives.

4.5   Computation of harmonics and intermodulations

These new results can also be used for computing characteristics directly related to the output, in contrast to NOFRFs based ones, which are related to functional components. Some possibilities are computing harmonics, specific intermodulations or separating transient from steady state components in their exact form. This can be useful for revealing further details about system properties in various applications.

The computation of harmonics using the analytical approach allows finding functions that describe how each harmonic varies with the driving input frequency. This can be useful as the monitoring of harmonics is widely used in applications for characterising nonlinear behaviour; however, this is usually carried out for a single frequency. When a nonlinear model of the system is available, a function describing how the harmonics vary with the input frequency can provide additional redundancy that can be useful for characterising further system features.

The procedure for finding the harmonics is similar to Algorithm 9, except that it is carried out for $Y(z) = Y_1(z) + Y_2(z) + \ldots + Y_p(z)$, instead of $Y_n(z)$. The harmonics are simply found as:

$$H(k\omega_h) = \mathcal{R}_Y(e^{jk\omega_h}) \tag{4.72}$$

This idea can also be extended for finding general intermodulation response functions. In this case, it is assumed that the input is represented as a sum of sinusoids:

$$U(z) = A_0 + \sum_{k=1}^{r} \frac{A_k}{z - e^{j\omega_k}} \tag{4.73}$$

And the intermodulation component for which $\omega = \omega_1 + \ldots + \omega_s$ is found as:

$$I(\omega) = \sum \mathcal{R}_Y(e^{j\omega_1 + \ldots + j\omega_s}) \tag{4.74}$$

Similarly, steady state components can be distinguished from transients by separating PF components whose poles are over the unit circle from those whose poles are inside the circle.

4.5.1   A note about NOFRFs

It has been observed that some particular ALEs produce situations where the NOFRFs are input-independent and can be more directly computed. These will be investigated in this section.

Consider an example, where a second order ALE is described as:

$$A \, y_2(t) = b \, u(t-1)^2 \tag{4.75}$$

The usual procedure for computing $G_2(z)$ from (4.75) is obtaining $Y_2(z)$ using the analytical approach and the partial fraction formulation, and dividing the result by the analytical form of $U_2(z)$, which can be computed via frequency convolutions. However, by noticing that:

$$\mathcal{Z}\{u(t-1)^2\} = z^{-1}\mathcal{Z}\{u(t)^2\} = z^{-1}U_2(z) \tag{4.76}$$

the second order NOFRF can be obtained in a much simpler way as:

$$G_2(z) = \frac{Y_2(z)}{U_2(z)} = \frac{b \, z^{-1}}{A(z)} \tag{4.77}$$

It is important to notice that, in this case, the NOFRF is input independent, which greatly simplifies the analysis. This procedure can be extended to a slightly more general situation where several similar terms are present in the right-hand side, for instance:

$$A \, y_2(t) = c_1 \, u(t-1)^2 + c_2 \, u(t-2)^2 + \ldots + c_p \, u(t-p)^2 \tag{4.78}$$

Notice that although all terms are nonlinear, they only differ from each other by time shifts. Moreover, the time-shifting operation can be interchanged with the nonlinearity, i.e., the term $u(t-l)^2$ can be obtained

$$u(t) \xrightarrow{\text{delay}} u(t-l) \xrightarrow{\text{square}} u(t-1)^2 \tag{4.79}$$

$$u(t) \xrightarrow{\text{square}} u(t)^2 \xrightarrow{\text{delay}} u(t-1)^2 \tag{4.80}$$

91

4. NEW METHODS FOR COMPUTATION OF NOFRFS OF NONLINEAR SYSTEMS

Therefore, the $\mathcal{Z}$-transform of any right-hand side term of (4.78) can be obtained as:

$$\mathcal{Z}\{u(t-l)^2\} = z^{-l}U_2(z) \tag{4.81}$$

Therefore, the NOFRF can be found as:

$$G_2(z) = \frac{c_1\,z^{-1} + c_2\,z^{-2} + \ldots + c_p\,z^{-p}}{A(z)} \tag{4.82}$$

which is, again, input independent. It is possible to conclude, then, that whenever the right-hand sides of the ALEs are in the same form as on the right-hand side of (4.78), the NOFRFs will be input independent.

Another possible situation arises from a different type of nonlinearity. For example, let:

$$A\,y_2(t) = c_1\,u(t-1)u(t-2) \tag{4.83}$$

In this case, it is difficult to establish a relationship between the $\mathcal{Z}$-transform of $u(t-1)u(t-2)$ and $U(z)$ and infer about the input independence of G_2. However, consider:

$$A\,y_2(t) = c_1\,u(t-1)u(t-2) + c_2\,u(t-3)u(t-4) \tag{4.84}$$

By noticing that:

$$\mathcal{Z}\{u(t-1)u(t-2)\} = z^{-1}\,\mathcal{Z}\{u(t)u(t-1)\} \tag{4.85}$$

$$= z^{-1}\,U'(z) \tag{4.86}$$

$$\mathcal{Z}\{u(t-3)u(t-4)\} = z^{-3}\,\mathcal{Z}\{u(t)u(t-1)\} \tag{4.87}$$

$$= z^{-3}\,U'(z) \tag{4.88}$$

equation (4.84) can be rewritten in the frequency domain as:

$$A(z)\,Y_2(z) = (c_1\,z^{-1} + c_2\,z^{-3})U'(z) \tag{4.89}$$

for which it is reasonable to define the filter:

$$G'(z) = \frac{c_1\,z^{-1} + c_2\,z^{-3}}{A(z)} \tag{4.90}$$

as one of the main characteristics of $Y_2(z)$. Obviously, a complete characterisation of the response requires analysing the nonlinear effects of term $u(t)u(t-1)$, which can be carried out using the frequency convolution approach. Also notice that the frequency support of $u(t)u(t-l)$ is the same support of $u(t)^2$, for any l. This means that dividing $Y_2(z)$ by the transforms of either should yield a FRF with the same properties of NOFRFs as currently defined.

The main point of these examples is that some nonlinear terms on the n-th order ALE right-hand sides can be clustered together according to their delaying properties and corresponding frequency representations. These clusters naturally form input-independent FRFs that play an important role in the composition of the spectrum of the n-th order component.

This reasoning is only possible for discrete-time systems, for which the delaying operation can be interchanged with the nonlinearities, *i.e.* $u(t-1)^2$ can be obtained as a delay and a squaring operations, or vice-versa. This does not apply for the continuous-time case, as this commutativity is not valid for terms based on derivatives, such as $\dot{u}(t)^2$.

4.6 Continuous-time case

Most of the results presented so far have been derived for DT systems, since the main objective of this research is to apply the developed techniques to practical DT models obtained from system identification and input-output data. However, these results can be extended to CT systems, which can be useful for analysing models obtained from first principles. This will be briefly discussed in this section.

The derivation of the system ALEs for the CT case follows the same principles of

the DT case, except for some minor differences. Usually, CT systems are represented
as differential equations, so that the CT equivalent of model (4.1) can be written as:

$$A\,y(t) = B\,u(t) + \sum_{m=1}^{M} c_m \prod_{l=0}^{L-1} \left(\frac{d^l y(t)}{dt^l}\right)^{p(m,l)} \left(\frac{d^l u(t)}{dt^l}\right)^{q(m,l)} \tag{4.91}$$

where

$$A\,y(t) = \frac{d^L y(t)}{dt^L} + \sum_{l=0}^{L-1} a_l \frac{d^l y(t)}{dt^l} \tag{4.92}$$

$$B\,u(t) = \sum_{l=0}^{L-1} b_l \frac{d^l u(t)}{dt^l} \tag{4.93}$$

As can be seen, the CT representation merely replaces a l-sample delay by the l-th
order derivative of signals. Because this does not affect the properties of operator $\mathcal{D}$,
the algorithm derivation and results are exactly the same and its implementation only
requires replacing delays by derivatives. Therefore, the CT-equivalent of equations
(4.5)-(4.6) can be described as:

$$A\,y_n(t) = B\,u(t) \qquad\qquad\qquad n = 1 \tag{4.94}$$

$$A\,y_n(t) = \sum_{m=1}^{M} c_m\,\psi_m(t) \sum_{S_m} \rho_m\,\phi_m(t) \tag{4.95}$$

where ρ_m is as described in (4.7) and:

$$\psi_m(t) = \prod_{l=0}^{L-1} \left[\frac{d^l u(t)}{dt^l}\right]^{q(m,l)} \tag{4.96}$$

$$\phi_m(t) = \prod_{l=0}^{L-1} \prod_{k=1}^{N_m} \left[\frac{d^l y_k(t)}{dt^l}\right]^{r(m,l,k)} \tag{4.97}$$

On the other hand, it is worth mentioning that a model of form (4.91) may not
be useful for analytical analysis of the ALEs, as it will be demonstrated in Section
4.7. This is due to the analytical framework that has been established being based on
partial fraction decomposition of signals, and the presence of derivatives can sometimes
compromise these forms. For this reason, it may be useful to consider an integral
formulation of model (4.91), as it is possible to guarantee that model operators will not

alter partial fraction forms. This can be accomplished by letting:

$$\tilde{y}(t) = \frac{d^L y(t)}{dt^L} \tag{4.98}$$

$$\tilde{u}(t) = \frac{d^L u(t)}{dt^L} \tag{4.99}$$

so that:

$$\frac{d^l y(t)}{dt^l} = \underbrace{\int_0^t \cdots \int_0^{\tau_3} \int_0^{\tau_2}}_{L-l} \tilde{y}(\tau_1) d\tau_1 d\tau_2 \ldots dt = \Delta^l \tilde{y}(t) \tag{4.100}$$

$$\frac{d^l u(t)}{dt^l} = \underbrace{\int_0^t \cdots \int_0^{\tau_1}}_{L-l} \tilde{u}(\tau_1) d\tau_1 \ldots dt = \Delta^l \tilde{u}(t) \tag{4.101}$$

and (4.91) can be rewritten as:

$$A\,\tilde{y}(t) = B\,\tilde{u}(t) + \sum_{m=1}^{M} c_m \prod_{l=1}^{L} \left(\Delta^l \tilde{y}(t)\right)^{p(m,l)} \left(\Delta^l u(t)\right)^{q(m,l)} \tag{4.102}$$

where

$$A\,\tilde{y}(t) = \tilde{y}(t) + \sum_{l=1}^{L} a_l\,\Delta^l \tilde{y}(t) \tag{4.103}$$

$$B\,\tilde{u}(t) = \sum_{l=1}^{L} b_l\,\Delta^l \tilde{u}(t) \tag{4.104}$$

The analysis of functionals order is not affected by the newly introduced operator Δ. Moreover, the form of model (4.102) is exactly the same as the DT model (4.1), which means that the ALEs can be obtained as (4.5)-(4.6) by simply replacing $u(t-l)$ and $y_k(t-l)$ respectively by $\Delta^l \tilde{u}(t)$ and $\Delta^l \tilde{y}_k(t)$. Obviously, when solutions are found, the original output signal must be recovered by differentiating the signal L times, as suggested by (4.98).

4.7 Example

To demonstrate the procedures presented in this chapter, a simple example will be used. To this end, consider the NARX model:

$$A\,y(t) = b\,u(t-1) + c\,y(t-2)^2 u(t-1) \tag{4.105}$$

where $b = 2$, $c = 5 \cdot 10^{-3}$ and:

$$A(z) = (z - 0.8 - j\,0.5)(z - 0.8 + j\,0.5)\,z^{-2} \tag{4.106}$$

Determination of the ALEs

For determining the ALEs up to order 3, the procedure is as follows. For $n = 1$:

$$A\,y_1(t) = b\,u(t - 1) \tag{4.107}$$

For $n = 2$, $J_1 = 2 - 3 = -1$, yielding the Diophantine system:

$$\begin{cases} 0 & = 2 \\ 0 & = -1 \end{cases} \tag{4.108}$$

which is inconsistent and implies that:

$$A\,y_2(t) = 0 \tag{4.109}$$

For $n = 3$, $J_1 = 3 - 3 + 1 = 1$, yielding:

$$\begin{cases} r(1, 1, 1) & = 2 \\ 0 & = 0 \end{cases} \tag{4.110}$$

which has only one solution which is already explicitly described as (4.110). This solution can be converted into the 3-rd order ALE described as:

$$A\,y_3(t) = c_1\,y_1(t - 2)^2\,u(t - 1) \tag{4.111}$$

Because of equation (4.109), $y_2(t) = 0$ and the ALEs can be further simplified before the characteristics are computed, yielding the following group of ALEs.

$$A\,y_1(t) = B\,u(t) \tag{4.112}$$

$$A\,y_3(t) = c_1\,y_1(t - 2)^2\,u(t - 1) \tag{4.113}$$

Sinusoidal probing

The procedures presented in sections 4.4.3 will be used for computing the nonparametric form of NOFRFs for a sinusoidal input. To this end, let $u(t)$ be a sinusoidal sequence of normalized frequency ω_h. The NOFRFs shall be computed for 100 different values of ω_h logarithmically spaced between 10^{-3} and $3 \cdot 10^{-1}$. Both analytical and numerical approaches will be used for the purpose of validating the results, i.e.: the NOFRFs computed via different approaches will be compared for verifying if they represent the same result.

The analytical forms of the NOFRFs computed at the harmonics are found as:

$$G_1(e^{j\omega_h}) = \frac{2.0\, e^{j\omega_h}}{0.89 - 1.6\, e^{j\omega_h} + e^{j2\omega_h}} \tag{4.114}$$

$$G_3(e^{j\omega_h}) = \frac{a_0 + a_1\, e^{j\omega_h} + \ldots + a_5\, e^{j5\omega_k}}{b_0 + b_1\, e^{j\omega_h} + \ldots + b_8\, e^{j8\omega_k}} \tag{4.115}$$

$$G_3(e^{j3\omega_h}) = \frac{0.02\, e^{j3\omega_h}}{c_0 + c_1\, e^{j\omega_h} + \ldots + c_{10}\, e^{j10\omega_h}} \tag{4.116}$$

where:

$$c_{10} = +1.0000 \cdot 10^{+0}$$

$$b_8 = +1.0000 \cdot 10^{+0} \qquad c_9 = -3.2000 \cdot 10^{+0}$$

$$b_7 = -6.5980 \cdot 10^{+0} \qquad c_8 = +4.3400 \cdot 10^{+0}$$

$$a_5 = +1.4980 \cdot 10^{-2} \qquad b_6 = +2.0100 \cdot 10^{+1} \qquad c_7 = -4.4480 \cdot 10^{+0}$$

$$a_4 = -2.3970 \cdot 10^{-2} \qquad b_5 = -3.6640 \cdot 10^{+1} \qquad c_6 = +5.9120 \cdot 10^{+0}$$

$$a_3 = +2.0000 \cdot 10^{-2} \qquad b_4 = +4.3560 \cdot 10^{+1} \qquad c_5 = -6.9440 \cdot 10^{+0}$$

$$a_2 = -1.1990 \cdot 10^{-2} \qquad b_3 = -3.4560 \cdot 10^{+1} \qquad c_4 = +5.4470 \cdot 10^{+0}$$

$$a_1 = +7.4910 \cdot 10^{-3} \qquad b_2 = +1.7890 \cdot 10^{+1} \qquad c_3 = -4.1150 \cdot 10^{+0}$$

$$a_0 = +0.0000 \cdot 10^{+0} \qquad b_1 = -5.5390 \cdot 10^{+0} \qquad c_2 = +3.8630 \cdot 10^{+0}$$

$$b_0 = +7.9210 \cdot 10^{-1} \qquad c_1 = -2.5350 \cdot 10^{+0}$$

$$c_0 = +7.0500 \cdot 10^{-1}$$

Figure 4.1 shows the comparison between the analytical and numerical calculations. The analytical results have been plotted with a normal line, while numerical results

4. NEW METHODS FOR COMPUTATION OF NOFRFS OF NONLINEAR SYSTEMS

are indicated with an "x" marker. It is important to mention that $G_3(e^{j3\omega_h})$ has only been computed up to $\omega = 0.3\pi$, since higher frequencies would yield third-order harmonics that would violate the Nyquist criterion. Figure 4.1 shows that there is a good agreement between results obtained from different methods.
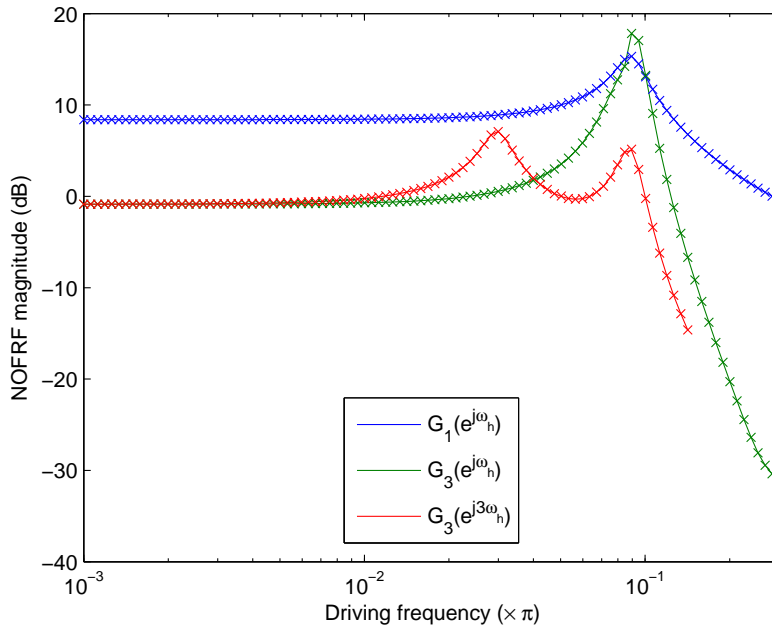
Figure 4.1: Comparison between NOFRFs computations.

Figure 4.1 also shows some interesting properties. More specifically, $G_3(e^{j3\omega_h})$ exhibits two resonance peaks, in contrast to the single peaks observed in $G_1(e^{j\omega_h})$ and $G_3(e^{j\omega_h})$, for which a single resonance peak is observed at approximately 0.09π. This is mainly due to the system linear characteristics, which can considerably affect both first and third order dynamics. On the other hand $G_3(e^{j3\omega_h})$ is affected only by third order components, and admits energy transfer between different bands. This is observed as the additional resonance peak at approximately 0.03π. This value is three times smaller than the original resonance, which is a nonlinear phenomenon typically related to polynomial nonlinearities. Harmonic excitations with this frequency are expected to

generate larger third order harmonics.

Sinc probing

The impulse response is an important characteristic of linear systems, because it provides, via a single input signal, the same information obtained from multiple sinusoidal excitations. This is not valid for nonlinear systems, since the superposition principle is not valid and this equivalence cannot be established. However, the impulse response transform is still an useful characteristic, since it can, in principle, describe how the system responds to an idealised case where the input possess a very large bandwidth.

However, the nonlinear components due to an impulse excitation can sometimes vanish for zero initial conditions, due to the particular forms of the system nonlinearities. This situation is problematic because it masks the system nonlinear characteristics, since the nonlinear components cannot be studied. This is the case of system (4.105), which can be better understood by analysing (4.113). When the input is the unit impulse, $u(t) = \delta(t)$ and the right-hand side term can be simplified as:

$$c\,y_1(t-2)^2 u(t-1) = c\,y_1(t-2)^2\delta(t-1)$$
$$= c\,y_1(-1)^2\delta(t-1)$$
$$= 0$$

since $y_n(t) = 0$ for $t < 0$ and any n. In fact, for system (4.105), the right-hand sides of all higher order ALEs ($n > 1$) vanish when $u(t) = \delta(t)$, yielding $y_n(t) = 0$ and preventing the investigation of higher order characteristics through this input.

For circumventing these difficulties, a non-ideal impulse function can be used. A non-ideal impulse is any function that possesses a short duration and a relatively broad and flat spectrum. One example is the sinc pulse, described as:

$$u(t) = \operatorname{sinc}\left(2bt - 2bt_0\right) h(t) \tag{4.117}$$

where b is the normalised bandwidth and t_0 is the pulse center. The sequence $h(t)$ is a Hamming windowing function used for reducing frequency leakage. The sinc function is defined as:

$$\mathrm{sinc}(x) = \begin{cases} \dfrac{\sin(\pi x)}{\pi x} & x \neq 0 \\ 1 & x = 0 \end{cases} \tag{4.118}$$

Notice that the n-th order NOFRF can only be reliably computed for $|\omega| \leq nb$, since $U_n(e^{j\omega})$ is zero otherwise. In addition, b should be chosen so that, for the largest n, nb does not exceed the Nyquist frequency.

The NOFRFs of system (4.105) for a 7000-sample sinc pulse were computed, using $b = 0.1\pi$ and $t_0 = 3500$. Figure 4.2 shows the first and third order generalised spectra. Figure 4.3 shows the magnitude of the resulting NOFRFs up to $3b = 0.3\pi$.
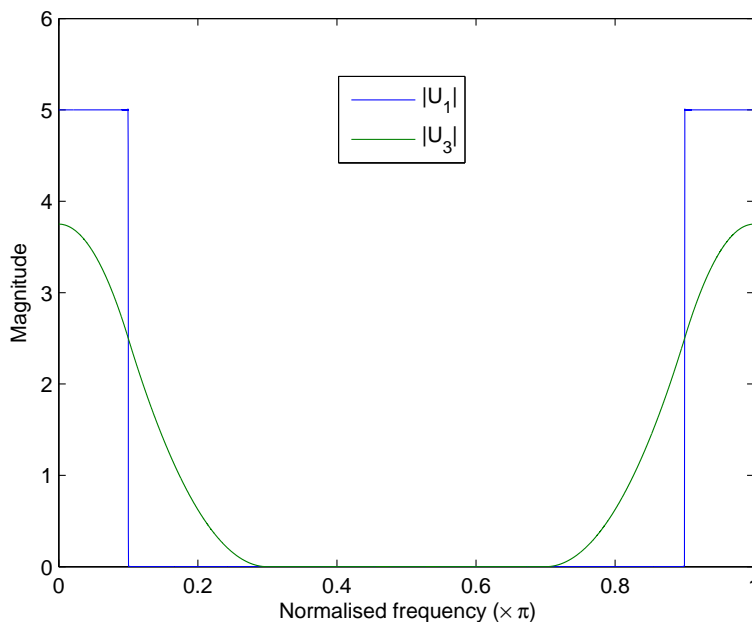
Figure 4.2: Generalised input spectra
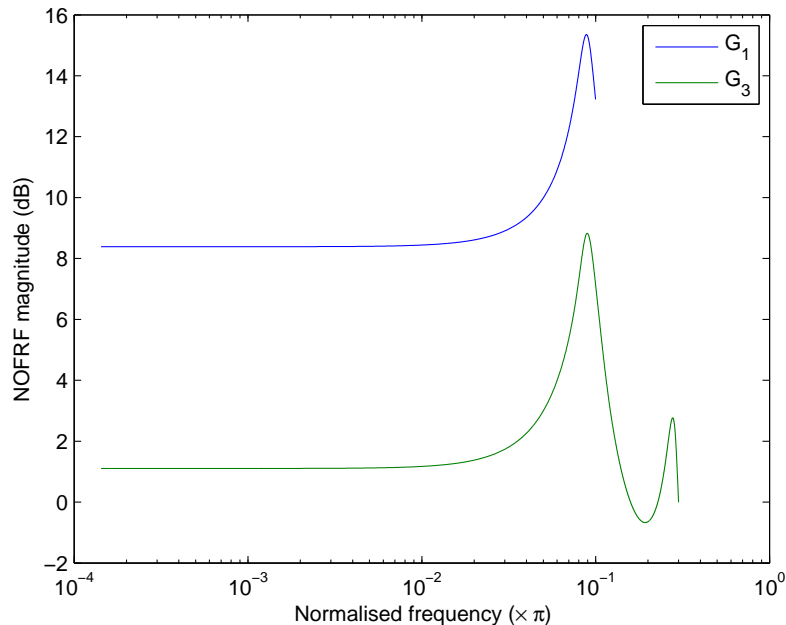
Figure 4.3: NOFRFs computed with sinc input

4.8 Conclusions

In this chapter, several new tools for computing NOFRFs were presented. These represent significant improvements over the previous approaches to this problem, as it is now possible to obtain the NOFRFs directly from a polynomial NARX model, both in numerical and analytical form, without needing to specify the truncation order in advance.

The results presented in chapter 3 regarding the extraction of the system ALEs were formalized, allowing a more efficient and systematic derivation of the recursive equations from a relatively general NARX model. This is particularly useful in practical situations where the models are obtained from real data and usually consist of several complex polynomial terms.

It was also demonstrated that these methods allow the computation of NOFRFs in both numerical and analytical forms. The numerical approach allows a fast computation

for an arbitrary input. The analytical approach, on the other hand, yields NOFRFs in rational form and, if necessary, in terms of varying parameters, such as the input frequency or a model coefficient, so its influence over the system response can be studied in more depth, which can be very useful for design. However, these computations can only be carried out for inputs that possess a closed form representation in the frequency domain, such as the impulse function and sinusoids.

The analytical computations are founded in the Residue Theorem, which allows computing the NOFRFs using only frequency domain operations and, therefore, avoiding alternating between different domains. However, when dealing with practical models with a large number of poles and nonlinear terms, the complexity of the calculations can be considerably large, causing accuracy and processing issues. It was then demonstrated that these problems can be alleviated by representing the transforms involved in the frequency convolutions into their corresponding partial fraction forms. In this way, the frequency convolutions are broken into much simpler operations which can be efficiently solved using a table look-up scheme, allowing the computation of higher order components in closed form.

This new set of tools provides an useful background for nonlinear systems analysis in the frequency domain. This will be better illustrated in the next chapter, where the applications of these new results to CM problems will be presented.

5

A new CM framework based on NOFRFs

5.1 Introduction

In this chapter, the theoretical results developed so far will be applied to condition monitoring problems. The aim is to investigate a systematic way of using NOFRFs in practical applications. This will be pursued by studying two specific problems, in order to identify the basic steps of the methodologies, so it can be generalised later.

The problems to be investigated are a simulated bilinear oscillator and an mechanical prototype used for studying the dynamics of impact systems. The bilinear oscillator consists of a single degree of freedom system that possesses the stiffness term described by piecewise linear function. It can be considered as an important benchmark in nonlinear systems studies, because it can exhibit both moderate (*e.g.* harmonics generations) and complex behaviours (*e.g.* bifurcation). The study conducted in this chapter, however, is carried out in conditions where only the moderate behaviours are observed, so that the Volterra series approach can be applied. The objective is to apply a condition monitoring philosophy in which it is assumed that the physical background about

the system is unknown, with the exception of the measurement of a few meaningful monitoring variables (*e.g.* the stiffness ratio). In this case, a black-box modelling approach is proposed for establishing the relationship between the input and output signals. It is also assumed that this relationship carries important physical information, characterised by the NOFRFs, which can be used for monitoring the variations of the monitoring parameter. It is then demonstrated that some NOFRFs based features can indeed be used for characterising the parameter changes, as it is progressively increased.

The second application problem is concerned with a laboratory prototype used for studying impact systems, developed by the University of Aberdeen. Under some simplifying assumptions, the bilinear oscillator investigated in the first case study can be seen as a simplified model of this system. However, the real prototype exhibits some additional challenges, such as the presence of modelling errors and noise. These circumstances make it difficult to extend the approach used in the first case study to this second problem. In this case, a different solution was developed, in which the system conditions to be monitored were grouped according to their similarities, *i.e.* they were not viewed as individual conditions controlled by the continuous variations of a parameters, but as cluster of similar conditions that can be characterised by a set of features that are geometrically localised close to each other on the representative feature space. Therefore, the task of condition monitoring is reduced to a classification problem that consists of computing the features associated to an unknown condition and classifying it into one of the known clusters, in order to characterise the fault conditions.

Before the case studies are discussed in more details, some basic concepts about condition monitoring problems will be discussed. After that, the general idea of the methodology will be explained, followed by the case studies. The chapter is finalised by a discussion that generalises the methodologies discussed in cases studies 1 and 2, so that they can be applied to address more problems.

5.2 Condition monitoring problems

As explained in Chapter 1, the need for strategies that automatically detect malfunctions in engineering systems is directly related to the growth and complexity of modern industrial processes. The aim of condition monitoring strategies is to fulfill this need, by providing ways of anticipating malfunctions which are difficult to be detected by human operators.

The term condition monitoring is usually employed in different engineering fields such as mechanical and structural engineering to refer to problems where the state of system critical components such as gears, shafts and structure materials is to be determined, often via inspection and tests, so that maintenance or repairs can be planned in a more optimised way (Barron, 1996). In order to do this, advanced measuring and signal processing techniques are used for identifying features that are capable of evidencing, explaining and possibly predicting the evolution of the component condition. Such methods are being increasingly investigated because some traditional ways of assessing structure or material condition involve invasive techniques, which is obviously economically infeasible. For this reason, CM strategies are closely related to Non-Destructive Testing (Buyukozturk et al., 2012).

Figure 5.1 shows the general strategy of traditional CM methods. In most cases, the basic idea is to acquire output data from the process during operation and analyse that data for finding useful features from which the process condition can be inferred. Usually, these features are quantities derived from specialised signal processing, *e.g.* statistical or spectral analysis (very common in vibration based CM), which are highly correlated to process changes. Once the features are extracted, the CM process is carried out, via, for instance, threshold checking or more complicated logic procedures.

This process usually requires some *a priori* information about the system, built from physical knowledge or process history. For example, in some vibration based CM, some common sources of problems are cracks or mass unbalance (Barron, 1996). In these
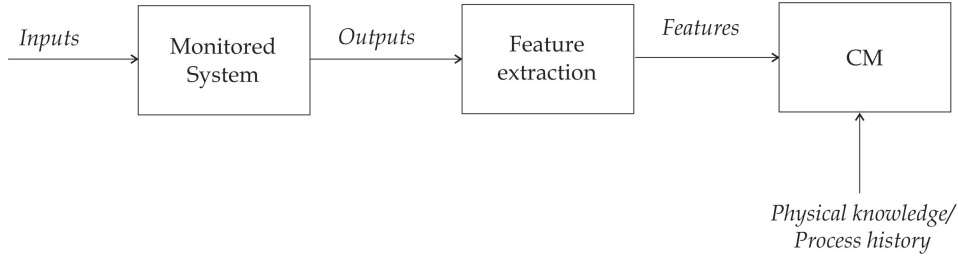
Figure 5.1: Traditional CM overview

cases, the symptoms are the abnormal levels of measured vibration (more specifically, acceleration, velocity or displacement) collected at different locations of the structure. The fault is usually explained as changes in the structure natural frequencies, which are greatly affected by cracks and mass unbalance; these changes tend to shift the structure natural frequencies to locations in the same range of frequencies of external inputs, which is what causes the large amplitudes of the structure response. This is a typical use of *a priori* knowledge applied to CM solutions.

It is worth mentioning that these principles are very similar to the fault diagnosis (FD) scenario, in particular, approaches based on parameter estimation (Isermann, 1993). The basic idea of this methodology is illustrated in Figure 5.2. The parameter estimation strategy is based in the principles that some fundamental physical properties of the system change when it is subject to abnormal conditions (Isermann, 2006; Venkatasubramanian et al., 2003c), similar to what was previously discussed about natural frequencies in CM problems. Notice that this formulation about faults should not be confused with what is used in other FD approaches in which faults are considered as unknown inputs, *e.g.* in parity equations (Chan et al., 2006) and observer based (Venkatasubramanian et al., 2003c) methods.

In some common parameter estimation FD approaches, the *a priori* physical knowledge about the system is used to construct a physical model whose parameters (*e.g.* model coefficients) are directly linked to system components. During on-line operation, these parameters are estimated and passed to the feature extraction stage. The
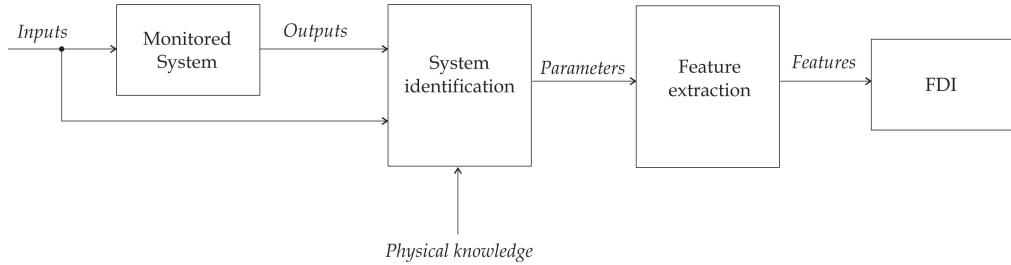
Figure 5.2: Oveview of parameter estimation based FDI

features can be the error between the estimate and a pre-specified nominal value or a more application oriented variable. Finally, the computed features are used in the FDI - Fault Detection and Isolation stage (Venkatasubramanian et al., 2003c; Isermann, 2006). The term *detection* refers to the binary task of verifying if a fault occurred or the system is working normally, while the term *isolation* can be interpreted as the diagnosis itself, where additional information about the fault is determined (*e.g.* fault location, severity, etc).

One important difference between CM as described in Figure 5.1 and FDI as described in Figure 5.2 is that FDI is usually carried out in real time - *e.g.* using recursive schemes (Isermann, 1993, 2005), while CM is more commonly done off-line (Barron, 1996). FDI is designed to work on-line because it is often applied to control loops, where a quick detection of faults is important. However, a more important aspect in the FDI scheme is that features are generated from model parameters, while in CM these are produced directly from output measurements. In this case, system identification can be seen as a pre-processing stage that generates primary features, *i.e.* model/model parameters, from which the actual fault features are later derived. This is a reasonable solution, since faults are assumed to possess a close relationship with the system physical properties, which should be, in principle, better observed from the model rather than a particular set of outputs, since the model carries information about how the system responds to a larger range of inputs.

The methodology proposed in this thesis lies in between the CM and FDI concepts

discussed so far. The basic idea is shown in Figure 5.3. The principle is very similar to the FDI scheme, where feature extraction is preceded by a system identification stage. The fundamental difference, however, is that system identification is done using a black-box polynomial NARX approach. This is useful because the physical *a priori* knowledge does not need to be taken into account at this stage, making the modelling process more systematic.
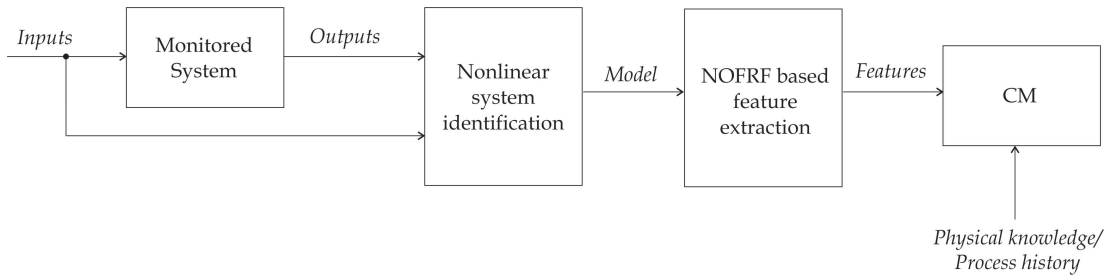
Figure 5.3: Overview of NOFRF based CM

In addition, the adoption of a nonlinear strategy allows the possibility of investigating system properties which could be difficult to observe if a linear model were used. This is additionally supported by the feature extraction stage, which is centred in the NOFRF approach. Once the NOFRFs based features are generated, the CM strategy, which can be designed either from physical knowledge or process history can be applied. The details about how this CM strategy can be developed is presented in the next section.

5.3   General framework

In this section, a few general considerations about the new NOFRF based CM framework will be discussed. The objective is to establish some problem assumption, in order to deal with CM problems involving nonlinear systems and feature generators based on the NOFRF approach.

For building CM system, it will be generally assumed that a detailed physical model

of the process is not available. This is consistent with many practical situations where the complexity and size of the process makes such modelling assumptions prohibitive. On the other hand, it will be assumed that input-output data is available, so that black-box models can be constructed for investigating the system characteristics.

The next important assumption is that a collection of data sets gathered during normal operation and under a few fault cases is available. This data form the core of the *a priori* knowledge that will be used for designing/training the CM system. It will also be assumed that, although faults are directly related to disturbances in physical parameters (*e.g.* material stiffness, electrical impedance), the actual values of these parameters are not necessarily known.

This means that each element of the *a priori* data set can be related to a known system condition, but this condition might not be well defined in terms of measurable quantities. Obviously, it is a more favourable situation if such information is available, so that it can be used for improving the diagnosis process. This is also a relatively reasonable assumption as it is the case of many practical situations, *e.g.* in crack detection in structures, where the characteristics of the crack (such as its geometry) not only are difficult to model, but also difficult to be quantified/measured; a similar problem occurs in monitoring of bearings and gear boxes.

Under these assumptions, the proposed CM scheme can be designed in the following steps: (i) identify a polynomial NARX model for each available fault case; (ii) compute the NOFRFs from the resulting models for each fault case; (iii) derive features from the NOFRFs that allow distinguishing between different fault cases; (iv) develop a classification procedure or a decision logic for characterising each fault case. This procedure is summarised in Figure 5.4.

Once the CM system has been designed, the diagnosis procedure can be conducted in a similar manner, as shown in Figure 5.5, except that the computed features represent an unknown system condition and need to be associated to one of the known fault
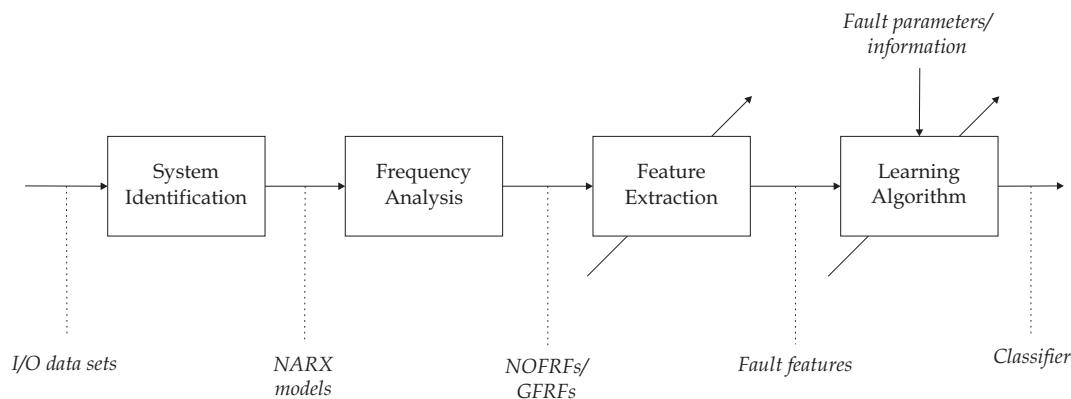
Figure 5.4: General diagnosis system design based on the new framework

cases. This can be interpreted as a classification or pattern recognition procedure (Theodoridis and Koutroumbas, 2008). Notice, however, that in exceptional cases where fault parameters are well defined, the diagnosis can also be given in terms of a continuous estimate of the faulty parameters. In this case, the problem can also be viewed as a classification/pattern recognition procedure, although the number of possible classes is infinite.
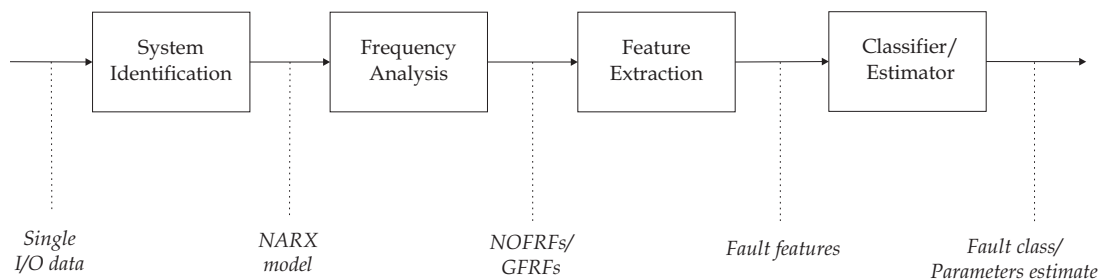
Figure 5.5: General diagnosis procedure based on the new framework

The proposed framework offers two fundamental features that are attractive for practical applications:

1. The modelling procedure is based on polynomial NARX models. This is interesting because it allows to expand the horizon of potential features by considering physical properties associated to nonlinear behaviour, while also making

the modelling process more systematic, which can be useful when physical knowledge about the process is scarce and process history data is abundant;

2. Features are computed in terms of GFRFs/NOFRFs. This is the main novelty of the framework, since nonlinear FRF representation has not been much explored in this kind of application. Nonlinear FRFs have been used in other scenarios (Lang and Peng, 2008; Peng et al., 2007a,b,?) where it was demonstrated that they can reveal interesting nonlinear systems' properties that not only cannot be studied using classical linear FRFs, but also can provide a more in-depth background for characterising faulty behaviour.

It is important to mention that although NOFRFs are generally preferred, GFRFs can also be used as fault features candidates (Tang et al., 2010). The new Algorithm 1 from chapter 3 makes this option more attractive, as GFRFs can be efficiently computed from general NARX models. However, this is seldom recommended because the multidimensional nature of the GFRFs makes the feature extraction process much more difficult. For this reason, only NOFRFs were explored in this work.

In the next sections, the principles of this new CM framework will be applied to address two CM problems. The objective is to verify the framework's feasibility and discuss some aspects that are important for the performance of the diagnosis system, but are relatively context-dependent and need to be investigated according to each particular situation.

5.4   Case study 1: bilinear oscillator simulation study

A simulation test of the CM strategy was carried out using a bilinear oscillator. This system is largely used for modelling important phenomena regarding impact and behaviour of cracked structures (Peng et al., 2007). The oscillator is inherently nonlinear and can exhibit a wide variety of nonlinear behaviour, including several types of bifur-

5. A NEW CM FRAMEWORK BASED ON NOFRFS

cations (Wiercigroch and Sin, 1998).

The bilinear oscillator is represented by a piecewise linear differential equation described as:

$$\begin{cases} \ddot{y}(t) + c\,\dot{y}(t) + k\,y(t) = u(t) & y(t) > 0 \\ \ddot{y}(t) + c\,\dot{y}(t) + k\,\beta\,y(t) = u(t) & y(t) \leq 0 \end{cases} \tag{5.1}$$

In the present study, parameters $c = 23.562$ and $k = 3.55 \cdot 10^4$ are assumed free of variations. The parameter values were extracted from (Peng et al., 2007) where a NOFRFs-based study of the bilinear oscillator was conducted. Parameter β is known as the *stiffness ratio* parameter, since it describes the relative change of the linear stiffness when the output undergoes variations from $y(t) \leq 0$ to $y(t) > 0$. In this case study, we shall investigate the system behaviour when β changes in the range $0.8 \leq \beta \leq 1.0$. Notice that for $\beta = 1$, the system becomes purely linear.

Variations in β can produce qualitative changes in the system nonlinear behaviour, therefore, monitoring β is an important way of tracking the system main characteristics. For example, in drilling processes, this simplified model can be used for better understanding the efficiency of the drill with respect to the static force applied to the rig. Attuning axial ultrasonic vibrations in the equipment is an efficient way of optimizing this and can be done by modelling the characteristics of the drilled material (Wiercigroch et al., 2005, 1999), which is mainly characterised by β. Different stiffness ratios can occur throughout the process due to different materials found by the drill, therefore, it is important to find a way to monitor changes in β. The problem can be formulated as a multiplicative condition monitoring situation with a single parameter.

Because of the system nonlinear characteristics, it is difficult to establish an explicit relationship between β and the output. Therefore, a monitoring procedure based on NOFRFs is proposed. As previously stated, the first step for designing such diagnosis system is to obtain models for different values of β. This was done using 10 different

values of β in the specified range and a chirp input described as:

$$u(t) = \sin\left[(0.1\omega_0 + 1.5\omega_0 t)t\right] \tag{5.2}$$

where $\omega_0 = \sqrt{k} = 188.4144$ is the system linear natural frequency. Data were initially sampled at 1000 Hertz and then down-sampled by a factor of 3. This step is usually required when the sampling period is over specified, which produces very similar consecutive samples and compromises the model identification.

NARMAX models with maximum delay $L = 4$ and nonlinearities up to order 3 were identified using the PRESS method. For the purpose of analysis, the moving average terms are neglected yielding NARX representations. Some of these models are shown bellow for the nonlinear cases with the smallest and largest β and the linear case. The full set of models is presented in Appendix A

$$
\left.
\begin{aligned}
y(t) \quad &= +8.3703 \cdot 10^{-06}\, u(t-1) \\
&+1.6590 \cdot 10^{+00}\, y(t-1) \\
&-9.3108 \cdot 10^{-01}\, y(t-2) \\
&+3.8721 \cdot 10^{-02}\, y(t-1)\, u(t-2) \\
&+6.4094 \cdot 10^{-03}\, y(t-4)\, u(t-5) \\
&-8.5746 \cdot 10^{-07}\, u(t-1)\, u(t-3)
\end{aligned}
\right\} \quad \beta = 0.80 \tag{5.3}
$$

$$
\left.
\begin{aligned}
y(t) \quad &= +8.8783 \cdot 10^{-06}\, u(t-1) \\
&+1.0634 \cdot 10^{+00}\, y(t-1) \\
&-5.2897 \cdot 10^{-01}\, y(t-3) \\
&+1.1440 \cdot 10^{-07}\, u(t-5) \\
&+5.4534 \cdot 10^{-03}\, y(t-1)\, u(t-2) \\
&+1.8209 \cdot 10^{-03}\, y(t-3)\, u(t-5) \\
&+4.1658 \cdot 10^{-06}\, u(t-2) \\
&-5.5919 \cdot 10^{-08}\, u(t-1)\, u(t-3)
\end{aligned}
\right\} \quad \beta = 0.98 \tag{5.4}
$$

$$
\left.\begin{aligned}
y(t) \quad &= +1.0603 \cdot 10^{+00}\, y(t-1) \\
&-5.3216 \cdot 10^{-01}\, y(t-3) \\
&+1.0570 \cdot 10^{-05}\, u(t-1) \\
&+3.3237 \cdot 10^{-06}\, u(t-3) \\
&-8.9887 \cdot 10^{-08}\, u(t-5) \\
&-1.4714 \cdot 10^{-09}\, u(t-1)\,u(t-2) \\
&-5.1091 \cdot 10^{-07}\, u(t-4) \\
&-7.3380 \cdot 10^{-10}\, u(t-5).^2 \\
&+1.8035 \cdot 10^{-09}\, u(t-2).^2
\end{aligned}\right\} \quad \beta = 1.00 \qquad (5.5)
$$

Notice that as β increases, not only model parameters change, but new model terms are included. This makes model comparison via the time-domain representation a difficult task, and justifies the use of a frequency-domain non-parametric representation such as the NOFRFs.

Sinusoidal characteristics

The sinusoidal response characteristics of each model was investigated using Algorithm 9 described in Section 4.4.3. To this end, a sinusoidal input of frequency ω_h is applied to the models and the NOFRFs are computed and analysed as a function of ω_h. The analytical approach was used to carry out this study, since the resulting representation is more flexible and compact.

In this study, only $G_1(e^{j\omega_h})$ and $G_2(e^{j2\omega_h})$ were computed, since it was noted that $G_2(0)$ does not add any significant information towards the monitoring goals. The analytical form of the linear FRFs is described as:

$$
G_1(e^{j\omega_h}) = \frac{B_1(e^{j\omega_h})}{A_1(e^{j\omega_h})} \qquad (5.6)
$$

where $p = e^{j\omega_h}$ and polynomials $A_1(e^{j\omega_h})$ and $B_1(e^{j\omega_h})$ for the cases $\beta = 0.80$, $\beta = 0.98$ and $\beta = 1.00$ are obtained from identified model i the corresponding case of β as given

below:

$$\beta = 0.80 \begin{cases} B_1(e^{j\omega_h}) = 8.3703 \cdot 10^{-6} \, p \\ A_1(e^{j\omega_h}) = p^2 - 1.6590 \, p + 0.9311 \end{cases} \tag{5.7}$$

$$\beta = 0.98 \begin{cases} B_1(e^{j\omega_h}) = 8.8783 \cdot 10^{-6} \left(p^4 + 0.4692 \, p^3 + 0.0129 \right) \\ A_1(e^{j\omega_h}) = p^5 - 1.0634 \, p^4 + 0.5290 \, p^2 \end{cases} \tag{5.8}$$

$$\beta = 1.00 \begin{cases} B_1(e^{j\omega_h}) = 1.0570 \cdot 10^{-5} \left(p^4 + 0.3145 \, p^2 - 0.0483 \, p - 0.0085 \right) \\ A_1(e^{j\omega_h}) = p^5 - 1.0603 \, p^4 + 0.5322 \, p^2 \end{cases} \tag{5.9}$$

The full set of polynomials for all studied cases are given in Appendix B.

For the second order NOFRFs, the general expression is similar and described as:

$$G_2(e^{j2\omega_h}) = \frac{B_2(e^{j\omega_h})}{A_2(e^{j\omega_h})}$$

where polynomials $B_2(e^{j\omega_h})$ and $A_2(e^{j\omega_h})$ are now described as:

$$\beta = 0.80 \begin{cases} B_2(e^{j\omega_h}) &= 1.4225 \cdot 10^{-6} \left(-0.3749 \, p^{11} + p^{10} - 0.5612 \, p^9 + 0.0377 \, p^5 \right) \\ A_2(e^{j\omega_h}) &= p^{15} - 1.6590 \, p^{14} - 0.7279 \, p^{13} + 2.7522 \, p^{12} - 0.6136 \, p^{11} \\ &\quad -1.5446 \, p^{10} + 0.8669 \, p^9 \end{cases} \tag{5.10}$$

$$\beta = 0.98 \begin{cases} B_2(e^{j\omega_h}) &= 8.2181 \cdot 10^{-8} \left(-0.0913 \, p^{15} + p^{14} - 0.3599 \, p^{12} + 0.0076 \, p^{11} \right. \\ &\qquad \left. +0.1967 \, p^{10} + 0.0923 \, p^9 + 0.0025 \, p^6 \right) \\ A_2(e^{j\omega_h}) &= p^{19} - 1.0634 \, p^{18} - 1.0634 \, p^{17} + 1.6597 \, p^{16} - 0.5625 \, p^{14} \\ &\quad +0.5290 \, p^{13} - 0.5625 \, p^{12} + 0.2798 \, p^{10} \end{cases}$$

$$\tag{5.11}$$

$$\beta = 1.00 \begin{cases} B_2(e^{j\omega_h}) &= 1.8035 \cdot 10^{-9} \left(-0.8159 \, p^{13} + p^{12} - 0.4069 \, p^6 \right) \\ A_2(e^{j\omega_h}) &= p^{16} - 1.0603 \, p^{14} + 0.5322 \, p^{10} \end{cases} \tag{5.12}$$

and the coefficients for all cases are provided in Appendix B.

Figures 5.8 and 5.9 show the magnitude of $G_1(e^{j\omega_h})$ and $G_2(e^{j2\omega_h})$ for different input frequencies ω_h and β.

A more in-depth analysis demonstrates that changes can be observed in $G_1(e^{j\omega_h})$, although they are not as significant as in $G_2(e^{j2\omega_h})$. The changes in $G_2(e^{j2\omega_h})$ occur
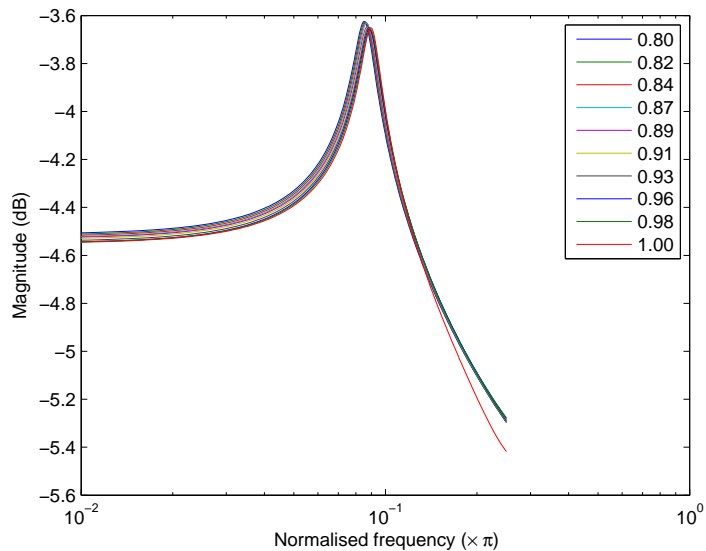
Figure 5.6: $G_1(e^{j\omega_h})$ for bilinear oscillator
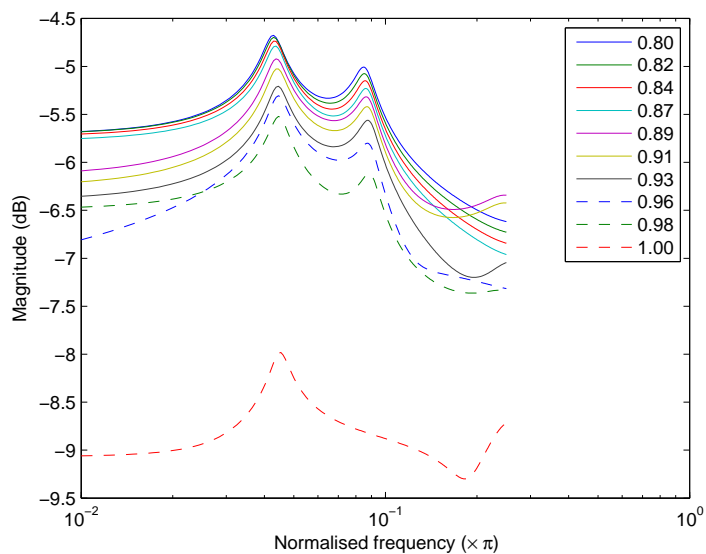
Figure 5.7: $G_2(e^{j2\omega_h})$ for bilinear oscillator

for all frequencies and in a relatively monotonic way. Therefore, a first investigation about these variations was carried out using the resonance characteristics of $G_1(e^{j\omega_h})$ and $G_2(e^{j2\omega_h})$, which are shown in Figures 5.8-5.11. The resonance characteristics are

the maxima of $|G_1(e^{j\omega_h})|$ and $|G_2(e^{j2\omega_h})|$ and their corresponding frequencies.

It is important to notice that $G_2(e^{j2\omega_h})$ possess an additional sub-resonance at approximately half the linear resonance frequency. The exception is the case for which $\beta = 1$ which is a purely linear case and no resonances can be observed in $|G_2(e^{j2\omega_h})|$, so that the case $\beta = 1.00$ is not shown in Figures 5.8-5.11.
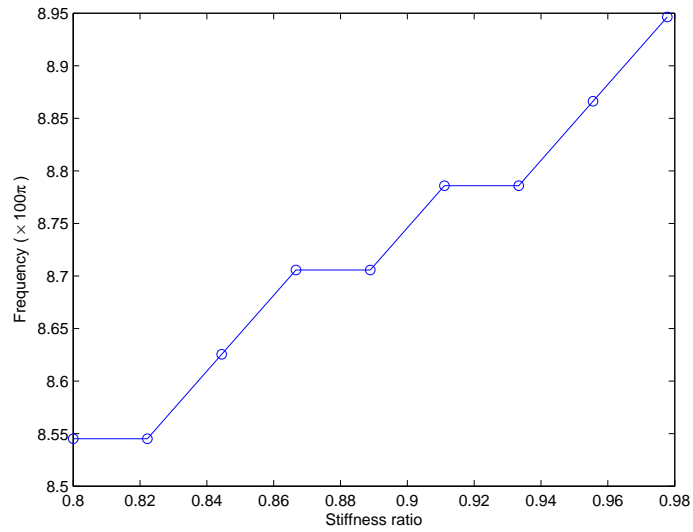
Figure 5.8: Resonance frequencies of $G_1(e^{j\omega_h})$

Figures 5.8-5.9 suggest that the resonance frequencies are not appropriate monitoring functions for β, since some variations in β result in no changes in these properties. In addition, the overall change in the resonance frequencies as β changes from 0.80 to 0.98 is very small: for $G_1(e^{j\omega_h})$, the total variation is 0.40; for $G_2(e^{j2\omega_h})$ the total variation is approximately 0.15 for the first resonance and 0.3 for the second resonance. This is problematic because such small changes can be mistaken with modelling errors. In addition, the second resonance of $G_2(e^{j2\omega_h})$ possess an anomalous behaviour at $\beta = 0.96$, where the resonance frequency decreases. This is a source of ambiguity (*i.e.* two different β that generate the same resonance frequency), that should either be avoided in practice or be used in conjunction with additional monitoring variables.
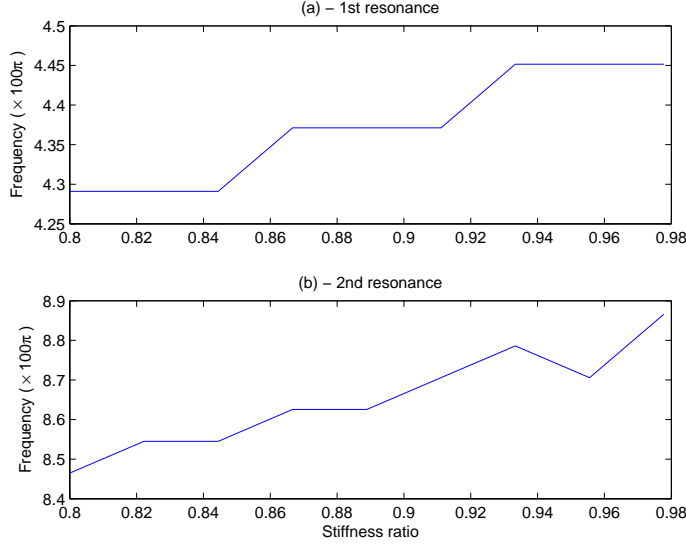
Figure 5.9: Resonance frequencies of $G_2(e^{j2\omega_h})$

Resonance peaks show a more favourable scenario for monitoring β, as shown in Figures 5.10 and 5.11. The first peak of $G_1(e^{j\omega_h})$ shows a strictly decreasing trend, although it is non-smooth. However, the total variation is relatively small: approximately 0.4 dB. This is reasonable though, as β is related to the system's nonlinear characteristics, which should be better observed from $G_2(e^{j2\omega_h})$. This is indeed the case, as seen in Figure 5.11, which exhibits a total decrease of 8 dB in the first resonance peak and 12 dB at the second resonance peak. In addition, the variations of the resonance peaks of $G_2(e^{j2\omega_h})$ are very smooth and completely monotonic, which makes these features ideal for monitoring β.

Based on these findings, a simple curve fitting procedure was conducted for building a 3-rd order polynomial function that can provide β from the resonance peaks measurements. The functions were found as:

$$\beta = 0.01169\, r_1^3 - 0.08731\, r_1^2 - 0.31\, r_1 - 4.909 \tag{5.13}$$

$$\beta = -0.0589\, r_2^3 - 0.1181\, r_2^2 - 0.2558\, r_2 - 5.303 \tag{5.14}$$
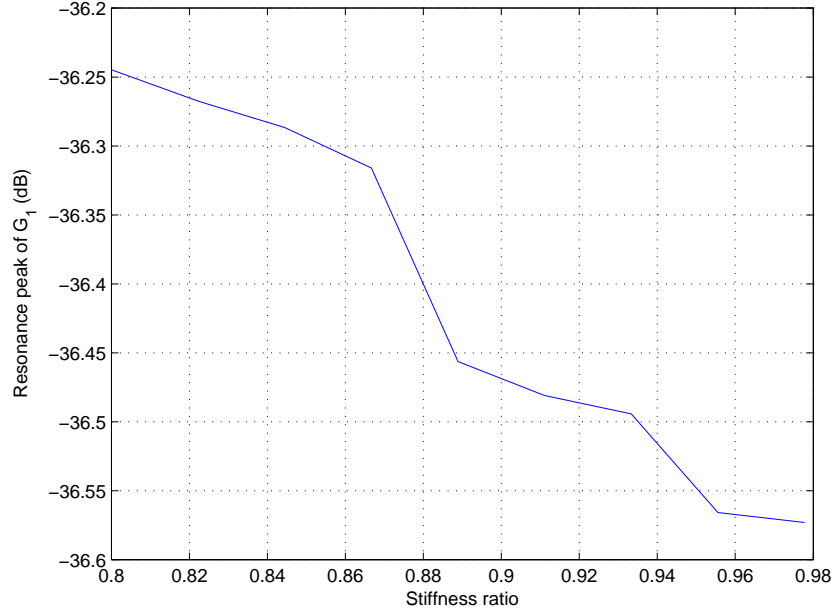
Figure 5.10: Resonance peaks of $G_1(e^{j\omega_h})$

where r_1 and r_2 denote the size of the first and second resonance peaks of $G_2(e^{j2\omega_h})$ in dB, respectively.

Notice that the choice of the resonance peaks of the NOFRFs is relatively arbitrary for this particular study case, since their behaviour for varying β is basically the same for almost all other frequencies. The exceptions are frequencies below 0.02, where the values of $G_2(e^{j2\omega_h})$ for $\beta = 0.96$ become smaller than what is observed for $\beta = 0.98$ (see Figure 5.7), which yields an ambiguity in the monitoring function. A similar behaviour is observed at some frequencies greater than 0.1. These results show that a complete monitoring procedure for β can be achieved via features based on sinusoidal NOFRFs.

Notice that the analytical approach is more convenient for this investigation because the features consisted of different NOFRFs evaluated at different input frequencies. If these were computed from the numerical approach, the steady state response would have to be extracted from a model simulation for each frequency, which is obviously a
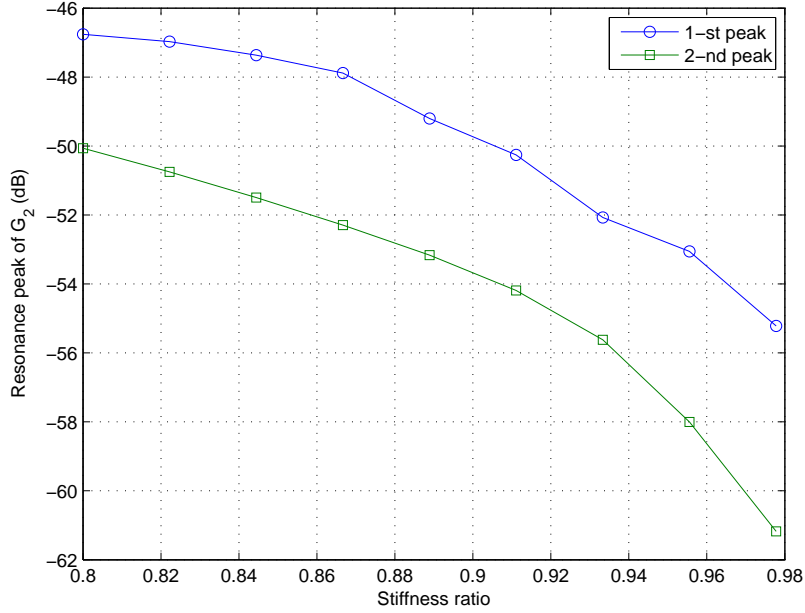
Figure 5.11: Resonance peaks of $G_2(e^{j2\omega_h})$

more laborious procedure.

Non-sinusoidal features

An additional investigation was carried out using a more simplified approach, in which the system is probed by a single input (instead of several sinusoids) whose energy is more widespread over the normalised frequency range. The most natural choice for this investigation is an ideal unit impulse:

$$u_0(t) = \delta(t) = \begin{cases} 1 & t = 0 \\ 0 & t \neq 0 \end{cases} \tag{5.15}$$

for which the energy is uniformly distributed over the whole normalised frequency range.

The NOFRFs for this input were determined using the analytical method, yielding

the $\mathcal{Z}$ domain representations as follows. The first order FRF is represented as:

$$G_1(z) = \frac{B_1(z)}{A_1(z)} \tag{5.16}$$

where the polynomials $B_1(z)$ and $A_1(z)$, for each analysed β, are described as:

$$\beta = 0.80 \begin{cases} B_1(z) & = 8.3703 \cdot 10^{-6}\, z \\ A_1(z) & = z^2 - 1.6590\, z + 0.9311 \end{cases} \tag{5.17}$$

$$\beta = 0.98 \begin{cases} B_1(z) & = 8.8783 \cdot 10^{-6}\left(z^4 + 0.4692\, z^3 + 0.0129 \right) \\ A_1(z) & = z^5 - 1.0634\, z^4 + 0.5290\, z^2 \end{cases} \tag{5.18}$$

$$\beta = 1.00 \begin{cases} B_1(z) & = 1.0570 \cdot 10^{-5}\left(z^4 + 0.3145\, z^2 - 0.0483\, z - 0.0085 \right) \\ A_1(z) & = z^5 - 1.0603\, z^4 + 0.5322\, z^2 \end{cases} \tag{5.19}$$

Notice that, as in the previous case, only a few cases were shown. The remaining NOFRFs are shown in Appendix C

Similarly, the second order NOFRF is represented as:

$$G_2(z) = \frac{B_2(z)}{A_2(z)} \tag{5.20}$$

where $B_2(z)$ and $A_2(z)$ are now described as:

$$\beta = 0.80 \begin{cases} B_2(z) & = 3.2411 \cdot 10^{-7}\left(z^3 + 0.1655 \right) \\ A_2(z) & = z^5 - 1.6590\, z^4 + 0.9311\, z^3 \end{cases} \tag{5.21}$$

$$\beta = 0.98 \begin{cases} B_2(z) & = 4.8417 \cdot 10^{-8}\left(z^3 + 0.5117 \right) \\ A_2(z) & = z^5 - 1.0634\, z^4 + 0.5290\, z^2 \end{cases} \tag{5.22}$$

$$\beta = 1.00 \begin{cases} B_2(z) & = 0.0000 \\ A_2(z) & = 1 \end{cases} \tag{5.23}$$

These formulas allow a more efficient extraction of the DFT representation of the NOFRFs, by simply letting $z = e^{j\omega}$ and evaluating the result for discrete values of ω. The magnitudes of NOFRFs obtained in this way are shown in Figures 5.12-5.13.
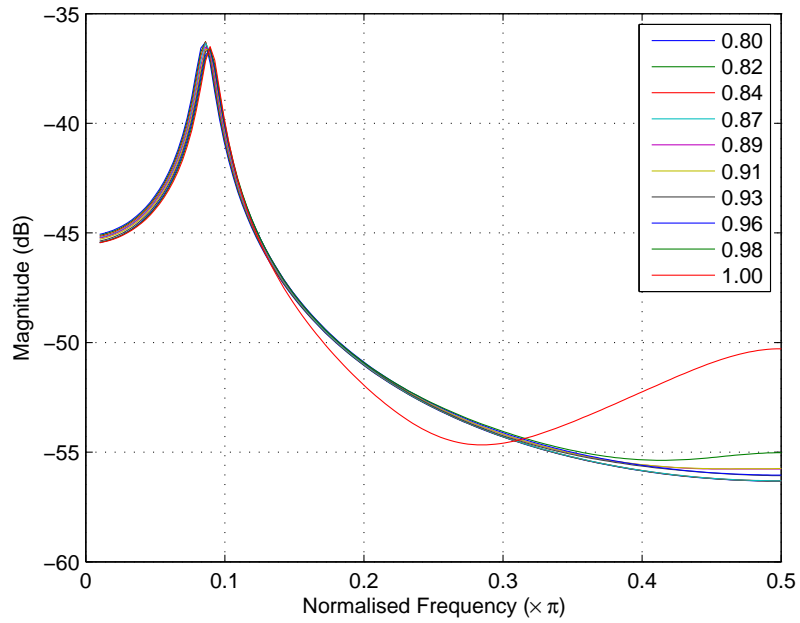
Figure 5.12: Linear FRFs for the impact oscillator
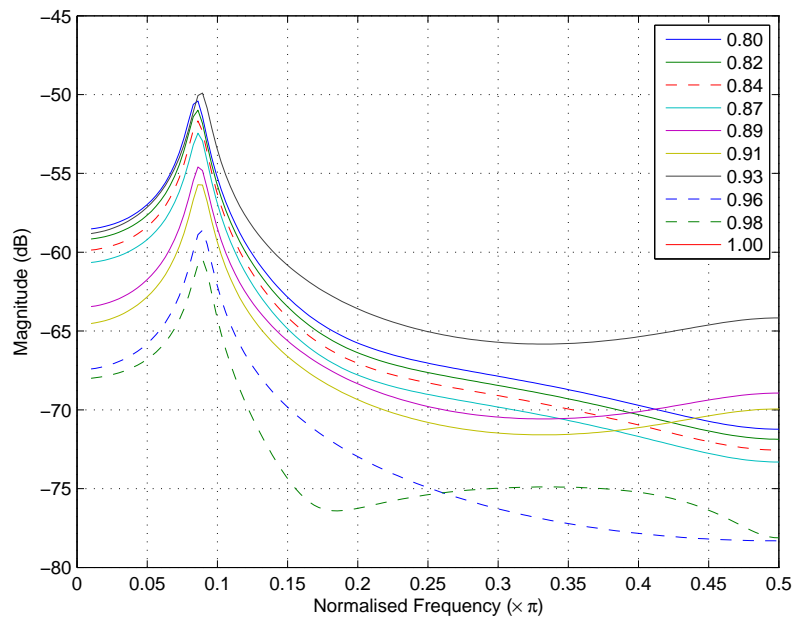
Figure 5.13: Second order NOFRFs for the impact oscillator

As in the sinusoidal case, different values of β cannot be well distinguished from the linear FRF. Notice, however, that the magnitude trends of the second order NOFRFs are not as monotonic as in the sinusoidal case. From Figure 5.13, we can see that they follow a different pattern and introduce ambiguities, which are problematic as discussed before. This can be explained from the multitone nature of the probing input, which allows energy transfers between different bands, producing more complicated spectra that are unsuited for the established monitoring goals.

One way to circumvent these difficulties is to use an alternative impulse function, as discussed in Section 4.7. In this case, we adopt the windowed sinc pulse:

$$u(t) = 2\,b\,\text{sinc}\,(2\,b\,t - 2\,b\,t_0)\,h(t - t_0) \tag{5.24}$$

where b is the bandwidth, t_0 is the pulse center and $h(t)$ is the Hamming window. It has been observed that the bandwidth b can be varied for yielding a more appropriate probing signal. In this case, the NOFRFs need to be computed via the numerical approach, Algorithm 7.

To illustrate this, the NOFRFs were computed for $b = 0.05$ and $b = 0.08$, using 300 samples of the input sequence. In order to simplify the results and generate a low dimensional feature, the following index was computed:

$$I_2 = \frac{\sum_{\Omega_2} |G_2(e^{j\omega})|^2}{\sum_{\Omega_1} |G_1(e^{j\omega})|^2} \tag{5.25}$$

where Ω_1 and Ω_2 are the frequency supports of $G_1(e^{j\omega})$ and $G_2(e^{j\omega})$ respectively.

Due to the input characteristics, these supports basically consists of discrete frequencies uniformly spaced in the intervals $[0, 2\pi b]$ for Ω_1 and $[0, 4\pi b]$ for Ω_2. The index basically reflects the weight of nonlinearities relative to the system linear characteristics. Therefore, the objective is to track the decrease of the system nonlinear behaviour as β increases towards 1.00, where the system becomes linear.

The index was plotted against β for various bandwidth values in Figure 5.14. The curves suggest that the optimal range for b is approximately between 0.05 and 0.08,

where the variation of the index with β is smooth and monotonic. For $b < 0.05$ the index shows non-monotonicity at $\beta = 0.98$, while for $b > 0.10$ the index shows a similar undesired behaviour at $\beta = 0.94$. The case where $b = 0.10$ can be considered acceptable, although the change of the index from $\beta = 0.96$ to $\beta = 0.98$ is very small, but still follows the decreasing trend.
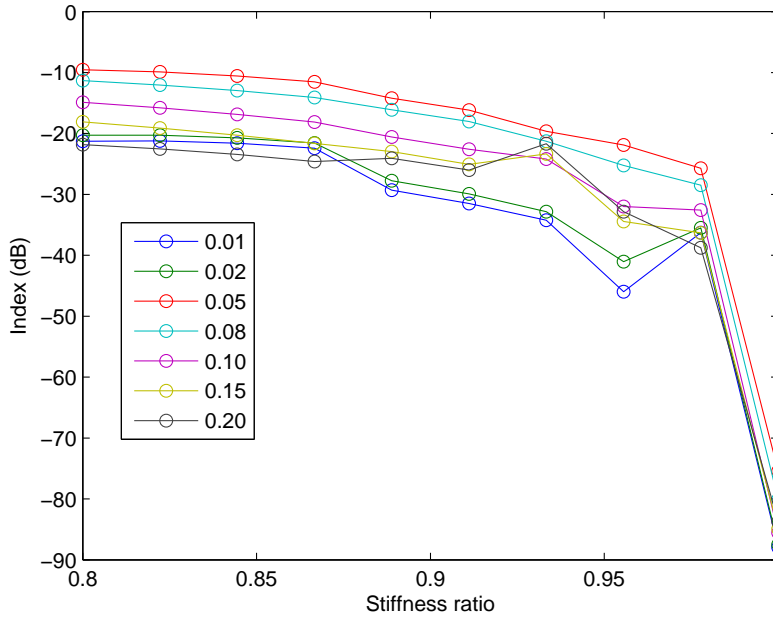
Figure 5.14: Index I_2 for different values of the input bandwidth B

This example shows that probing the system model for specific characteristics is not always a trivial task, especially when multiple fault cases are involved. The new frequency analysis framework is useful in this context, because it allows optimising the NOFRF features towards the fault isolation goals.

5.5 Case study 2: experimental impact oscillator

The simulation results of the previous section were confronted with experimental data produced by a real prototype of the impact oscillator, built at the Centre for Applied

Dynamics Research, School of Engineering, Kings College, Aberdeen University.

The oscillator consists of the rig originally studied in (Wiercigroch and Sin, 1998) and later adapted in (Ing, 2008). The experimental apparatus is illustrated in Figure 5.15. The rig operates over a dynamic shaker and consists of a block of mild steel weighting 1 kg, supported by two parallel leaf springs that permits vertical displacement and prevents rotational motion. The lengths of the leaf springs can be varied for adjusting the system's primary stiffness. Large amplitude vibrations produce contact between the mass and one or two removable spring steel beams. The gap between those can be adjusted via extendible bolts and by changing the size of the beams. In this form an independent control of the secondary stiffness can be achieved.

The displacement of the leaf springs at the fixed end is used as the source of displacement measurement, using an eddy current probe, whose voltage-displacement characteristics were experimentally determined via a specific test and a least squares fit. The base acceleration, which can be considered as the input, is measured using accelerometers. Data is sampled using a National Instruments PCI-MIO-16E-1 acquisition board in conjunction with Labview at the rate of 2000 samples/second.

The tests were carried out for twelve stiffness ratios (β): 19.01, 20.92, 22.14, 24.36, 24.51, 26.96, 28.22, 31.24, 32.69, 34.72, 36.19, and 38.30. For each of these cases, a sinusoidal excitation with frequency 7 Hz was applied at throughout three different experiments. It is worth mentioning that this is not the ideal choice of excitation for an identification experiment, but it was the only available option for the circumstances at the time the experiments were conducted.

Data was initially smoothed using the Savitsky-Golay algorithm (Savitzky and Golay, 1964) and down-sampled by a factor of 12. This was necessary as the presence of noise and the high sample rate can compromise the identification, yielding unstable models. One NARX model was identified for each available β, each describing the relationship between the base acceleration (input) and the mass displacement (output).

Figure 5.15: Rig prototype (by the University of Aberdeen)

Both ERR and PRESS approaches were used for this task. However, PRESS provided models with a very reduced number of terms and inconsistent responses, which for

this reason were discarded. ERR provided more satisfactory models, but had to be adjusted for using pure input terms, *e.g.* $u(t-1)$, $u(t-2)^2$, $u(t-1)u(t-3)$, etc., because the inclusion of output terms was often producing unstable models. In order to improve model generalisation, each estimation was carried out by using data from all three waveforms collected for each β. This significantly improved model prediction, as it provided a reasonable alternative for compensating the narrow bandwidth of the input used for the experiments. A comparison between the measured output and model prediction is provided in Figures 5.16 and 5.17
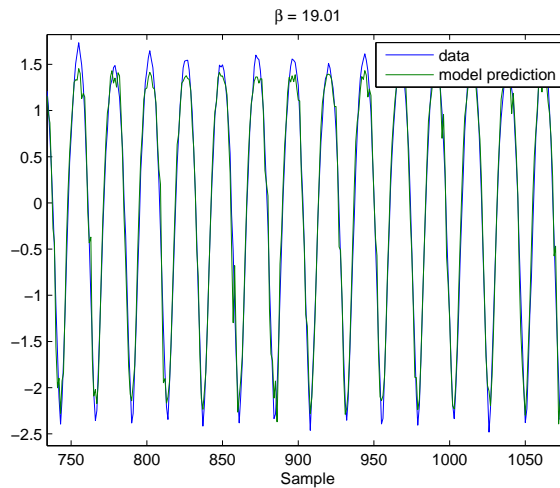
Figure 5.16: Steady state model prediction, $\beta = 19.01$

It is worth mentioning that obtaining satisfactory models for the system was a much more difficult task than in the simulation case, as the obtained models were occasionally unstable or yielded bad predictions. These difficulties can be attributed to three main reasons:

1. Increased complexity of the system in comparison to the idealised simulation model

2. Presence of random noise in the measurements
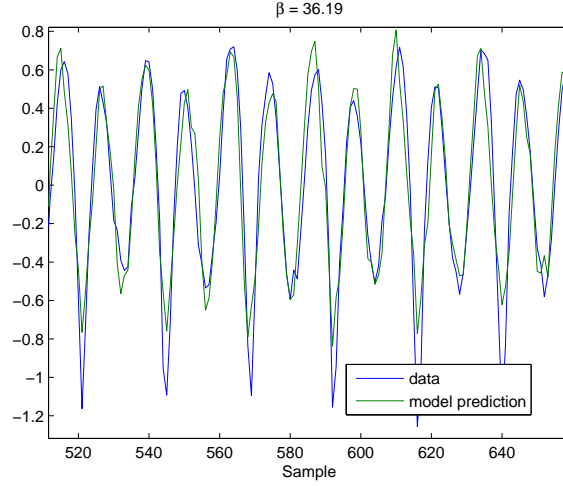
Figure 5.17: Steady sate model prediction, $\beta = 36.19$

3. Narrow band excitation (sinusoid), preventing the acquirement of more detailed information about the system

The list of identified models is given in Appendix D. As in the simulation case, changing the stiffness ratio causes the model structure to change significantly, but in a way that cannot be easily distinguished from the difference equation. The presence of noise is an additional complication, since, in these circumstances, repeating the identification procedure during real time operation can produce different models, even though β might not have changed.

A preliminary analysis based on the sinc pulse (5.24) similarly to the previous section was conducted for the identified models. As before, several different bandwidths were tested, in the attempt of finding features that exhibit a monotonic trend. The results of a few tests in which $0.001 \leq b \leq 0.15$ are shown in Figure 5.18. In these tests, an increasing trend can be observed for all indices, although it was not possible to find a probing input that resulted on an index that behaves monotonically for all β samples. This is mainly caused by the presence of noise, which introduces severe variations in model structure and consequently in the NOFRFs, preventing the obser-

vation of smooth monitoring functions based on index (5.25). This was also observed in a previous (although not presented) simulation test in which the inclusion of noise produced similar behaviour in the index values.
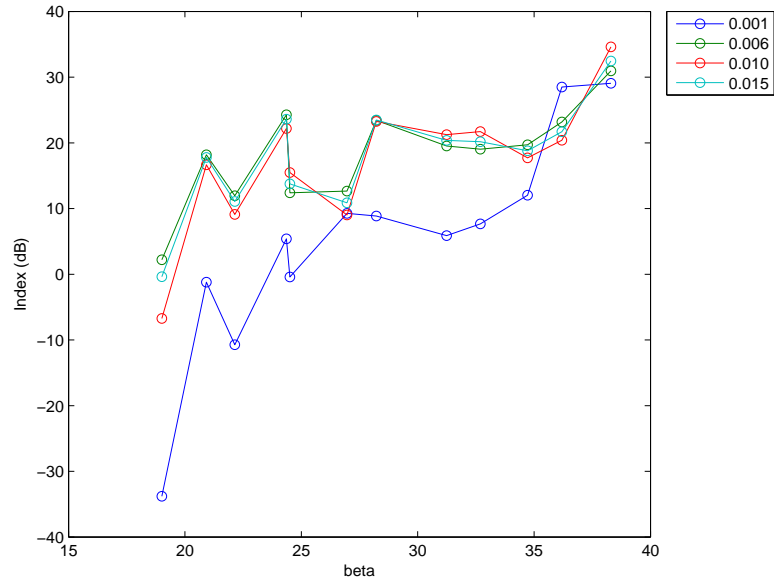
Figure 5.18: Index computed for different input bandwidth (experimental rig)

Due to the stochastic nature of the data, a second attempt based on sinusoidal features and statistical processing was carried out for improving the monitoring strategy. As in case study 1, the objective was to obtain the NOFRFs for sinusoidal inputs of different frequencies and use this information for deriving the monitoring procedure. However, the diagnosis objectives had to be slightly shifted towards a classification/clustering approach.

The basic idea consists of partitioning all fault cases using the k-means clustering algorithm. Because each fault is represented by a single variable in this application, this clustering procedure is equivalent to dividing the *a priori* stiffness ratio range into small intervals. However, the clustering algorithm is a more systematic approach, since it is more adequate for situations where faults are represented by multiple parameters.

5. A NEW CM FRAMEWORK BASED ON NOFRFS

The diagnosis strategy consists of associating an unknown fault to one of the established clusters, by using features derived from NOFRF data. Due to the presence of noise, it is reasonable to consider several NOFRF frequency components in the attempt to provide sufficient redundancy. However, using a large number of NOFRF measurements brings issues for characterising and visualising the clusters. To circumvent this problem, a new reduced set of features produced by linear transformations designed via PCA/PLS is proposed. The resulting features are considered adequate if the features associated to a particular cluster remain on a well defined region, with little overlap between clusters. In this case study, both PCA and PLS approaches were computed for verifying which one provides the best results.

PCA works as an unsupervised feature generation, in which the clustering results are not used, while PLS directly use this information for providing feature separation. The main objective of these techniques is to reduce the dimensionality of the original NOFRF data for better characterising each fault cluster. The resulting features can be considered adequate if the features associated to a particular cluster remain on a well defined region, with small overlapping between different clusters.

The primary NOFRF features were computed by extracting the sinusoidal NOFRFs from the models obtained for each β, and building the basic NOFRF data vector described as:

$$\boldsymbol{x}(\beta) = \left[\begin{array}{cccccc} M_1(\omega_1) & \ldots & M_1(\omega_s) & M_2(\omega_1) & \ldots & M_2(\omega_s) \end{array} \right] \qquad (5.26)$$

where

$$M_1(\omega_h) = \log_{10} |G_1(e^{j\omega_h})| \qquad (5.27)$$

$$M_2(\omega_h) = \log_{10} |G_2(e^{j2\omega_h})| \qquad (5.28)$$

For convenience, the input frequencies ω_h were logarithmically spaced in the interval $[2\pi \cdot 10^{-4}, 0.2\pi]$. After some tests, it was noticed that a large number of points is not able to produce significantly better features, therefore only $s = 5$ frequencies were used,

yielding $\omega_h \in \{0.0001\pi, 0.0007\pi, 0.0045\pi, 0.0299\pi, 0.2\pi\}$. After computing the data vectors, the following data matrix was constructed:

$$
X = \begin{bmatrix}
x(19.01) \\
x(20.92) \\
\vdots \\
x(36.19) \\
x(38.30)
\end{bmatrix}
\tag{5.29}
$$

Because PCA and PLS work with zero mean data, the mean value of each column of X was removed and stored for future processing. For convenience, the data matrix with removed means was denoted as X_0.

For the purposes of classification, the values of β were divided into 3 groups using the k-means partitioning methodology. This was done using all stiffness ratios, except $\beta = 19.01$, which was left out of the clustering procedure for serving as validation data. The clusters were found as:

$$
\text{C1: } 20.92 \le \beta \le 24.51 \tag{5.30}
$$

$$
\text{C2: } 26.96 \le \beta \le 31.24 \tag{5.31}
$$

$$
\text{C3: } 32.69 \le \beta \le 38.30 \tag{5.32}
$$

For describing the relationship between each feature (row of X_0) a partition matrix C was built. The (i, j)-th element of the partition matrix is 1 if the i-th feature vector (row of X_0) belongs to cluster j and 0 otherwise. According to the construction of matrix X in (5.29) and the results of the k-means clustering described above, the

partition matrix was obtained as:

$$
\boldsymbol{C} = \begin{bmatrix}
1 & 0 & 0 \\
1 & 0 & 0 \\
1 & 0 & 0 \\
1 & 0 & 0 \\
1 & 0 & 0 \\
0 & 1 & 0 \\
0 & 1 & 0 \\
0 & 1 & 0 \\
0 & 0 & 1 \\
0 & 0 & 1 \\
0 & 0 & 1 \\
0 & 0 & 1
\end{bmatrix}
\tag{5.33}
$$

Two different dimensionality reduction techniques were applied to the data matrix $\boldsymbol{X}_0$: PCA and PLS. In both approaches, the objective is to find a transformation $\boldsymbol{T}$ for producing a new features $\boldsymbol{Z} = \boldsymbol{X_0 T}$, whose variability is concentrated in the first few columns of $\boldsymbol{Z}$. PCA acts as an unsupervised method, for which no clustering information is used for determining the new features. PLS, on the other hand, can use the partition matrix $\boldsymbol{C}$ and can be interpreted as a supervised learning procedure. It is also interesting to notice that the PLS method offers an estimate of the class scores (5.33), which are provided in Appendix E

The usual criterion for selecting the features is the total percentage of variance explained by the new variables. For the PCA features, the first two PCs contain 89.6% of the total variance while the first three PCs contain 97.4%. PLS yielded 89.3% for the first two latent variables and 97.1 % for the first three latents, a very similar scenario. For both alternatives the two variables option was chosen, since it is very convenient for visualisation while still retaining about 90% of the total variance.

The transformation matrices were found as:

$$\boldsymbol{T}_1 = \begin{bmatrix} 0.4522 & 0.2570 \\ 0.4519 & 0.2566 \\ 0.4413 & 0.2415 \\ 0.3500 & 0.1209 \\ 0.2541 & 0.0761 \\ -0.3150 & 0.6421 \\ -0.2566 & 0.5142 \\ -0.1536 & 0.2450 \\ -0.1099 & 0.0759 \\ -0.0934 & 0.2167 \end{bmatrix} \qquad \boldsymbol{T}_2 = \begin{bmatrix} 0.1370 & -0.1000 \\ 0.1369 & -0.0999 \\ 0.1342 & -0.0960 \\ 0.1084 & -0.0750 \\ 0.0779 & -0.0413 \\ -0.0836 & -0.3407 \\ -0.0702 & -0.2966 \\ -0.0395 & -0.1296 \\ -0.0233 & 0.0560 \\ -0.0065 & 0.2027 \end{bmatrix} \tag{5.34}$$

where $\boldsymbol{T}_1$ is the PCA transformation matrix and $\boldsymbol{T}_2$ is the PLS transformation matrix. Notice that both possess 10 rows, 5 corresponding to the coefficients for $M_1(\omega_h)$ and the other 5 corresponding to the coefficients for $M_2(\omega_h)$. Scatter plots of the transformed variables $\boldsymbol{Z}_1 = \boldsymbol{X}_0\boldsymbol{T}_1$ and $\boldsymbol{Z}_2 = \boldsymbol{X}_0\boldsymbol{T}_2$ are respectively shown in Figures 5.19 and 5.20.

A set of boundaries between each class is shown as dashed straight lines. It is important to notice that although the choice of boundaries is not unique, other choices are easy to find due to the clear separable patterns the resulting features exhibit. In this case, automatic recognition can be achieved by neural or statistical classifiers. For the PLS features, the class regions are described as follows:

$$\text{Class 1:} \quad \begin{cases} y + 11.1670x - 0.1255 < 0 \\ y - 1.6908x - 0.1101 < 0 \end{cases} \tag{5.35}$$

$$\text{Class 2:} \quad \begin{cases} y + 11.1670x - 0.1255 < 0 \\ y - 1.6908x - 0.1101 > 0 \end{cases} \tag{5.36}$$

$$\text{Class 3:} \quad y + 11.1670x - 0.1255 > 0 \tag{5.37}$$

where x and y denote the horizontal and vertical coordinates of Figure 5.19. Similarly,
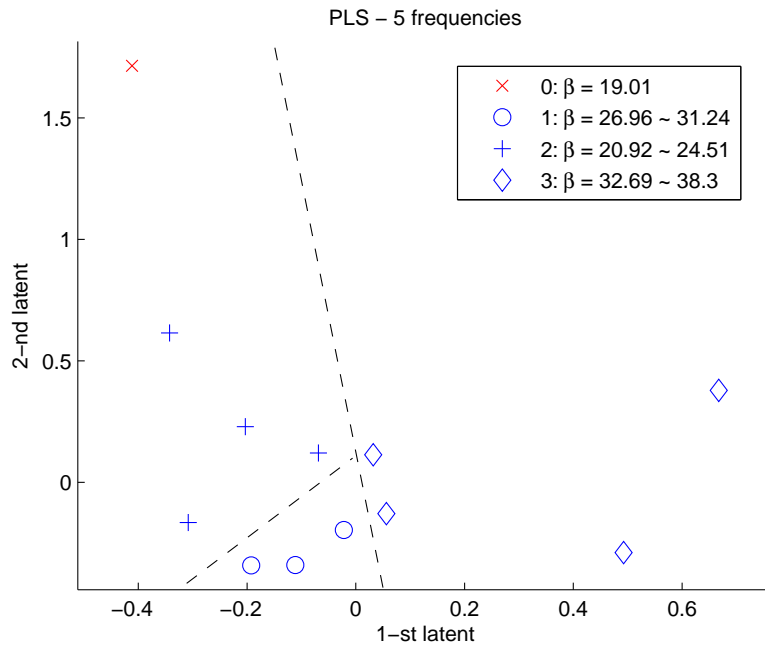
Figure 5.19: Classification results using PLS features
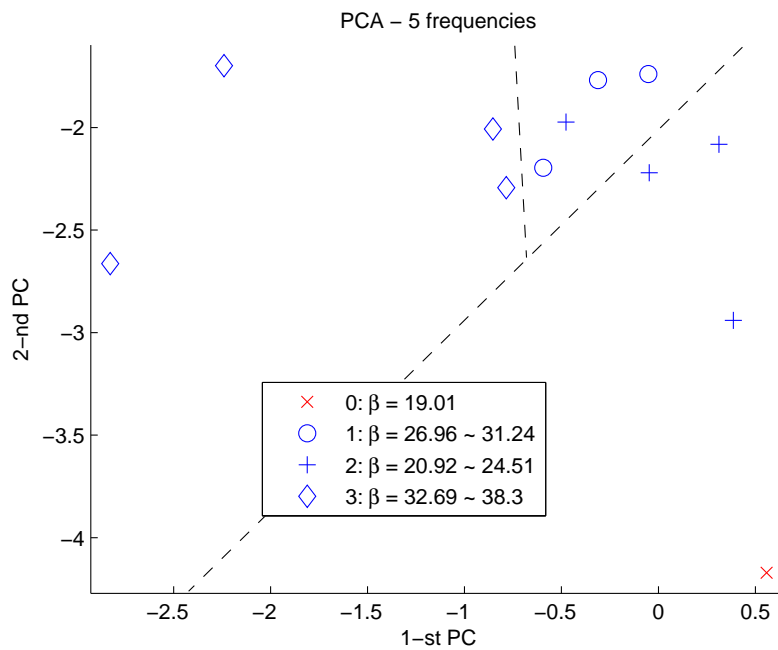
Figure 5.20: Classification results using PCA features

the boundaries shown in Figure 5.20 are described as:

$$\text{Class 1:} \begin{cases} y + 16.9475x + 14.1582 > 0 \\ y - 0.9286x + 2.0108 > 0 \end{cases} \tag{5.38}$$

$$\text{Class 2:} \ y + 16.9475x + 14.1582 < 0 \tag{5.39}$$

$$\text{Class 3:} \begin{cases} y + 16.9475x + 14.1582 < 0 \\ y - 0.9286x + 2.0108 > 0 \end{cases} \tag{5.40}$$

The PCA features are relatively well split, although there is a small overlapping region between clusters 1 and 2. This is a reasonable intersection, as these clusters represent adjacent intervals of β. The lack of more data prevents a more detailed visualisation of the overlapping region, which could provide an estimate about how frequent a misclassification in this region can occur. In practice, this problem can be alleviated by soft partitioning the PCA clusters using, for example, fuzzy clusters. Despite these issues, the overall characteristics of both PCA and PLS features can be considered satisfactory, as they provide clear distinction between different cases in the training data.

The validation case $\beta = 19.01$, labelled as cluster "0", is also shown in Figures 5.19 and 5.20. The feature corresponding to this case was marked as a red 'x'. Although classifiers were not trained, the geometric arrangement of the features suggest that $\beta = 19.01$ can be considered as belonging to cluster 1 ($20.92 \leq \beta \leq 24.51$), since this is the closest cluster to the corresponding point. This is a reasonable approximation, considering the small size of the training data. Another possible scenario is to recognise $\beta = 19.01$ as a new kind of fault, because although cluster 1 is the closest fault pattern, the distance to the corresponding point is relatively larger than the average distance between the *a priori* points of cluster 1.

Similar results can be obtained by using other points as validation data, although in some of them, cluster separability is deteriorated for both PLS and PCA. This can be explained by the small number of training samples, for which a removal of a single

template (the one that will be used as validation) can produce a significant impact in the mean values of the data matrix, therefore introducing large displacements of the features. Another possibility is the modelling error produced by noise and the narrow bandwidth of the excitation, which can introduce ambiguities, as discussed before. As previously shown, this is partly alleviated by PLS in some cases, since the learning is supervised, although not always possible.

Despite the difficulties encountered at the realisation of the experiment, the results presented at this section were found satisfactory. The obtained features can clearly demonstrate that NOFRFs can be used in conjunction with well established pattern recognition tools for producing meaningful features that allow visual interpretation of fault clusters and can be used, in principle, for training autonomous classifiers. In order to make the method more understandable, the procedures for training and implementing the diagnosis system are summarised as follows.

Training procedure:

1. For each available model the sinusoidal NOFRFs $G_1^i(e^{j\omega_h})$ and $G_2^i(e^{j2\omega_h})$ were computed at the pre-specified frequencies:

$$\omega_h = \{\omega_1, \ldots, \omega_5\}$$

$$\omega_1 = 0.0001\pi \qquad\qquad \omega_2 = 0.0007\pi$$

$$\omega_3 = 0.0045\pi \qquad\qquad \omega_4 = 0.0299\pi$$

$$\omega_5 = 0.2\pi$$

where $i \in \{1, \ldots, 12\}$

2. NOFRF data vectors were constructed for each model as:

$$\boldsymbol{x}^i = \begin{bmatrix} x_1^i & \ldots & x_5^i & x_6^i & \ldots x_{10}^i \end{bmatrix}$$

$$x_k^i = \begin{cases} 10 \log_{10} |G_1^i(e^{j\omega_k})| & k = \{1, \ldots, 5\} \\ 10 \log_{10} |G_2^i(e^{j\omega_{k-s}})| & k = \{6, \ldots, 10\} \end{cases}$$

3. The mean values for each component of $\boldsymbol{x}$ were computed:

$$\boldsymbol{\mu} = \left[\begin{array}{ccc} \mu_1 & \ldots & \mu_{10} \end{array} \right]$$

$$\mu_k = \frac{1}{m} \sum_{i=1}^{12} x_k^i$$

4. A zero-mean data matrix $\boldsymbol{X}$ was constructed as:

$$\boldsymbol{X} = \left[\begin{array}{c} \boldsymbol{x}^1 - \boldsymbol{\mu} \\ \vdots \\ \boldsymbol{x}^{12} - \boldsymbol{\mu} \end{array} \right]$$

5. The available values of β were partitioned into $c = 3$ clusters, using the k-means algorithm;

6. A partition matrix $\boldsymbol{C}_{m \times c}$ describing the clusters was constructed, where $C_{ij} = 1$ if β_i is in cluster j and 0 otherwise;

7. Compute the new features using PCA/PLS and the transformation matrix $\boldsymbol{T}$;

8. Train a classifier using the PCA/PLS features and the partition matrix (if required).

Diagnosis procedure:

1. Obtain a NARX model from input-output data;

2. Compute the NOFRFs $G_1(e^{j\omega_h})$ and $G_2(e^{j2\omega_h})$ at the pre-specified frequencies $\omega_h = \{\omega_1, \ldots, \omega_s\}$;

3. Build the zero-mean NOFRF vector $\boldsymbol{x}_0$ as follows:

$$\boldsymbol{x} = \left[\begin{array}{cccc} x_1 & \ldots & x_s & x_{s+1} & \ldots x_{2s} \end{array} \right]$$

$$x_k = \begin{cases} 10 \log_{10} |G_1(e^{j\omega_k})| & k = \{1, \ldots, s\} \\ 10 \log_{10} |G_2(e^{j\omega_{k-s}})| & k = \{s+1, \ldots, 2s\} \end{cases}$$

$$\boldsymbol{x}_0 = \boldsymbol{x} - \boldsymbol{\mu}$$

4. Apply the transformation matrix for finding the features $\boldsymbol{z} = \boldsymbol{T}\,\boldsymbol{x}_0$;

5. Classify the feature according to its distance to the closest cluster (or apply the features to the classifier, if available)

5.6   Generalisation of the CM strategies

The previous sections presented direct applications of the new CM framework to particular problems. In the present section, these ideas will be discussed in more general terms so the CM strategies can be extended for other problems.

5.6.1   Problem formulation

Consider a single-input-single-output continuous-time nonlinear system described as:

$$y(t) = F[u(t); \boldsymbol{p}] \qquad\qquad \text{Condition: } \mathcal{C} \qquad\qquad (5.41)$$

where $y(t)$ is the output, $u(t)$ is the input, $\boldsymbol{p}$ is a parameter vector, F is a nonlinear operator and $\mathcal{C}$ is a condition label (*e.g.* "normal", "fault 1", etc.).

Faults are characterised by changes in operator F. When the parameter vector $\boldsymbol{p}$ is well defined (*i.e.* it is associated to a physical or measurable system property), these changes can be directly associated to variations in $\boldsymbol{p}$ and the CM problem basically consists of recovering its real value. When $\boldsymbol{p}$ is not well defined, the characterisation of faults is still possible, but needs to be done via experience and process knowledge. In this case, each fault is identified via different conditions $\mathcal{C}$.

The CM strategies are constructed for dealing with the following problem scenario:

(i) The form of functional F in (5.41) is unknown;

(ii) Sampled input-output data are available;

(iii) The input can be freely adjusted;

(iv) Fault transients are negligible

(v) Off-line experiments under known conditions can be conducted for building a basis of *a priori* knowledge.

This formulation is consistent with many practical situations in which controlled tests can be conducted prior to system operation, so that the system behaviour under faulty conditions can be better understood, similar to case study 2. The main limitation is the time-independence assumption in (iv), since faults always exhibit some time dependent characteristics as systems can transit from a normal to a faulty state at a particular instant or over a period of time. In this case, it will be assumed that the fault transient is fast and does not play an important role for characterising the fault itself. This is a reasonably practical assumption in situations where the evolution of the defect is difficult to track. For example, in structure condition monitoring, the development of cracks over time is very difficult to observe, although the collection of data before and after its appearance is manageable. This limitation implies a loss of information that could be useful for estimating the time when the defect occurs, however, the problem can be partly alleviated by periodically performing the diagnosis procedure so that a reasonable detection window can be found.

According to the results from case studies 1 and 2, the design of the diagnosis is mainly influenced by the noise levels/modelling errors and if the parameter vector is well defined. Based on this assumption, two diagnosis strategies are proposed.

5.6.2 CM based on monitoring functions

This strategy is based on case study 1, where noise levels/modelling errors are small and fault parameters are well defined (in case study 1, the stiffness ratio). A monitoring function can be defined as any NOFRF-based feature x for which variations in $\boldsymbol{p}$ produces significant changes in x. In case study 1, this was represented by the second resonance peak of the second order NOFRF or the energy index (5.25). Using

the problem formulation, the k-th monitoring function can be defined as:

$$x_k = f_k(\boldsymbol{p}) \tag{5.42}$$

where x_k is the computable NOFRF feature. For CM purposes, it is better to consider a set of monitoring functions, which can be described in vector form as:

$$\boldsymbol{x} = \boldsymbol{f}(\boldsymbol{p}) \tag{5.43}$$

where

$$\boldsymbol{x} = \left[\begin{array}{ccc} x_1 & \ldots & x_r \end{array} \right] \tag{5.44}$$

$$\boldsymbol{f}(\boldsymbol{p}) = \left[\begin{array}{ccc} f_1(\boldsymbol{p}) & \ldots & f_r(\boldsymbol{p}) \end{array} \right] \tag{5.45}$$

Theoretically, the function $\boldsymbol{f}$ admits an inverse $\boldsymbol{f}^{-1}$ if $\boldsymbol{f}$ is bijective. For the univariate case ($\boldsymbol{p} = p$ is a scalar), this can be easily detected by plotting the measured NOFRF feature x_k versus the measured parameter p; if the curve does not exhibit any ambiguous points - *i.e.* there are no points (p_1, x_k^1) and (p_2, x_k^2) for which $p_2 \neq p_1$ and $x_k^1 = x_k^2$ - then the inverse function must exist. This procedure is more difficult to follow in the multivariate case, although the principle is the same.

When the inverse $\boldsymbol{f}^{-1}$ exists, its form can usually be found by applying a curve fitting procedure, using the measured parameters $\boldsymbol{p}$ as outputs and the computed features as inputs. The result is represented as:

$$\hat{\boldsymbol{p}} = \boldsymbol{f}^{-1}(\boldsymbol{x}) \tag{5.46}$$

The computation of the inverse in closed form allows an efficient way of estimating the fault parameters, as illustrated in case study 1. However, for the general case where multiple fault parameters exist and $\boldsymbol{f}$ is nonlinear, finding the inverse in closed form is seldom possible.

When the inverse does not exist or is difficult to compute, an alternative approach can still be applied in the attempt to recover the fault parameters. The basic idea

is to use additional monitoring functions (at least as many as the dimension of $\boldsymbol{p}$) for generating sufficient redundancy to counterbalance the ambiguities of $\boldsymbol{f}$. Then, the problem can be treated as a search for the roots of a system of nonlinear algebraic equations. The procedure can be described as follows: first, a closed form representation for the monitoring function $\boldsymbol{f}$ in (5.43) is found via curve fitting. During on-line operation, the features $\boldsymbol{x}$ are measured and substituted in (5.43), yielding a system of nonlinear equations. Then, special algorithms (*e.g.* Newton's method) can be applied for recovering the fault parameters $\boldsymbol{p}$.

Notice that this is the same strategy proposed by parameter estimation techniques (Isermann, 2005), except that it is a more general case where the process is nonlinear and the estimation scheme is constructed in terms of NOFRF features, instead of mapping discrete-time parameters into continuous-time parameters.

The design procedure and diagnosis implementation are summarised as Algorithms 10 and 11.

It is worth mentioning that a critical point of Algorithm 10 is step 4, in which the NOFRF features are selected. The exact choice is highly dependent on the particular characteristics of each problem. At the present, the selection needs to be made by trial and error, although there are some general aspects that can be considered. This will be discussed in more detail in Section 5.6.4.

5.6.3 Diagnosis based on fault clusters

The second strategy is based on the principle that CM can be treated as a classification problem. This is particularly well suited for situations where the parameter vector is not well defined and, therefore, cannot be recovered. In this case, the *a priori* knowledge consists of a bank of fault cases (conditions) that share similar features that need to be uncovered and used for grouping similar faults into *fault clusters* (or *classes*) in the feature space. The diagnosis procedure, then, consists of fitting an unknown

5. A NEW CM FRAMEWORK BASED ON NOFRFS

Algorithm 10 Design of CM system based on monitoring functions

---

1. Collect m input-output data sets and the corresponding fault parameters

2. For each parameter sample, identify a NARX model

3. For each identified NARX model, compute the NOFRFs

4. Select the NOFRF features that will be used as monitoring functions

5. If possible, plot the features versus the fault parameters and verify if the relationship is bijective and its inverse exists

6. If the inverse function exists, apply curve fitting for finding the inverse in closed form

7. If the inverse cannot be found, but the monitoring functions are smooth, apply curve fitting for finding the monitoring function in closed form

---

Algorithm 11 CM procedure based on monitoring functions

---

1. Acquire input-output data

2. Identify a NARX model

3. Compute the NOFRFs and measure the target features $\boldsymbol{x}$

4. If the inverse function was determined in closed form, obtain the estimates of the fault parameters as $\hat{\boldsymbol{p}} = \boldsymbol{f}^{-1}(\boldsymbol{x})$

5. If the inverse function was not determined, apply a numerical method for solving $\boldsymbol{x} = \boldsymbol{f}(\boldsymbol{p})$ with respect to $\boldsymbol{p}$

---

condition into a particular established cluster provided that its corresponding features are sufficiently close to the cluster under consideration.

Another circumstance for which this approach is useful is when significant noise is present at the output measurements. The noise produces random variations in the NOFRFs computations, producing biased features that can easily be mistaken as fault-related conditions. The strategy uses a feature generation scheme that possess some interesting statistical properties that provide a slight reduction of the noise effects in the resulting features. Moreover, the cluster formulation provides some additional robustness to the diagnosis, as faults can still be recognised as one of the defined clusters, as long as it lies sufficiently close to one of them. Therefore, this strategy can be seen as a potential alternative to the one presented in the previous section, whenever fault parameters is not well defined or significant noise is present.

The fault clusters are determined by grouping the known fault cases by either using *a priori* knowledge or specialized clustering methods, such as the k-means algorithm. The algorithmic approach was used in case study 2 and is relatively systematic, providing a straightforward way for dealing with the general case in which p can be of any dimension. However, this procedure does not need to be followed if the clusters are known in advance, based on *a priori* knowledge from experienced operators. This is an interesting situation, since the lack of accurate fault parameter values that characterise each fault is not problematic, as the other steps of the methodology only requires the clustering information, not the actual values of the fault parameters.

Due to the stochastic nature of the measurements, the NOFRF features associated to each fault cluster usually need to be computed for several frequencies, since they seldom yield comprehensible patterns that allow an appropriate selection of only a few key NOFRF frequency components. In this case, a dimensionality reduction techniques such as PCA or PLS can be applied for allowing a better visualisation of data and adjusting the clusters structures, if necessary. At this final stage, the number of fault clusters and the selected NOFRF features play an important role, and some trial and error might be required until satisfactory PCA/PLS feature patterns can be found. The

main results of this stage are the PCA/PLS transformation matrix and the features associated to each fault clusters, which need to stored for comparison with real faults.

The entire design procedure is summarised as Algorithm 12, while the corresponding diagnosis procedure is summarised in Algorithm 13.

Algorithm 12 Design of CM system based on fault clusters

---

1. Measure m input-output data sets and their corresponding fault parameters

2. For each fault sample, identify a NARX model

3. For each identified NARX model, compute the NOFRFs

4. Select the NOFRF measurements to be used as primary features and build the sample data vectors $\boldsymbol{x}^i$, $i = \{1, \ldots, m\}$

5. Compute the mean values of the primary features $\boldsymbol{\mu}$

6. Compute the zero mean data vectors $\boldsymbol{x}_0^i = \boldsymbol{x}^i - \boldsymbol{\mu}$

7. Find c clusters of known faults and the corresponding partition matrix $\boldsymbol{C}$

8. Build the data matrix $\boldsymbol{X}_0$ whose rows are vectors $\boldsymbol{x}_0^i$

9. Apply PCA/PLS using $\boldsymbol{X}_0$ and $\boldsymbol{C}$ and obtain the resulting transformation matrix $\boldsymbol{T}$

10. Verify the consistency of the new features with respect to the cluster structure

11. Train a classifier using the new features (optional)

The main advantage of the CM algorithm 13 is that it is designed to directly deal with situations where moderate noise can be observed in data. Moreover, because faults are viewed as clusters, the values of the fault parameters are not essential (although can still be used) when the fault clusters are known *a priori*.

Algorithm 13 CM procedure based on fault clusters

---

1. Acquire input-output data

2. Identify a NARX model

3. Compute the NOFRFs

4. Build the data vector $\boldsymbol{x}$ according to the structure established at the design stage

5. Compute the zero mean data vector as $\boldsymbol{x}_0 = \boldsymbol{x} - \boldsymbol{\mu}$

6. Compute the fault features as $\boldsymbol{z} = \boldsymbol{x}_0 \boldsymbol{T}$

7. Apply the features $\boldsymbol{z}$ to the trained classifier or plot the relevant coordinates with the pre established clusters for manual classification

---

When the resulting PCA/PLS features are clearly separable, they are usually easy to interpret and do not require an autonomous classifier to be trained, which was stated in step 11 of Algorithm 12. The main difficulties occur, when the resulting features exhibit excessive overlapping between them, which prevents an unique association between a unknown fault and the known clusters. This issue is application specific and a general solution is difficult to establish, although it is possible to list some suggested guidelines for improving the situation.

Fault overlapping is similar to the ambiguity problem observed in the monitoring function approach. This issue can usually be improved by using additional redundancy, which, in this case, consists of using a larger number of fault cases, so the structures of clusters can be refined. Another option is to increase the number of fault clusters, which can lead to a better understanding about the frontiers between each cluster. Alternatively, the whole situation can be re-interpreted in terms of fuzzy clustering, in

which the overlapping is quantitatively described, allowing the development of a more flexible decision logic that may yield better classification results.

5.6.4 Basic aspects about selection of NOFRF measurements

In the methodologies described above, the process of selecting the NOFRFs plays an important role in the design of the core elements of the CM approaches. Although selecting the ideal NOFRF features is a problem-dependent issue, some guidelines can still be discussed in general terms.

The basic idea in each approach is to construct a data vector $\boldsymbol{x}$ where each component is a NOFRF measurement, such as amplitude, real part, etc. The most straightforward choices for the k-th component of $\boldsymbol{x}$ are described as:

$$x_k = \Re\big[G_n(e^{j\omega_i})\big] \tag{5.47}$$

$$x_k = \Im\big[G_n(e^{j\omega_i})\big] \tag{5.48}$$

$$x_k = |G_n(e^{j\omega_i})| \tag{5.49}$$

$$x_k = \log_{10}|G_n(e^{j\omega_i})| \tag{5.50}$$

$$x_k = \angle G_n(e^{j\omega_i}) \tag{5.51}$$

where $i \in \{1, 2, \ldots, s\}$, s is the dimension of $\boldsymbol{x}$, $\Re$ denotes real part, $\Im$ denotes imaginary part and $\angle$ denotes unwrapped phase angle. Notice that many choices are available, considering that (5.47)-(5.51) can be computed at different frequencies ω and combined in the same data vector $\boldsymbol{x}$.

The possibility of computing the components x_i at different frequencies represents an additional freedom for the feature design. However, it should be noticed that, depending on the probing input used, the NOFRFs $G_n(e^{j\omega})$ need to be computed in different ways and also possess different interpretations.

As discussed in section 4.4, there are two cases that need to be considered: sinusoidal and non-sinusoidal inputs. For a non-sinusoidal input, such as the unit impulse or a

low-pass pulse such as the sinc function, the computation of the n-th order NOFRF results in a *single function* defined for a range of frequencies ω, typically $\omega \leq n\,b$, where b is the bandwidth of the low-pass input. Usually b should be chosen so that $n\,b$ is less than the Nyquist frequency. Notice that, if the input possesses a closed form representation, $G_n(e^{j\omega})$ can be obtained either numerically or analytically. The numerical computation is usually preferred in this situation, as it is faster and its accuracy is essentially equivalent to the analytical method.

In contrast, when the input is sinusoidal, $G_n(e^{j\omega})$ can only be computed at the super-harmonics of the input frequency ω_h, so that ω can be replaced by $k\omega_h$ in (5.47)-(5.51), where $k \in \{0, \ldots, n\}$. The advantage of using a sinusoidal input is that the NOFRFs are input-independent and carry useful system information that may be able to provide good fault information. Usually, we will be interested in the values of $G_n(e^{jk\omega_h})$ for various ω_h, which is interpreted as probing the system with different inputs for yielding *several distinct functions*. This is equivalent to computing a linear system FRF by applying several sinusoids of different frequencies. The computation can be carried out via the numerical method, which requires long simulations (for the response reaching steady state) that need to conducted multiple times (one for each value of ω_h). For this reason, the analytical approach should be preferred, as the availability of a closed formula provides great flexibility for computing the NOFRFs at various frequencies, which is relatively useful for the design stage where we usually need to test different ranges or number of frequency components.

In addition to directly using the NOFRF values, energy indices, such as (5.25) introduced in case study 1 can also be used as components of the data vector $\boldsymbol{x}$. The general form of the indices is described as:

$$x_k = I_n = \frac{\displaystyle\sum_{\Omega_n} |G_n(e^{j\omega})|^2}{\displaystyle\sum_{\Omega_1} |G_1(e^{j\omega})|^2} \tag{5.52}$$

which is a rough measure of the relative impact of nonlinearities of degree n in the

response. In (5.52), the summations are computed for all $\omega \in \Omega_n$, where Ω_n represents the frequency support of $G_n(e^{j\omega})$, which is usually a sequence of frequencies easily obtained from the DTFT analysis of the n-th order Volterra series component. It is worth mentioning that the denominator was chosen as the energy of the linear FRF because the linear component is usually the dominant part of the response, but different possibilities should be considered if that is not the case. Notice, however, that these indices contain less information than the NOFRF measurements (5.47)-(5.51), since they average the NOFRF amplitude over all possible frequencies.

5.7   Conclusions

In this chapter, a new general CM framework based on nonlinear systems modelling and frequency domain analysis was proposed. The framework was designed for dealing with practical situations where nonlinear behaviour and multiplicative faults need to be considered. The main idea consists of four basic steps: model identification, computation of NOFRFs, extraction of features from the NOFRFs and fault classification according to the obtained features. Based on this framework, two new CM strategies were developed and successfully tested.

The first strategy is based on the concept of monitoring functions and can be applied in situations where a fault parameter is well defined and noise levels and modelling errors are small. The basic idea is to identify NOFRF measurements, such as resonance peaks or an energy index, that exhibit significant sensitivity to the fault parameters, so they can be used for tracking the evolution of the defect. The diagnosis procedure can be implemented in two different ways: by finding the inverse of the monitoring function for directly computing the fault parameters from the NOFRF measurements; or by numerically solving a system of nonlinear algebraic equations, built from all available monitoring functions. The choice between these two implementations depends on how ambiguous the monitoring functions are, which directly depends on the modelling

errors and the level of noise observed in the sensors. This method was tested by both simulation and experimental data analysis and satisfactory results have been achieved.

The second CM methodology was introduced to deal with a more realistic scenario, where significant noise and modelling errors are present or fault parameters are not well defined. It consists of working with fault clusters instead of computing a continuous estimate of the fault parameters, so that the diagnosis objective is reduced to fitting an unknown condition into one of the *a priori* clusters (or defining a new one, in case none of the clusters is sufficiently similar). The features that characterise each cluster and system condition are designed via PCA/PLS, which provides the statistical treatment required for dealing with the variations of NOFRF computations due to presence of noise in output measurements. The approach was successfully tested using experimental data analysis.

These satisfactory results demonstrate that the new framework offers a solid background for developing CM solutions. Moreover, it is worth mentioning that, despite some similarities with system identification approaches, important novelties were involved in these developments, which make them fundamentally different from the system identification methodology; these novelties are: (i) the use of black-box nonlinear modelling and (ii) the use of NOFRFs-based features obtained via the new algorithms proposed in chapter 4.

6

Conclusion

In this research work, new methods were developed for the analysis of nonlinear systems in the frequency domain. Then, the CM problem was studied under a new framework where the time-domain modelling and the new methods based on frequency domain analysis were applied. This approach was taken due to some difficulties observed in basic CM methodologies, after comprehensively reviewing the recent advances in the field, with a specific focus on model-based and process history techniques. What was observed is that there is only a small number of approaches that are capable of dealing with systems that exhibit nonlinear behaviour and the so called multiplicative faults, which is the case of many practical situations.

In this context, it is generally difficult to extend some of the principal model-based techniques such as parity equations and observers to this problem scenario, basically due to the difficulties of dealing with nonlinear models. The system identification approach, on the other hand, is a more suited method for dealing with these issues, since it is focused in the isolation of faults by directly identifying the physical quantities associated to them. Although the method does not find any significant difficulties in dealing with nonlinearities, the necessity of establishing maps between fault parameters (usually associated to CT models) and model parameters (associated to DT representations)

imposes a severe limitation, because this procedure requires process knowledge that is often very difficult to obtain.

A reasonable solution to this problem, at least for the linear cases, is to monitor the system state via frequency domain parameters such as resonance characteristics, bandwidth etc., because whether computed from DT or CT models, the values of such parameters should be the same. Therefore, in order to extend this approach to nonlinear systems, a new frequency domain formulation need to be considered.

It is well established that nonlinear system analysis can be carried out via the Volterra series approach. This methodology can be applied to the so-called fading memory systems, which comprises a wide class of nonlinear systems of practical interest. Using the Volterra series approach, several FRF concepts from linear systems theory can be generalised, *e.g.* , the Generalised Frequency Response Functions, although identifying key system properties that can be useful for CM is not as simple as in the linear case. This is due to the multidimensional nature of the GFRFs, which brings several complications to both graphical and analytical techniques. For this reason, alternative nonlinear FRF concepts, such as the NOFRFs have been proposed, in the attempt to capture the system's essential properties while maintaining the dimensionality of the frequency features low.

Despite NOFRFs have been successfully applied to practical problems and theoretical analysis, there are still fundamental problems related to their computation and analysis that required investigation, which was the main focus of this work. Throughout the research, several significant advances in this area were obtained, which altogether comprise a new framework for carrying out practical nonlinear systems analysis in the frequency domain and the application of the analysis to engineering systems condition monitoring/fault diagnosis. These results have then enabled the development of new systematic approaches to CM which has been successfully verified by both simulation and experimental studies.

6.1   Contributions of this research

This research produced some significant contributions both in the field of nonlinear system frequency analysis and CM. The overall results were satisfactory, although it is worth emphasising some particular points:

(i) A new algorithm that allows extracting the system GFRFs in a recursive form was proposed. The method was designed for dealing with very general nonlinear systems that may possess complicated polynomial terms. For this reason, it is very useful for practical situations where such models are obtained from real data by using system identification techniques.

The method can be considered as an alternative to the well known harmonic probing method. Though both approaches provide the same result, the algorithm proposed in this thesis is more efficient and comprehensible, as the implementation does not require recursive symbolic calculations and the formulas are provided in their most compact form.

In addition to providing a more effective way of determining GFRFs, the techniques used in deriving the new algorithm also provided an important basis for the development of a new method for determination of NOFRFs.

(ii) A new method for determination of NOFRFs of nonlinear systems was proposed. The method consists of extracting the system ALEs by using an algorithm that follows the same philosophy of the new GFRF extraction algorithm, computing the Volterra series components in the frequency domain and then evaluating the NOFRFs from the results. The advantage of this new method is that it allows to efficiently compute the Volterra functional components and then, the corresponding NOFRFs up to arbitrary order, without recurring to any multidimensional calculations. In addition, the method allows obtaining the NOFRFs in two different forms: numerical and analytical. The numer-

ical computation allows a straightforward and general way of obtaining the NOFRFs for any input, although it is not very efficient if an unknown parameter is involved or the NOFRFs need to be recomputed at different scenarios. For these situations, the analytical approach is more convenient, as it can provide great insight into how unknown parameters can affect the NOFRFs of nonlinear systems under study.

The new method is a significant development in NOFRF based nonlinear system analysis, since it provides a more efficient way to compute these functions. Using the numerical approach, NOFRFs can be computed in numerical format for any arbitrary input. Because the core of these computations are the system ALEs, which are recursive in nature, the computation of lower order NOFRFs is not affected by their higher order counterparts, a problem that is very likely to occur when available methods are used.

On the other hand, the analytical approach offers a new perspective over NOFRF-based analysis. The symbolic nature of this approach allows the NOFRF to be determined, in terms of some unknown parameters of interest. This can be useful for situations in which the effect of these parameters on the NOFRF based system representation are to be investigated, for example, for selecting optimal NOFRF features for fault classification. In addition, for particular types of inputs, the NOFRFs can be obtained in conventional rational form which allows, in principle, to carry out the analysis in terms of familiar concepts such as poles and residues, further reinforcing the similarities between FRF analysis of linear systems and NOFRF-based nonlinear system analysis.

(iii) The new framework for condition monitoring/fault diagnosis was established. This is a time-domain modelling and frequency domain analysis based framework, where the new GFRFs/NOFRFs evaluation methods are the very basis

of the required frequency analysis. Under the new framework, new CM approaches based on monitoring functions and faults clusters were introduced. These can be considered as hybrid approaches, as their basic principles are founded in model-based and process history methods. The advantage, however, is that they were designed for dealing with practical contexts, where: (a) the only *a priori* knowledge available for CM design is in the form of input-output data and fault characterisation; (b) physical knowledge about the process is limited; (c) fault features need to be extracted from nonlinear black box models. The novelty of the methods is in the use of NOFRF measurements, which can provide a good fault discerning scenario as demonstrated in the case studies, one of which presented substantial difficulties due to noise and experimental circumstances. However, it is worth mentioning that the CM design is not always straightforward, as there are many aspects that need to be considered for finding good features, such as the probing input, the order of the NOFRFs, what measurements to use (magnitude, phase, etc.) and the frequencies over which the NOFRFs are computed. Although it is true that these elements provide additional freedom to the CM design, they also introduce further complexity as they need to be constantly considered throughout the design process.

6.2   Future work

In the present study, new nonlinear systems frequency analysis methods were developed and based on these new methods, a new CM framework and associated strategies were proposed. However, there are many subjects that require further investigation or are interesting subjects for future studies. Some of these are as follows:

(i) Investigate the possibility of applying the new frequency analysis framework,

in particular the analytical approach, to other nonlinear systems studies, such as control design. Introducing feedback into NARX models produce new NARX models, which, although more complicated in form, can be systematically analysed using the ALE extraction algorithm. The analytical framework provides the background for analysing the influence of controller parameters over the response, allowing a better prediction of the nonlinear distortions and possibly tuning controller gains for alleviating their effects.

(ii) There are also several other fields in which the Volterra series approach is applied, such as channel equalisation, echo cancelling and analysis of neuronal signals, which can all be investigated using the new frequency framework.

(iii) The analytical approach also provides an interesting background for developing a new CM scheme in which faults are formulated as unknown inputs, similar to the parity equation approach. This is due to the possibility of exactly computing each component of the response, for example, due to a step input (sudden fault). In this case, it is possible to derive formulas in terms of the step amplitude that might be able to aid the fault isolation procedure.

(iv) Another issue that requires a more in-depth investigation is how to tune NOFRF-related parameters, such as frequency components and the probing input. In the context of CM, this is an important problem as it directly influences the separability of fault clusters. It is conjectured that using nonlinear optimization tools can yield a better tuning of these parameters, but this needs to be more appropriately addressed.

These are a few possible routes that can be taken from the present state of this research. Other possibilities include the optimisation of software routines for dealing with problems associated with a more in-depth investigation of the NOFRF concept and relevant techniques which, as demonstrated by the work of this thesis, will have a

wide range of potential applications

6. CONCLUSION

References

Ron Barron. *Engineering Condition Monitoring: Practice, Methods and Applications.* Practice, Methods and Applications. Longman, 1996. ISBN 9780582246560. 5, 105, 107

R. S. Bayma and Z. Q. Lang. A new method for determining the generalised frequency response functions of nonlinear systems. *IEEE Transactions On Circuits and Systems I-regular Papers*, 59(12):3005–3014, December 2012. doi: 10.1109/TCSI.2012.2206454. 10, 26, 30, 35, 43

R S Bayma and Z Q Lang. Fault diagnosis methodology based on nonlinear system modelling and frequency analysis. In *19th IFAC World Congress*. IFAC, August 2014. 10

S. Benedetto and Ezio Biglieri. Nonlinear equalization of digital satellite channels. *Selected Areas in Communications, IEEE Journal on*, 1(1):57–62, 1983. ISSN 0733-8716. doi: 10.1109/JSAC.1983.1145885. 2

Ezio Biglieri, S. Barberis, and M. Catena. Analysis and compensation of nonlinearities in digital transmission systems. *Selected Areas in Communications, IEEE Journal on*, 6(1):42–51, 1988. ISSN 0733-8716. doi: 10.1109/49.192728. 2

S. A. Billings and Z. Q. Lang. Non-linear systems in the frequency domain: energy

REFERENCES

transfer filters. *International Journal of Control*, 75(14):1066–1081, September 2002. doi: 10.1080/00207170210157575. 4

S. A. Billings and L. M. Li. Reconstruction of linear and non-linear continuous-time system models from input/output data using the kernel invariance algorithm. *Journal of Sound and Vibration*, 233(5):877–896, June 2000. doi: 10.1006/jsvi.1999.2843. 3

S.A. Billings. *Nonlinear System Identification: Narmax Methods in the Time, Frequency, and Spatio-Temporal Domains*. John Wiley & Sons, 2013. ISBN 9781118535547. 1, 36, 37

S.A Billings and Hua-Liang Wei. A new class of wavelet networks for nonlinear system identification. *Neural Networks, IEEE Transactions on*, 16(4):862–874, 2005. ISSN 1045-9227. 36

S. Boyd and L. O. Chua. Fading memory and the problem of approximating nonlinear operators with Volterra series. *IEEE Transactions On Circuits and Systems*, 32(11): 1150–1161, 1985. doi: 10.1109/TCS.1985.1085649. 2, 16

Churchill Ruel V. Brown, James Ward. *Complex variables and applications*. McGraw-Hill Higher Education, Boston, MA, 2009. 79, 80

O. Buyukozturk, M.A. Tasdemir, O. Gunes, and Y. Akkaya. *Nondestructive Testing of Materials and Structures: Proceedings of NDTMS-2011, Istanbul, Turkey, May 15-18, 2011*. Rilem Bookseries. Springer, 2012. ISBN 9789400707221. 105

R. J. G. B. Campello, G. Favier, and W. C. do Amaral. Optimal expansions of discrete-time Volterra models using Laguerre functions. *Automatica*, 40(5):815–822, May 2004. doi: 10.1016/j.automatica.2003.11.016. 33

A. Carini, G.L. Sicuranza, and V. John Mathews. Equalization and linearization of nonlinear systems. In *Acoustics, Speech and Signal Processing, 1998. Proceedings of*

the 1998 IEEE International Conference on, volume 3, pages 1617–1620 vol.3, 1998. doi: 10.1109/ICASSP.1998.681763. 17

J. Casar-Corredera, M. Garcia-Otero, and A. Figueiras-Vidal. Data echo nonlinear cancellation. In *Acoustics, Speech, and Signal Processing, IEEE International Conference on ICASSP '85.*, volume 10, pages 1245–1248, 1985. doi: 10.1109/ICASSP. 1985.1168120. 17

C. W. Chan, Song Hua, and Hong-Yue Zhang. Application of fully decoupled parity equation in fault detection and identification of DC motors. *IEEE TRANSACTIONS ON INDUSTRIAL ELECTRONICS*, 53(4):1277–1284, AUG 2006. ISSN 0278-0046. doi: {10.1109/TIE.2006.878304}. 106

K.-Y. Chen and C.-C. Huang. Characterisation of gaas pseudomorphic high electron mobility transistors for volterra-series circuit analysis. *Microwaves, Antennas & Propagation, IET*, 3(2):228–234, 2009. ISSN 1751-8725. 2

S. Chen and S. A. Billings. Representations of non-linear systems - the narmax model. *International Journal of Control*, 49(3):1013–1032, March 1989. doi: 10.1080/00207178908547379. 36

S. Chen, S. A. Billings, and W. Luo. Orthogonal least squares methods and their application to nonlinear system identification. Technical Report 343, The University of Sheffield, August 1988. 38

D. Coca and S. A. Billings. Nonlinear system identification using wavelet multiresolution models. Technical Report 763, The University of Sheffield, December 1999. 36

J. A. V. Feijoo, K. Worden, and R. Stanway. System identification using associated linear equations. *Mechanical Systems and Signal Processing*, 18(3):431–455, May 2004. doi: 10.1016/S0888-3270(03)00078-5. 27

REFERENCES

J. A. V. Feijoo, K. Worden, and R. Stanway. Associated linear equations for Volterra operators. *Mechanical Systems and Signal Processing*, 19(1):57–69, January 2005. doi: 10.1016/j.ymssp.2004.03.003. 8, 27, 70

J. A. V. Feijoo, K. Worden, and R. Stanway. Analysis of time-invariant systems in the time and frequency domain by associated linear equations (ales). *Mechanical Systems and Signal Processing*, 20(4):896–919, May 2006. doi: 10.1016/j.ymssp.2005.03.004. 27, 70

D. A. George. Continuous nonlinear systems. Technical Report 355, Massachusetts Institute of Technology. Research Laboratory of Electronics, July 1959. 3, 4, 18

S.S. Haykin. *Neural networks: a comprehensive foundation.* Prentice Hall, 1999. ISBN 9780132733502. 36

R. Hermann. Volterra modeling of digital magnetic saturation recording channels. *Magnetics, IEEE Transactions on*, 26(5):2125–2127, 1990. ISSN 0018-9464. doi: 10.1109/20.104642. 17

James Ing. *Near grazing dynamics of piecewise linear oscillators.* PhD thesis, University of Aberdeen, 2008. 125

R. Isermann. Fault-diagnosis of machines via parameter estimation and knowledge processing - Tutorial Paper. *Automatica*, 29(4):815–835, JUL 1993. ISSN 0005-1098. doi: {10.1016/0005-1098(93)90088-B}. 106, 107

R. Isermann. Model-based fault-detection and diagnosis - status and applications. *Annual Reviews In Control*, 29(1):71–85, 2005. doi: 10.1016/j.arcontrol.2004.12.002. 107, 141

R. Isermann. *Fault-diagnosis systems: an introduction from fault detection to fault tolerance.* Springer, 2006. 5, 6, 106, 107

X. J. Jing, Z. Q. Lang, and S. A. Billings. Mapping from parametric characteristics to generalized frequency response functions of non-linear systems. *International Journal of Control*, 81(7):1071–1088, 2008. doi: 10.1080/00207170701636542. 3, 35, 65

JJ Joseph and BK Ghosh. A volterra approach to dynamic modeling of the visual cortex. In *PROCEEDINGS OF THE 2003 AMERICAN CONTROL CONFERENCE, VOLS 1-6*, PROCEEDINGS OF THE AMERICAN CONTROL CONFERENCE, pages 3579–3584, 345 E 47TH ST, NEW YORK, NY 10017 USA, 2003. Amer Automat Control Council; IFAC, IEEE. ISBN 0-7803-7896-2. Annual American Control Conference (ACC 2003), DENVER, CO, JUN 04, 2003-JUN 06, 2006. 2

G. Karam and H. Sari. Analysis of predistortion, equalization, and isi cancellation techniques in digital radio systems with nonlinear transmit amplifiers. *Communications, IEEE Transactions on*, 37(12):1245–1253, 1989. ISSN 0090-6778. doi: 10.1109/26.44196. 17

M. Korenberg, S. A. Billings, Y. P. Liu, and P. J. Mcilroy. Orthogonal parameter-estimation algorithm for non-linear stochastic-systems. *International Journal of Control*, 48(1):193–210, July 1988. doi: 10.1080/00207178808906169. 36, 38

M. J. Korenberg. An orthogonal parameter estimation algorithm for nonlinear stochastic systems. Technical Report 307, University of Sheffield. Department of Control Engineering, 1987. 37, 38

Z. Q. Lang and S. A. Billings. Output frequency characteristics of nonlinear systems. *International Journal of Control*, 64:1049–1067, 1996. 2, 18

Z. Q. Lang and S. A. Billings. Output frequencies of nonlinear systems. *International Journal of Control*, 67(5):713–730, July 1997. 19

Z. Q. Lang and S. A. Billings. Energy transfer properties of non-linear systems in the

frequency domain. *International Journal of Control*, 78(5):345–362, March 2005. doi: 10.1080/00207170500095759. 4, 9, 20, 21, 22, 67

Z. Q. Lang and Z. K. Peng. A novel approach for nonlinearity detection in vibrating systems. *Journal of Sound and Vibration*, 314(3-5):603–615, July 2008. doi: 10.1016/ j.jsv.2008.01.043. 4, 25, 111

Z. Q. Lang, S. A. Billings, R. Yue, and J. Li. Output frequency response function of nonlinear volterra systems. *Automatica*, 43(5):805–816, May 2007. doi: 10.1016/j. automatica.2006.11.013. 4

Y. W. Lee and M. Schetzen. Measurement of Wiener kernels of a nonlinear system by cross-correlation. *International Journal of Control*, 2(3):237–&, 1965. 3, 16, 30, 32

I. J. Leontaritis and S. A. Billings. Input output parametric models for non-linear systems .1. deterministic non-linear systems. *International Journal of Control*, 41 (2):303–328, 1985. doi: 10.1080/0020718508961129. 34, 36, 48

L. M. Li and S. A. Billings. Continuous time non-linear system identification in the frequency domain. *International Journal of Control*, 74(11):1052–1061, July 2001. doi: 10.1080/00207170110052239. 3

P. Li, H. L. Wei, S. A. Billings, M. A. Balikhin, and R. Boynton. Nonlinear model identification from multiple data sets using an orthogonal forward search algorithm. *Journal of Computational and Nonlinear Dynamics*, 8(4):41001–41001, October 2013. 36

P. Z. Marmarelis and K. I. Naka. Identification of multi-input biological-systems. *IEEE Transactions On Biomedical Engineering*, BM21(2):88–101, 1974. doi: 10. 1109/TBME.1974.324293. 2, 3, 17

V. J. Mathews and G. L. Sicuranza. *Polynomial signal processing*. New York, Chich-ester, John Wiley & Sons, 2000. 17

R.H. Myers. *Classical and Modern Regression with Applications*. Duxbury classic series. Duxbury/Thompson Learning, 1990. ISBN 9780534380168. 40

P. Palumbo and L. Piroddi. Harmonic analysis of non-linear structures by means of generalised frequency response functions coupled with narx models. *Mechanical Systems and Signal Processing*, 14(2):243–265, March 2000. doi: 10.1006/mssp.1999. 1264. 19

R. Patton, P. Frank, and R. Clark. *Fault diagnosis in dynamic systems - Theory and application*. Prentice Hall, 1989. 6

Z. K. Peng, Z. Q. Lang, and S. A. Billings. Crack detection using nonlinear output frequency response functions. *Journal of Sound and Vibration*, 301(3-5):777–788, April 2007a. doi: 10.1016/j.jsv.2006.10.039. 4, 25, 111

Z. K. Peng, Z. Q. Lang, and S. A. Billings. Resonances and resonant frequencies for a class of nonlinear systems. *Journal of Sound and Vibration*, 300(3-5):993–1014, March 2007b. doi: 10.1016/j.jsv.2006.09.012. 5, 24, 25, 111

Z. K. Peng, Z. Q. Lang, S. A. Billings, and G. R. Tomlinson. Comparisons between harmonic balance and nonlinear output frequency response function in nonlinear system analysis. *Journal of Sound and Vibration*, 311(1-2):56–73, March 2008. doi: 10.1016/j.jsv.2007.08.035. 24

Z. K. Peng, Z. Q. Lang, C. Wolters, S. A. Billings, and K. Worden. Feasibility study of structural damage detection using narmax modelling and nonlinear output frequency response function based analysis. *Mechanical Systems and Signal Processing*, 25(3): 1045–1061, April 2011. doi: 10.1016/j.ymssp.2010.09.014. 4, 5, 25

Z. K. Peng, Z. Q. Lang, S. A. Billings, and Y. Lu. Analysis of bilinear oscillators under harmonic loading using nonlinear output frequency response functions. *INTERNA-*

REFERENCES

TIONAL JOURNAL OF MECHANICAL SCIENCES, 49(11):1213–1225, NOV 2007. ISSN 0020-7403. doi: {10.1016/j.ijmecsci.2007.03.009}. 5, 24, 111, 112

J. C. Peyton Jones. Simplified computation of the Volterra frequency response functions of non-linear systems. *Mechanical Systems and Signal Processing*, 21(3):1452–1468, April 2007. doi: 10.1016/j.ymssp.2005.10.013. 30, 34, 43

J. C. Peyton Jones and S. A. Billings. A recursive algorithm for computing the frequency response of a class of nonlinear difference equation models. Technical Report 354, University of Sheffield. Department of Control Engineering, 1988. 34

J. C. Peyton Jones and S. A. Billings. Recursive algorithm for computing the frequency-response of a class of non-linear difference equation models. *International Journal of Control*, 50(5):1925–1940, November 1989. 3, 8, 30, 34, 43

A.D. Poularikas. *The Transforms and Applications: Handbook*. The Electrical Engineering Handbook Series. Taylor & Francis Group, 2000. ISBN 9780849385957. 80

G. Ramponi. Edge extraction by a class of second-order nonlinear filters. *Electronics Letters*, 22(9):482–484, 1986. ISSN 0013-5194. doi: 10.1049/el:19860328. 2, 17

W. Rudin. *Principles of Mathematical Analysis*. International series in pure and applied mathematics. McGraw-Hill International, 1976. ISBN 9780070856134. 15

Wilson J. Rugh. *Nonlinear system theory : the Volterra/Wiener approach*. Baltimore ; London : Johns Hopkins University Press, 1981. 3, 26, 41

P. Sakian, R. Mahmoudi, and A van Roermund. A circuit-level analysis of third order intermodulation mechanisms in cmos mixers using time-invariant power and volterra series. In *Microwave Conference (EuMC), 2011 41st European*, pages 595–598, 2011. 2

Abraham. Savitzky and M. J. E. Golay. Smoothing and differentiation of data by simplified least squares procedures. *Analytical Chemistry*, 36(8):1627–1639, 1964. doi: 10.1021/ac60214a047. 125

M. Schetzen. Theory of pth-order inverses of nonlinear-systems. *IEEE Transactions On Circuits and Systems*, 23(5):285–291, 1976. doi: 10.1109/TCS.1976.1084219. 16

M. Schetzen. Nonlinear system modeling based on the Wiener theory. *Proceedings of the IEEE*, 69(12):1557 – 1573, dec. 1981. ISSN 0018-9219. doi: 10.1109/PROC.1981. 12201. 3, 30, 32, 33

Martin Schetzen. *The Volterra and Wiener theories of nonlinear systems*. John Wiley, 1980. 1, 2, 16, 26, 31, 33

George P.H. Styan. Hadamard products and multivariate statistical analysis. *Linear Algebra and its Applications*, 6(0):217 – 240, 1973. ISSN 0024-3795. doi: http:// dx.doi.org/10.1016/0024-3795(73)90023-2. URL http://www.sciencedirect.com/ science/article/pii/0024379573900232. 73

H. Tang, Y. H. Liao, J. Y. Cao, and H. Xie. Fault diagnosis approach based on Volterra models. *Mechanical Systems and Signal Processing*, 24(4):1099–1113, May 2010. doi: 10.1016/j.ymssp.2009.09.001. 19, 66, 111

S. Theodoridis and K. Koutroumbas. *Pattern Recognition*. Elsevier Science, 2008. ISBN 9780080949123. 110

V. Venkatasubramanian, R. Rengaswamy, and S. N. Kavuri. A review of process fault detection and diagnosis part ii: Quantitative model and search strategies. *Computers & Chemical Engineering*, 27(3):313–326, March 2003a. doi: 10.1016/S0098-1354(02) 00161-8. 6

V. Venkatasubramanian, R. Rengaswamy, S. N. Kavuri, and K. Yin. A review of process fault detection and diagnosis part iii: Process history based methods. *Computers &*

REFERENCES

Chemical Engineering, 27(3):327–346, March 2003b. doi: 10.1016/S0098-1354(02)
00162-X. 6

V. Venkatasubramanian, R. Rengaswamy, K. Yin, and S. N. Kavuri. A review of process
fault detection and diagnosis part i: Quantitative model-based methods. *Computers
& Chemical Engineering*, 27(3):293–311, March 2003c. doi: 10.1016/S0098-1354(02)
00160-6. 6, 106, 107

V. Volterra. *Theory of functionals and of integral and integro-differential equations.*
Dover Phoenix editions, 1959. 14

LP Wang and WR Cluett. Use of PRESS residuals in dynamic system identi-
fication. *AUTOMATICA*, 32(5):781–784, MAY 1996. ISSN 0005-1098. doi:
{10.1016/0005-1098(96)00003-9}. 39

D.D. Weiner and J.F. Spina. *Sinusoidal analysis and modeling of weakly nonlinear
circuits: with application to nonlinear interference effects.* Van Nostrand Reinhold,
1980. ISBN 9780442260934. 2, 3, 4, 17

Eric W. Weisstein. Diophantine equation. From MathWorld–A Wolfram Web Resource,
August 2014a. URL `http://mathworld.wolfram.com/DiophantineEquation.`
`html`. 51

Eric W. Weisstein. Euclidean algorithm. From MathWorld–A Wolfram Web Resource,
August 2014b. URL `http://mathworld.wolfram.com/EuclideanAlgorithm.html`.
57

Eric W. Weisstein. Partition. From MathWorld–A Wolfram Web Resource, August
2014c. URL `http://mathworld.wolfram.com/Partition.html`. 57

Eric W. Weisstein. Gram-schmidt orthonormalization. From MathWorld–A Wol-
fram Web Resource, August 2014d. URL `http://mathworld.wolfram.com/`
`Gram-SchmidtOrthonormalization.html`. 38

Eric W. Weisstein. Singular value decomposition. From MathWorld–A Wolfram Web Resource, August 2014e. URL http://mathworld.wolfram.com/SingularValueDecomposition.html. 38

N. Wiener. *Nonlinear problems in random theory.* The MIT press, 1958. 16, 30

M. Wiercigroch and V. W. T. Sin. Experimental study of a symmetrical piecewise base-excited oscillator. *Journal of Applied Mechanics*, 65(3):657–663, September 1998. ISSN 0021-8936. doi: 10.1115/1.2789108. 112, 125

M Wiercigroch, RD Neilson, and MA Player. Material removal rate prediction for ultrasonic drilling of hard materials using an impact oscillator approach. *PHYSICS LETTERS A*, 259(2):91–96, AUG 9 1999. ISSN 0375-9601. doi: {10.1016/S0375-9601(99)00416-8}. 112

M Wiercigroch, J Wojewoda, and AM Krivtsov. Dynamics of ultrasonic percussive drilling of hard rocks. *JOURNAL OF SOUND AND VIBRATION*, 280(3-5):739–757, FEB 23 2005. ISSN 0022-460X. doi: {10.1016/j.jsv.2003.12.045}. 112

X. F. Wu, Z. Q. Lang, and S. A. Billings. Analysis of output frequencies of nonlinear systems. *IEEE Transactions On Signal Processing*, 55(7):3239–3246, July 2007. doi: 10.1109/TSP.2007.894387. 19

R. Yue, S. A. Billings, and Z. Q. Lang. An investigation into the characteristics of non-linear frequency response functions. part 1: Understanding the higher dimensional frequency spaces. *International Journal of Control*, 78(13):1031–1044, September 2005a. doi: 10.1080/00207170500144417. 3, 20

R. Yue, S. A. Billings, and Z. Q. Lang. An investigation into the characteristics of non-linear frequency response functions. part 2: New analysis methods based on symbolic expansions and graphical techniques. *International Journal of Control*, 78(14):1130–1149, September 2005b. doi: 10.1080/00207170500144524. 4, 20

REFERENCES

X. Zhao, Jinaming Lu, and T. Yahagi. A design method of noise canceller using parallel adaptive volterra filter. In *Industrial Technology, 2005. ICIT 2005. IEEE International Conference on*, pages 987–990, 2005. doi: 10.1109/ICIT.2005.1600779. 17

Appendices

Appendix A

NARX models for case study 1

The following polynomial NARX models were identified for the impact oscillator for several values of stiffness ratios. Models were identified using the forward orthogonal estimator with structure selection based on the PRESS criterion.

$$
\left.
\begin{aligned}
y(t) \quad &= +8.3703 \cdot 10^{-06}\, u(t-1) \\
&+1.6590 \cdot 10^{+00}\, y(t-1) \\
&-9.3108 \cdot 10^{-01}\, y(t-2) \\
&+3.8721 \cdot 10^{-02}\, y(t-1)\, u(t-2) \\
&+6.4094 \cdot 10^{-03}\, y(t-4)\, u(t-5) \\
&-8.5746 \cdot 10^{-07}\, u(t-1)\, u(t-3)
\end{aligned}
\right\} \quad \beta = 0.80 \qquad (A.1)
$$

$$
\left.
\begin{aligned}
y(t) \quad &= +8.3781 \cdot 10^{-06}\, u(t-1) \\
&+1.6556 \cdot 10^{+00}\, y(t-1) \\
&-9.3102 \cdot 10^{-01}\, y(t-2) \\
&+3.3622 \cdot 10^{-02}\, y(t-1)\, u(t-2) \\
&+5.7585 \cdot 10^{-03}\, y(t-4)\, u(t-5) \\
&-6.6151 \cdot 10^{-07}\, u(t-1)\, u(t-3)
\end{aligned}
\right\} \quad \beta = 0.82 \qquad (A.2)
$$

A. NARX MODELS FOR CASE STUDY 1

$$
\left.
\begin{aligned}
y(t) \quad &= +8.3821 \cdot 10^{-06}\, u(t-1) \\
&+1.6523 \cdot 10^{+00}\, y(t-1) \\
&-9.3100 \cdot 10^{-01}\, y(t-2) \\
&+2.8813 \cdot 10^{-02}\, y(t-1)\, u(t-2) \\
&+5.0720 \cdot 10^{-03}\, y(t-4)\, u(t-5) \\
&-5.0445 \cdot 10^{-07}\, u(t-1)\, u(t-3)
\end{aligned}
\right\} \quad \beta = 0.84 \qquad (A.3)
$$

$$
\left.
\begin{aligned}
y(t) \quad &= +8.3834 \cdot 10^{-06}\, u(t-1) \\
&+1.6490 \cdot 10^{+00}\, y(t-1) \\
&-9.3099 \cdot 10^{-01}\, y(t-2) \\
&+2.4281 \cdot 10^{-02}\, y(t-1)\, u(t-2) \\
&+4.3514 \cdot 10^{-03}\, y(t-4)\, u(t-5) \\
&-3.8194 \cdot 10^{-07}\, u(t-1)\, u(t-3)
\end{aligned}
\right\} \quad \beta = 0.87 \qquad (A.4)
$$

$$
\left.
\begin{aligned}
y(t) \quad &= +8.6427 \cdot 10^{-06}\, u(t-1) \\
&+1.0791 \cdot 10^{+00}\, y(t-1) \\
&-5.2461 \cdot 10^{-01}\, y(t-3) \\
&+2.2964 \cdot 10^{-02}\, y(t-2)\, u(t-3) \\
&+2.2879 \cdot 10^{-05}\, u(t-1)\, y(t-5) \\
&+4.5229 \cdot 10^{-06}\, u(t-2) \\
&+1.0033 \cdot 10^{-02}\, y(t-1)\, u(t-1) \\
&-6.5211 \cdot 10^{-07}\, u(t-1)\, u(t-5)
\end{aligned}
\right\} \quad \beta = 0.89 \qquad (A.5)
$$

$$
\left.
\begin{aligned}
y(t) \;=\;& +8.6459 \cdot 10^{-06}\, u(t-1) \\
& +1.0747 \cdot 10^{+00}\, y(t-1) \\
& -5.2566 \cdot 10^{-01}\, y(t-3) \\
& +1.8164 \cdot 10^{-02}\, y(t-2)\, u(t-3) \\
& +4.7072 \cdot 10^{-04}\, u(t-1)\, y(t-5) \\
& +4.5236 \cdot 10^{-06}\, u(t-2) \\
& +8.3476 \cdot 10^{-03}\, y(t-1)\, u(t-1) \\
& -5.3680 \cdot 10^{-07}\, u(t-1)\, u(t-5)
\end{aligned}
\right\} \quad \beta = 0.91 \qquad (A.6)
$$

$$
\left.
\begin{aligned}
y(t) \;=\;& +8.5119 \cdot 10^{-06}\, u(t-1) \\
& +1.0709 \cdot 10^{+00}\, y(t-1) \\
& -5.2686 \cdot 10^{-01}\, y(t-3) \\
& +1.3663 \cdot 10^{-02}\, y(t-1)\, u(t-3) \\
& -6.4812 \cdot 10^{-08}\, u(t-5) \\
& -6.1215 \cdot 10^{-07}\, u(t-1)\, u(t-5) \\
& +4.0332 \cdot 10^{-07}\, u(t-3).^2 \\
& +4.6296 \cdot 10^{-06}\, u(t-2)
\end{aligned}
\right\} \quad \beta = 0.93 \qquad (A.7)
$$

$$
\left.
\begin{aligned}
y(t) \;=\;& +8.5705 \cdot 10^{-06}\, u(t-1) \\
& +1.6355 \cdot 10^{+00}\, y(t-1) \\
& -9.2865 \cdot 10^{-01}\, y(t-2) \\
& +6.1344 \cdot 10^{-03}\, y(t-1)\, u(t-2) \\
& +4.8693 \cdot 10^{-05}\, y(t-4)\, u(t-5) \\
& -2.9044 \cdot 10^{-07}\, u(t-2) \\
& -7.7364 \cdot 10^{-08}\, u(t-1)\, u(t-4) \\
& +3.4722 \cdot 10^{-03}\, y(t-3)\, u(t-3) \\
& -2.1788 \cdot 10^{-07}\, u(t-2)\, u(t-5)
\end{aligned}
\right\} \quad \beta = 0.96 \qquad (A.8)
$$

$$
\left.
\begin{aligned}
y(t) \quad &= +8.8783 \cdot 10^{-06}\, u(t-1) \\
&+1.0634 \cdot 10^{+00}\, y(t-1) \\
&-5.2897 \cdot 10^{-01}\, y(t-3) \\
&+1.1440 \cdot 10^{-07}\, u(t-5) \\
&+5.4534 \cdot 10^{-03}\, y(t-1)\, u(t-2) \\
&+1.8209 \cdot 10^{-03}\, y(t-3)\, u(t-5) \\
&+4.1658 \cdot 10^{-06}\, u(t-2) \\
&-5.5919 \cdot 10^{-08}\, u(t-1)\, u(t-3)
\end{aligned}
\right\} \quad \beta = 0.98 \qquad \text{(A.9)}
$$

$$
\left.
\begin{aligned}
y(t) \quad &= +1.0603 \cdot 10^{+00}\, y(t-1) \\
&-5.3216 \cdot 10^{-01}\, y(t-3) \\
&+1.0570 \cdot 10^{-05}\, u(t-1) \\
&+3.3237 \cdot 10^{-06}\, u(t-3) \\
&-8.9887 \cdot 10^{-08}\, u(t-5) \\
&-1.4714 \cdot 10^{-09}\, u(t-1)\, u(t-2) \\
&-5.1091 \cdot 10^{-07}\, u(t-4) \\
&-7.3380 \cdot 10^{-10}\, u(t-5).^2 \\
&+1.8035 \cdot 10^{-09}\, u(t-2).^2
\end{aligned}
\right\} \quad \beta = 1.00 \qquad \text{(A.10)}
$$

Appendix B

Description of sinusoidal NOFRFs for case study 1

Sinusoidal NOFRFs up to second order were computed in analytical form for the impact oscillator. The general expression of the linear FRF is described as:

$$G_1(e^{j\omega_h}) = \frac{B_1(e^{j\omega_h})}{A_1(e^{j\omega_h})} \tag{B.1}$$

where the coefficients for each β are described as:

$$\beta = 0.80 \begin{cases} B_1(e^{j\omega_h}) = 8.3703 \cdot 10^{-6} \, p \\ A_1(e^{j\omega_h}) = p^2 - 1.6590 \, p + 0.9311 \end{cases} \tag{B.2}$$

$$\beta = 0.82 \begin{cases} B_1(e^{j\omega_h}) = 8.3781 \cdot 10^{-6} \, p \\ A_1(e^{j\omega_h}) = p^2 - 1.6556 \, p + 0.9310 \end{cases} \tag{B.3}$$

$$\beta = 0.84 \begin{cases} B_1(e^{j\omega_h}) = 8.3821 \cdot 10^{-6} \, p \\ A_1(e^{j\omega_h}) = p^2 - 1.6523 \, p + 0.9310 \end{cases} \tag{B.4}$$

$$\beta = 0.87 \begin{cases} B_1(e^{j\omega_h}) = 8.3834 \cdot 10^{-6} \, p \\ A_1(e^{j\omega_h}) = p^2 - 1.6490 \, p + 0.9310 \end{cases} \tag{B.5}$$

B. DESCRIPTION OF SINUSOIDAL NOFRFS FOR CASE STUDY 1

$$\beta = 0.89 \begin{cases} B_1(e^{j\omega_h}) = 8.6427 \cdot 10^{-6} \left(p^2 + 0.5233\,p \right) \\ A_1(e^{j\omega_h}) = p^3 - 1.0791\,p^2 + 0.5246 \end{cases} \tag{B.6}$$

$$\beta = 0.91 \begin{cases} B_1(e^{j\omega_h}) = 8.6459 \cdot 10^{-6} \left(p^2 + 0.5232\,p \right) \\ A_1(e^{j\omega_h}) = p^3 - 1.0747\,p^2 + 0.5257 \end{cases} \tag{B.7}$$

$$\beta = 0.93 \begin{cases} B_1(e^{j\omega_h}) = 8.5119 \cdot 10^{-6} \left(p^4 + 0.5439\,p^3 - 0.0076 \right) \\ A_1(e^{j\omega_h}) = p^5 - 1.0709\,p^4 + 0.5269\,p^2 \end{cases} \tag{B.8}$$

$$\beta = 0.96 \begin{cases} B_1(e^{j\omega_h}) = 8.5705 \cdot 10^{-6} \left(p - 0.0339 \right) \\ A_1(e^{j\omega_h}) = p^2 - 1.6355\,p + 0.9286 \end{cases} \tag{B.9}$$

$$\beta = 0.98 \begin{cases} B_1(e^{j\omega_h}) = 8.8783 \cdot 10^{-6} \left(p^4 + 0.4692\,p^3 + 0.0129 \right) \\ A_1(e^{j\omega_h}) = p^5 - 1.0634\,p^4 + 0.5290\,p^2 \end{cases} \tag{B.10}$$

$$\beta = 1.00 \begin{cases} B_1(e^{j\omega_h}) = 1.0570 \cdot 10^{-5} \left(p^4 + 0.3145\,p^2 - 0.0483\,p - 0.0085 \right) \\ A_1(e^{j\omega_h}) = p^5 - 1.0603\,p^4 + 0.5322\,p^2 \end{cases} \tag{B.11}$$

where for convenience we used $p = e^{j\omega_h}$

For the second order NOFRF, the general expression is also described as:

$$G_2(e^{j\omega_h}) = \frac{B_2(e^{j\omega_h})}{A_2(e^{j\omega_h})} \tag{B.12}$$

where the coefficients are now described as:

$$\beta = 0.80 \begin{cases} B_2(e^{j\omega_h}) & = 1.4225 \cdot 10^{-6} \left(-0.3749\,p^{11} + p^{10} - 0.5612\,p^9 + 0.0377\,p^5 \right) \\ A_2(e^{j\omega_h}) & = p^{15} - 1.6590\,p^{14} - 0.7279\,p^{13} + 2.7522\,p^{12} - 0.6136\,p^{11} \\ & \quad -1.5446\,p^{10} + 0.8669\,p^9 \end{cases}$$

$$\tag{B.13}$$

$$\beta = 0.82 \begin{cases} B_2(e^{j\omega_h}) & = 1.0952 \cdot 10^{-6} \left(-0.3468\,p^{11} + p^{10} - 0.5623\,p^9 + 0.0441\,p^5 \right) \\ A_2(e^{j\omega_h}) & = p^{15} - 1.6556\,p^{14} - 0.7246\,p^{13} + 2.7411\,p^{12} - 0.6104\,p^{11} \\ & \quad -1.5414\,p^{10} + 0.8668\,p^9 \end{cases}$$

$$\tag{B.14}$$

$$\beta = 0.84 \begin{cases} B_2(e^{j\omega_h}) & = 8.3351 \cdot 10^{-7} \left(-0.3155\,p^{11} + p^{10} - 0.5634\,p^9 + 0.0510\,p^5\right) \\ A_2(e^{j\omega_h}) & = p^{15} - 1.6523\,p^{14} - 0.7213\,p^{13} + 2.7302\,p^{12} - 0.6073\,p^{11} \\ & \quad -1.5383\,p^{10} + 0.8668\,p^9 \end{cases}$$

$$\text{(B.15)}$$

$$\beta = 0.87 \begin{cases} B_2(e^{j\omega_h}) & = 6.2983 \cdot 10^{-7} \left(-0.2832\,p^{11} + p^{10} - 0.5646\,p^9 + 0.0579\,p^5\right) \\ A_2(e^{j\omega_h}) & = p^{15} - 1.6490\,p^{14} - 0.7180\,p^{13} + 2.7193\,p^{12} - 0.6043\,p^{11} \\ & \quad -1.5352\,p^{10} + 0.8667\,p^9 \end{cases}$$

$$\text{(B.16)}$$

$$\beta = 0.89 \begin{cases} B_2(e^{j\omega_h}) & = 8.0776 \cdot 10^{-7} \left(+0.1073\,p^{12} + 0.0562\,p^{11} - 0.5616\,p^9 + p^8\right. \\ & \qquad \left. +0.0001\,p^7 - 0.4235\,p^6\right) \\ A_2(e^{j\omega_h}) & = p^{15} - 1.0791\,p^{14} - 1.0791\,p^{13} + 1.6891\,p^{12} - 0.5661\,p^{10} \\ & \quad +0.5246\,p^9 - 0.5661\,p^8 + 0.2752\,p^6 \end{cases}$$

$$\text{(B.17)}$$

$$\beta = 0.91 \begin{cases} B_2(e^{j\omega_h}) & = 6.6312 \cdot 10^{-7} \left(+0.1088\,p^{12} + 0.0569\,p^{11} - 0.5727\,p^9 + p^8\right. \\ & \qquad \left. +0.0032\,p^7 - 0.4255\,p^6\right) \\ A_2(e^{j\omega_h}) & = p^{15} - 1.0747\,p^{14} - 1.0747\,p^{13} + 1.6806\,p^{12} - 0.5649\,p^{10} \\ & \quad +0.5257\,p^9 - 0.5649\,p^8 + 0.2763\,p^6 \end{cases}$$

$$\text{(B.18)}$$

$$\beta = 0.93 \begin{cases} B_2(e^{j\omega_h}) & = 2.2363 \cdot 10^{-7} \left(+0.5200\,p^{10} - 0.6510\,p^9 + p^8 - 0.4960\,p^6\right) \\ A_2(e^{j\omega_h}) & = p^{15} - 1.0709\,p^{14} - 1.0709\,p^{13} + 1.6736\,p^{12} - 0.5642\,p^{10} \\ & \quad +0.5269\,p^9 - 0.5642\,p^8 + 0.2776\,p^6 \end{cases}$$

$$\text{(B.19)}$$

$$\beta = 0.96 \begin{cases} B_2(e^{j\omega_h}) & = 3.5533 \cdot 10^{-7} \left(+0.1480\,p^{11} - 0.2227\,p^{10} + 0.3561\,p^9\right. \\ & \qquad \left. -0.7316\,p^8 + p^7 - 0.5694\,p^6 + 0.0012\,p^5 - 0.0000\,p^4\right) \\ A_2(e^{j\omega_h}) & = p^{15} - 1.6355\,p^{14} - 0.7069\,p^{13} + 2.6749\,p^{12} - 0.5902\,p^{11} \\ & \quad -1.5188\,p^{10} + 0.8624\,p^9 \end{cases}$$

$$\text{(B.20)}$$

B. DESCRIPTION OF SINUSOIDAL NOFRFS FOR CASE STUDY 1

$$
\beta = 0.98 \begin{cases} B_2(e^{j\omega_h}) & = 8.2181 \cdot 10^{-8} \left(-0.0913\,p^{15} + p^{14} - 0.3599\,p^{12} + 0.0076\,p^{11} \right. \\ & \quad \left. +0.1967\,p^{10} + 0.0923\,p^{9} + 0.0025\,p^{6} \right) \\ A_2(e^{j\omega_h}) & = p^{19} - 1.0634\,p^{18} - 1.0634\,p^{17} + 1.6597\,p^{16} - 0.5625\,p^{14} \\ & \quad +0.5290\,p^{13} - 0.5625\,p^{12} + 0.2798\,p^{10} \end{cases}
$$

$$(B.21)$$

$$
\beta = 1.00 \begin{cases} B_2(e^{j\omega_h}) & = 1.8035 \cdot 10^{-9} \left(-0.8159\,p^{13} + p^{12} - 0.4069\,p^{6} \right) \\ A_2(e^{j\omega_h}) & = p^{16} - 1.0603\,p^{14} + 0.5322\,p^{10} \end{cases}
$$

$$(B.22)$$

where $p = e^{j\omega_h}$.

Appendix C

Description of impulsive NOFRFs for case study 1

In Section (), the NOFRFs up to second order were analytically derived for a pure impulse input. The analytical formulas for $G_1(z)$ and $G_2(z)$, from which the NOFRFs are computed later, are described as follows.

For the linear FRF:

$$G_1(z) = \frac{B_1(z)}{A_1(z)} \tag{C.1}$$

where the polynomials $B(z)$ and $A_2(z)$ are, for each analysed β, described as:

$$\beta = 0.80 \begin{cases} B_1(z) & = 8.3703 \cdot 10^{-6}\, z \\[2mm] A_1(z) & = z^2 - 1.6590\, z + 0.9311 \end{cases} \tag{C.2}$$

$$\beta = 0.82 \begin{cases} B_1(z) & = 8.3781 \cdot 10^{-6}\, z \\[2mm] A_1(z) & = z^2 - 1.6556\, z + 0.9310 \end{cases} \tag{C.3}$$

$$\beta = 0.84 \begin{cases} B_1(z) & = 8.3821 \cdot 10^{-6}\, z \\[2mm] A_1(z) & = z^2 - 1.6523\, z + 0.9310 \end{cases} \tag{C.4}$$

$$\beta = 0.87 \begin{cases} B_1(z) & = 8.3834 \cdot 10^{-6}\, z \\[2mm] A_1(z) & = z^2 - 1.6490\, z + 0.9310 \end{cases} \tag{C.5}$$

C. DESCRIPTION OF IMPULSIVE NOFRFS FOR CASE STUDY 1

$$\beta = 0.89 \begin{cases} B_1(z) & = 8.6427 \cdot 10^{-6} \left(z^2 + 0.5233\, z \right) \\ A_1(z) & = z^3 - 1.0791\, z^2 + 0.5246 \end{cases} \tag{C.6}$$

$$\beta = 0.91 \begin{cases} B_1(z) & = 8.6459 \cdot 10^{-6} \left(z^2 + 0.5232\, z \right) \\ A_1(z) & = z^3 - 1.0747\, z^2 + 0.5257 \end{cases} \tag{C.7}$$

$$\beta = 0.93 \begin{cases} B_1(z) & = 8.5119 \cdot 10^{-6} \left(z^4 + 0.5439\, z^3 - 0.0076 \right) \\ A_1(z) & = z^5 - 1.0709\, z^4 + 0.5269\, z^2 \end{cases} \tag{C.8}$$

$$\beta = 0.96 \begin{cases} B_1(z) & = 8.5705 \cdot 10^{-6} \left(z - 0.0339 \right) \\ A_1(z) & = z^2 - 1.6355\, z + 0.9286 \end{cases} \tag{C.9}$$

$$\beta = 0.98 \begin{cases} B_1(z) & = 8.8783 \cdot 10^{-6} \left(z^4 + 0.4692\, z^3 + 0.0129 \right) \\ A_1(z) & = z^5 - 1.0634\, z^4 + 0.5290\, z^2 \end{cases} \tag{C.10}$$

$$\beta = 1.00 \begin{cases} B_1(z) & = 1.0570 \cdot 10^{-5} \left(z^4 + 0.3145\, z^2 - 0.0483\, z - 0.0085 \right) \\ A_1(z) & = z^5 - 1.0603\, z^4 + 0.5322\, z^2 \end{cases} \tag{C.11}$$

The second order NOFRFs are described by a similar formula:

$$G_2(z) = \frac{B_2(z)}{A_2(z)} \tag{C.12}$$

where $B_2(z)$ and $A_2(z)$ are now described, for each β, as:

$$\beta = 0.80 \begin{cases} B_2(z) & = 3.2411 \cdot 10^{-7} \left(z^3 + 0.1655 \right) \\ A_2(z) & = z^5 - 1.6590\, z^4 + 0.9311\, z^3 \end{cases} \tag{C.13}$$

$$\beta = 0.82 \begin{cases} B_2(z) & = 2.8168 \cdot 10^{-7} \left(z^3 + 0.1713 \right) \\ A_2(z) & = z^5 - 1.6556\, z^4 + 0.9310\, z^3 \end{cases} \tag{C.14}$$

$$\beta = 0.84 \begin{cases} B_2(z) & = 2.4151 \cdot 10^{-7} \left(z^3 + 0.1760 \right) \\ A_2(z) & = z^5 - 1.6523\, z^4 + 0.9310\, z^3 \end{cases} \tag{C.15}$$

$$\beta = 0.87 \begin{cases} B_2(z) & = 2.0356 \cdot 10^{-7} \left(z^3 + 0.1792 \right) \\ A_2(z) & = z^5 - 1.6490\, z^4 + 0.9310\, z^3 \end{cases} \tag{C.16}$$

$$\beta = 0.89 \begin{cases} B_2(z) & = 1.9847 \cdot 10^{-7} \\ A_2(z) & = z^3 - 1.0791\, z^2 + 0.5246 \end{cases} \tag{C.17}$$

$$\beta = 0.91 \begin{cases} B_2(z) & = 1.5704 \cdot 10^{-7} \\ A_2(z) & = z^3 - 1.0747\, z^2 + 0.5257 \end{cases} \tag{C.18}$$

$$\beta = 0.93 \begin{cases} B_2(z) & = 5.9111 \cdot 10^{-7} \\ A_2(z) & = z^3 - 1.0709\, z^2 + 0.5269 \end{cases} \tag{C.19}$$

$$\beta = 0.96 \begin{cases} B_2(z) & = 5.2575 \cdot 10^{-8} \\ A_2(z) & = z^2 - 1.6355\, z + 0.9286 \end{cases} \tag{C.20}$$

$$\beta = 0.98 \begin{cases} B_2(z) & = 4.8417 \cdot 10^{-8} \left(z^3 + 0.5117 \right) \\ A_2(z) & = z^5 - 1.0634\, z^4 + 0.5290\, z^2 \end{cases} \tag{C.21}$$

$$\beta = 1.00 \begin{cases} B_2(z) & = 0.0000 \\ A_2(z) & = 1 \end{cases} \tag{C.22}$$

Appendix D

NARX models for case study 2

In case study 2, a NARX model was identified for each stiffness ratio. The models are described as follows:

For $\beta = 19.01$

$$
\begin{aligned}
y(t) \cdot 10^{-4} ={}& 0.0017\,u(t-3) + 0.0128\,u(t-2)\,u(t-3) + 0.0002\,u(t-2) \\
& - 0.0129\,u(t-2)^2 + 0.4722\,u(t-2)^2\,u(t-3) - 0.0039\,u(t-3)^2 \\
& + 0.0225\,u(t-3)^3 + 0.4022\,u(t-1)\,u(t-2)^2 + 0.0152\,u(t-1)\,u(t-2) \\
& - 0.2714\,u(t-2)\,u(t-3)^2 - 0.5640\,u(t-1)\,u(t-2)\,u(t-3) - 0.0010\,u(t-1) \\
& - 0.8994\,u(t-2)\,u(t-3)^3 - 0.0006\,u(t-1)^2 - 0.2393\,u(t-2)^3 \\
& + 0.4747\,u(t-2)^3\,u(t-3) + 0.2250\,u(t-3)^4 - 0.2115\,u(t-1)^2\,u(t-2) \\
& + 0.2332\,u(t-1)\,u(t-3)^2 - 1.2259\,u(t-1)\,u(t-2)^2\,u(t-3) \\
& + 0.9048\,u(t-2)^2\,u(t-3)^2 + 1.7593\,u(t-1)\,u(t-2)^3 - 0.8672\,u(t-2)^4 \\
& - 1.0231\,u(t-1)^2\,u(t-2)^2 + 0.0515\,u(t-1)^3 + 0.2319\,u(t-1)\,u(t-3)^3 \\
& - 0.0106\,u(t-1)\,u(t-3) + 0.1010\,u(t-1)^2\,u(t-3) \\
& + 0.0625\,u(t-1)^3\,u(t-3) + 0.4446\,u(t-1)^2\,u(t-2)\,u(t-3) \\
& - 0.2405\,u(t-1)\,u(t-2)\,u(t-3)^2 + 0.1473\,u(t-1)^3\,u(t-2)
\end{aligned}
$$

$$- 0.0059\,u(t-1)^4 + 0.0129\,u(t-1)^2\,u(t-3)^2 \tag{D.1}$$

For $\beta = 20.92$

$$
\begin{aligned}
y(t) \cdot 10^{-5} = {}&+0.0006\,u(t-2)\,u(t-3) - 0.0003\,u(t-3)^2 - 0.0012\,u(t-2)^2 \\
&+ 0.0024\,u(t-1)\,u(t-2) - 0.0043\,u(t-2)\,u(t-3)^2 \\
&+ 0.0143\,u(t-2)^2\,u(t-3) - 0.0000\,u(t-2) + 0.0001\,u(t-3) \\
&- 0.0057\,u(t-3)^3 - 0.0372\,u(t-1)\,u(t-2)\,u(t-3) \\
&+ 0.7744\,u(t-2)\,u(t-3)^3 + 0.0112\,u(t-1)\,u(t-2)^2 \\
&- 0.0016\,u(t-1)\,u(t-3) + 0.0242\,u(t-1)\,u(t-3)^2 - 0.0270\,u(t-3)^4 \\
&- 0.0000\,u(t-1) - 2.4171\,u(t-2)^4 + 4.9550\,u(t-1)\,u(t-2)^3 \\
&+ 4.9258\,u(t-2)^3\,u(t-3) - 8.5613\,u(t-1)\,u(t-2)^2\,u(t-3) \\
&- 0.0038\,u(t-2)^3 + 0.7320\,u(t-1)^3\,u(t-2) - 3.3208\,u(t-1)^2\,u(t-2)^2 \\
&- 0.6349\,u(t-1)\,u(t-3)^3 + 0.0000\,u(t-1)^2 - 0.6502\,u(t-1)^3\,u(t-3) \\
&+ 4.5149\,u(t-1)^2\,u(t-2)\,u(t-3) - 0.0252\,u(t-1)^4 \\
&+ 4.2867\,u(t-1)\,u(t-2)\,u(t-3)^2 - 1.2910\,u(t-1)^2\,u(t-3)^2 \\
&- 3.2601\,u(t-2)^2\,u(t-3)^2 + 0.0004\,u(t-1)^3 \tag{D.2}
\end{aligned}
$$

For $\beta = 22.14$

$$
\begin{aligned}
y(t) \cdot 10^{-5} = {}&+0.0006\,u(t-2)\,u(t-3) + 0.0018\,u(t-1)\,u(t-2) + 0.0002\,u(t-3) \\
&+ 0.1667\,u(t-2)^2\,u(t-3) + 0.0001\,u(t-3)^2 \\
&+ 0.0130\,u(t-3)^3 - 0.0000\,u(t-2) + 0.1426\,u(t-1)\,u(t-2)^2 \\
&- 0.0894\,u(t-2)\,u(t-3)^2 - 0.0009\,u(t-2)^2 - 0.1001\,u(t-2)^3 \\
&- 0.3324\,u(t-2)\,u(t-3)^3 - 0.0016\,u(t-1)\,u(t-3) - 0.0001\,u(t-1) \\
&- 0.1653\,u(t-1)\,u(t-2)\,u(t-3) - 0.7755\,u(t-2)^4 \\
&+ 0.0732\,u(t-3)^4 - 0.0000\,u(t-1)^2 + 0.0521\,u(t-1)\,u(t-3)^2
\end{aligned}
$$

$$+ 0.6833\, u(t-2)^3\, u(t-3) + 1.5274\, u(t-1)\, u(t-2)^3$$

$$+ 0.0069\, u(t-1)^3\, u(t-3) - 0.9169\, u(t-1)^2\, u(t-2)^2$$

$$+ 0.0106\, u(t-1)^3 + 0.1507\, u(t-1)\, u(t-3)^3$$

$$- 1.1412\, u(t-1)\, u(t-2)^2\, u(t-3) + 0.1378\, u(t-1)^3\, u(t-2)$$

$$+ 0.4421\, u(t-1)^2\, u(t-2)\, u(t-3) + 0.0123\, u(t-1)^4$$

$$- 0.0643\, u(t-1)^2\, u(t-2) + 0.0102\, u(t-1)^2\, u(t-3)^2$$

$$+ 0.0336\, u(t-1)^2\, u(t-3) + 0.2097\, u(t-2)^2\, u(t-3)^2$$

$$- 0.0875\, u(t-1)\, u(t-2)\, u(t-3)^2 \tag{D.3}$$

For $\beta = 24.36$

$$y(t)\cdot 10^{-5} = +0.0008\, u(t-2)\, u(t-3) - 0.0017\, u(t-2)^2 - 0.0003\, u(t-3)^2$$

$$+ 0.0033\, u(t-1)\, u(t-2) + 0.0592\, u(t-2)\, u(t-3)^2$$

$$- 0.0025\, u(t-1)\, u(t-3) - 0.0733\, u(t-2)^2\, u(t-3) - 0.0000\, u(t-2)$$

$$+ 0.0174\, u(t-2)^3 + 0.7037\, u(t-2)\, u(t-3)^3 - 0.0182\, u(t-3)^3$$

$$+ 7.8152\, u(t-1)\, u(t-2)^2\, u(t-3) - 0.0037\, u(t-1)\, u(t-2)^2$$

$$- 2.6240\, u(t-2)^3\, u(t-3) + 0.0513\, u(t-1)\, u(t-2)\, u(t-3)$$

$$+ 0.0001\, u(t-3) - 0.0114\, u(t-1)\, u(t-3)^2$$

$$- 4.8467\, u(t-1)^2\, u(t-2)\, u(t-3) - 0.2222\, u(t-3)^4$$

$$+ 0.0066\, u(t-1)^3 - 1.2366\, u(t-1)^3\, u(t-2)$$

$$+ 1.2091\, u(t-1)^2\, u(t-3)^2 + 0.0003\, u(t-1)^2 + 1.9058\, u(t-2)^4$$

$$+ 0.3290\, u(t-1)\, u(t-3)^3 - 0.0206\, u(t-1)^2\, u(t-3)$$

$$- 0.0085\, u(t-1)^2\, u(t-2) + 0.3813\, u(t-2)^2\, u(t-3)^2$$

$$+ 4.1938\, u(t-1)^2\, u(t-2)^2 - 5.2808\, u(t-1)\, u(t-2)^3$$

$$+ 0.9327\, u(t-1)^3\, u(t-3) + 0.0631\, u(t-1)^4 - 0.0000\, u(t-1)$$

$$- 3.3217\, u(t-1)\, u(t-2)\, u(t-3)^2 \tag{D.4}$$

D. NARX MODELS FOR CASE STUDY 2

For $\beta = 24.51$

$$
\begin{aligned}
y(t) \cdot 10^{-5} = {}& +0.0099\, u(t-2)\, u(t-3) - 0.0047\, u(t-2)^2 - 0.3772\, u(t-2)^2\, u(t-3) \\
& - 0.0034\, u(t-3)^2 - 0.0001\, u(t-2) - 0.0641\, u(t-3)^3 + 0.1574\, u(t-2)^3 \\
& + 0.2708\, u(t-2)\, u(t-3)^2 + 0.0002\, u(t-3) - 2.5787\, u(t-2)\, u(t-3)^3 \\
& - 0.0054\, u(t-1)\, u(t-3) + 0.0029\, u(t-1)\, u(t-2) \\
& + 0.2962\, u(t-1)\, u(t-2)\, u(t-3) - 0.1658\, u(t-1)\, u(t-2)^2 \\
& - 3.1651\, u(t-2)^3\, u(t-3) + 0.5284\, u(t-3)^4 - 0.0008\, u(t-1)^4 \\
& - 0.1046\, u(t-1)\, u(t-3)^2 - 0.0625\, u(t-1)^2\, u(t-3) \\
& - 0.0027\, u(t-1)^3\, u(t-3) - 0.0046\, u(t-1)^2\, u(t-2)^2 \\
& - 0.0158\, u(t-1)^2\, u(t-2)\, u(t-3) - 0.0000\, u(t-1) - 0.4612\, u(t-1)\, u(t-2)^3 \\
& - 0.0179\, u(t-1)^2\, u(t-3)^2 + 0.6660\, u(t-1)\, u(t-3)^3 \\
& + 0.0510\, u(t-1)^2\, u(t-2) + 0.7670\, u(t-2)^4 + 0.0006\, u(t-1)^2 \\
& - 0.0017\, u(t-1)^3 - 1.8407\, u(t-1)\, u(t-2)\, u(t-3)^2 \\
& + 4.4011\, u(t-2)^2\, u(t-3)^2 + 1.7253\, u(t-1)\, u(t-2)^2\, u(t-3) \qquad \text{(D.5)}
\end{aligned}
$$

For $\beta = 26.96$

$$
\begin{aligned}
y(t) \cdot 10^{-3} = {}& +0.0070\, u(t-3) + 0.0031\, u(t-2) - 2.3120\, u(t-2)\, u(t-3)^2 \\
& - 0.2212\, u(t-2)\, u(t-3) + 0.1064\, u(t-3)^2 - 0.0072\, u(t-1) \\
& + 5.8013\, u(t-2)\, u(t-3)^3 - 2.0600\, u(t-3)^4 \\
& + 8.5428\, u(t-2)^3\, u(t-3) + 1.8171\, u(t-1)\, u(t-2)^2 - 0.2177\, u(t-1)\, u(t-2) \\
& + 0.1972\, u(t-2)^2 + 0.8885\, u(t-1)\, u(t-3)^2 \\
& + 0.0552\, u(t-1)^2 - 0.2054\, u(t-1)^2\, u(t-3)^2 + 1.2858\, u(t-1)\, u(t-3)^3 \\
& + 0.0322\, u(t-1)^3 - 1.5084\, u(t-2)^3 \\
& - 9.4109\, u(t-2)^2\, u(t-3)^2 + 0.6865\, u(t-1)^2\, u(t-3) \\
& - 4.2096\, u(t-1)^2\, u(t-2)\, u(t-3) + 0.4672\, u(t-1)^2\, u(t-2)^2
\end{aligned}
$$

$$+ 0.0886\, u(t-1)\, u(t-3) + 3.2793\, u(t-2)^2\, u(t-3)$$

$$- 2.6453\, u(t-1)\, u(t-2)\, u(t-3) - 4.2281\, u(t-2)^4 + 2.6375\, u(t-1)\, u(t-2)^3$$

$$+ 1.4089\, u(t-1)^3\, u(t-3) - 0.7306\, u(t-1)^2\, u(t-2)$$

$$+ 0.5016\, u(t-3)^3 - 0.0865\, u(t-1)^3\, u(t-2) \tag{D.6}$$

For $\beta = 28.22$

$$y(t) \cdot 10^{-5} = -0.0037\, u(t-2)\, u(t-3) + 0.0044\, u(t-2)^2 + 0.0001\, u(t-3)$$

$$+ 0.0010\, u(t-3)^2 + 0.0000\, u(t-2)$$

$$- 0.0611\, u(t-2)\, u(t-3)^2 + 0.0992\, u(t-2)^2\, u(t-3)$$

$$- 0.0497\, u(t-2)^3 - 0.0052\, u(t-1)\, u(t-2)$$

$$+ 0.0099\, u(t-3)^3 + 4.7870\, u(t-2)^3\, u(t-3)$$

$$+ 0.0521\, u(t-1)\, u(t-2)^2 + 2.8289\, u(t-2)\, u(t-3)^3$$

$$+ 0.0010\, u(t-1)\, u(t-3) + 0.0027\, u(t-1)^2$$

$$- 5.2450\, u(t-1)\, u(t-2)^2\, u(t-3) - 1.2416\, u(t-2)^4$$

$$- 0.0001\, u(t-1) - 0.4821\, u(t-3)^4$$

$$- 5.8287\, u(t-2)^2\, u(t-3)^2 + 0.0327\, u(t-1)\, u(t-3)^2$$

$$- 0.0075\, u(t-1)^4 + 1.5049\, u(t-1)\, u(t-2)^3$$

$$- 0.0117\, u(t-1)^3\, u(t-2) + 4.7475\, u(t-1)\, u(t-2)\, u(t-3)^2$$

$$- 0.4646\, u(t-1)^2\, u(t-2)^2 - 0.0536\, u(t-1)^3\, u(t-3)$$

$$- 1.2113\, u(t-1)\, u(t-3)^3 - 0.0806\, u(t-1)\, u(t-2)\, u(t-3)$$

$$+ 0.0086\, u(t-1)^2\, u(t-3) + 1.6039\, u(t-1)^2\, u(t-2)\, u(t-3)$$

$$- 0.0121\, u(t-1)^2\, u(t-2) - 0.9268\, u(t-1)^2\, u(t-3)^2$$

$$+ 0.0009\, u(t-1)^3 \tag{D.7}$$

D. NARX MODELS FOR CASE STUDY 2

For $\beta = 31.24$

$$
\begin{aligned}
y(t) \cdot 10^{-5} = {}& -0.0046\,u(t-2)\,u(t-3) + 0.0037\,u(t-2)^2 + 0.0011\,u(t-3)^2 \\
& + 0.0241\,u(t-2)\,u(t-3)^2 - 0.0302\,u(t-2)^2\,u(t-3) \\
& + 0.2369\,u(t-2)\,u(t-3)^3 + 0.0000\,u(t-2) - 0.0028\,u(t-1)\,u(t-2) \\
& + 0.0015\,u(t-1)\,u(t-3) + 0.0120\,u(t-2)^3 \\
& + 0.0477\,u(t-1)\,u(t-2)\,u(t-3) - 0.0396\,u(t-1)\,u(t-2)^2 \\
& - 0.0084\,u(t-3)^3 - 0.0100\,u(t-3)^4 + 0.0010\,u(t-1)^2 \\
& + 1.3070\,u(t-2)^3\,u(t-3) - 0.0233\,u(t-1)^2\,u(t-3) \\
& - 0.9120\,u(t-2)^2\,u(t-3)^2 + 0.2993\,u(t-1)\,u(t-2)\,u(t-3)^2 \\
& + 0.0326\,u(t-1)^2\,u(t-3)^2 + 0.0001\,u(t-3) - 0.0001\,u(t-1) \\
& - 0.6109\,u(t-2)^4 - 0.0189\,u(t-1)^3\,u(t-2) - 0.0069\,u(t-1)^3 \\
& - 0.1062\,u(t-1)^2\,u(t-2)^2 - 0.0129\,u(t-1)\,u(t-3)^3 \\
& + 0.0335\,u(t-1)^2\,u(t-2) - 0.0093\,u(t-1)\,u(t-3)^2 \\
& + 0.5695\,u(t-1)\,u(t-2)^3 - 0.8752\,u(t-1)\,u(t-2)^2\,u(t-3) \\
& + 0.0808\,u(t-1)^2\,u(t-2)\,u(t-3) + 0.0217\,u(t-1)^3\,u(t-3) \\
& - 0.0007\,u(t-1)^4 \tag{D.8}
\end{aligned}
$$

For $\beta = 32.69$

$$
\begin{aligned}
y(t) \cdot 10^{-5} = {}& +0.0049\,u(t-2)\,u(t-3) - 0.0033\,u(t-2)^2 - 0.0018\,u(t-3)^2 \\
& + 0.0125\,u(t-2)\,u(t-3)^2 - 0.0000\,u(t-2) \\
& + 0.0020\,u(t-1)\,u(t-2) - 0.0137\,u(t-2)^2\,u(t-3) + 0.4312\,u(t-2)\,u(t-3)^3 \\
& - 0.0047\,u(t-1)\,u(t-2)^2 + 1.2730\,u(t-2)^3\,u(t-3) \\
& + 0.0038\,u(t-2)^3 + 0.0006\,u(t-1)^2 - 0.0526\,u(t-3)^4 \\
& - 1.1333\,u(t-2)^2\,u(t-3)^2 + 0.0001\,u(t-3) - 0.0025\,u(t-1)\,u(t-3) \\
& - 0.0027\,u(t-1)\,u(t-3)^2 - 0.0043\,u(t-3)^3
\end{aligned}
$$

$$-1.5486\,u(t-1)\,u(t-2)^2\,u(t-3) + 0.8788\,u(t-1)\,u(t-2)^3$$

$$+\,0.0114\,u(t-1)\,u(t-2)\,u(t-3) - 0.2351\,u(t-1)\,u(t-3)^3$$

$$-\,0.5669\,u(t-2)^4 + 1.0546\,u(t-1)\,u(t-2)\,u(t-3)^2$$

$$+\,0.4017\,u(t-1)^2\,u(t-2)\,u(t-3) + 0.0018\,u(t-1)^4$$

$$+\,0.0092\,u(t-1)^3\,u(t-2) - 0.3605\,u(t-1)^2\,u(t-2)^2$$

$$+\,0.0367\,u(t-1)^3\,u(t-3) - 0.0000\,u(t-1) - 0.1896\,u(t-1)^2\,u(t-3)^2$$

$$+\,0.0020\,u(t-1)^2\,u(t-2) - 0.0053\,u(t-1)^2\,u(t-3)$$

$$+\,0.0006\,u(t-1)^3 \tag{D.9}$$

For $\beta = 34.72$

$$y(t)\cdot 10^{-4} = +0.0031\,u(t-2)\,u(t-3) - 0.0053\,u(t-2)^2 - 0.0047\,u(t-3)^2$$

$$-\,0.5489\,u(t-2)\,u(t-3)^2 + 0.0121\,u(t-1)\,u(t-2)$$

$$+\,0.0001\,u(t-2) + 1.0022\,u(t-2)^2\,u(t-3) + 0.9839\,u(t-1)\,u(t-2)^2$$

$$-\,1.9246\,u(t-2)^3\,u(t-3) + 0.0702\,u(t-3)^4$$

$$-\,1.0977\,u(t-1)\,u(t-2)\,u(t-3) - 0.2055\,u(t-2)\,u(t-3)^3$$

$$+\,0.0880\,u(t-3)^3 + 1.1699\,u(t-2)^2\,u(t-3)^2$$

$$+\,0.4812\,u(t-1)\,u(t-2)^2\,u(t-3) + 0.0006\,u(t-3) + 0.0007\,u(t-1)^2$$

$$-\,0.0069\,u(t-1)\,u(t-3) - 0.0892\,u(t-1)\,u(t-2)\,u(t-3)^2$$

$$-\,0.0005\,u(t-1) + 0.1008\,u(t-1)^3 + 0.9197\,u(t-2)^4$$

$$-\,1.7901\,u(t-1)^2\,u(t-2)^2 + 0.3388\,u(t-1)\,u(t-3)^2 - 0.6066\,u(t-2)^3$$

$$-\,0.5206\,u(t-1)^2\,u(t-2)$$

$$+\,1.4171\,u(t-1)^2\,u(t-2)\,u(t-3) - 0.2254\,u(t-1)\,u(t-3)^3 - 0.2935\,u(t-1)^4$$

$$+\,0.2585\,u(t-1)^2\,u(t-3) + 1.2612\,u(t-1)^3\,u(t-2)$$

$$-\,0.2985\,u(t-1)^2\,u(t-3)^2 - 0.4868\,u(t-1)^3\,u(t-3) \tag{D.10}$$

D. NARX MODELS FOR CASE STUDY 2

For $\beta = 36.19$

$$y(t) \cdot 10^{-5} = +0.0007\,u(t-2)\,u(t-3) - 0.0013\,u(t-2)^2 - 0.0005\,u(t-3)^2$$
$$+ 0.0249\,u(t-2)^2\,u(t-3) + 0.0000\,u(t-3)$$
$$+ 0.0015\,u(t-1)\,u(t-2) + 0.6199\,u(t-2)^3\,u(t-3)$$
$$- 1.3227\,u(t-1)\,u(t-2)^2\,u(t-3) - 0.0600\,u(t-3)^4 - 0.0008\,u(t-1)\,u(t-3)$$
$$+ 0.4314\,u(t-2)\,u(t-3)^3 + 0.0000\,u(t-2)$$
$$- 0.0276\,u(t-1)\,u(t-2)\,u(t-3) + 0.0002\,u(t-1)^2 + 0.0351\,u(t-1)\,u(t-2)^2$$
$$- 0.8944\,u(t-2)^2\,u(t-3)^2 - 0.0082\,u(t-2)\,u(t-3)^2$$
$$- 0.0774\,u(t-1)^3\,u(t-2)$$
$$+ 1.2188\,u(t-1)\,u(t-2)\,u(t-3)^2 - 0.0218\,u(t-2)^3 - 0.3095\,u(t-1)\,u(t-3)^3$$
$$- 0.0185\,u(t-1)^2\,u(t-2) + 0.0045\,u(t-1)^2\,u(t-3)$$
$$+ 0.7348\,u(t-1)^2\,u(t-2)\,u(t-3) + 0.0187\,u(t-1)^4$$
$$+ 0.0908\,u(t-1)\,u(t-2)^3 - 0.3537\,u(t-1)^2\,u(t-3)^2 - 0.0000\,u(t-1)$$
$$- 0.0962\,u(t-1)^3\,u(t-3) + 0.0042\,u(t-1)^3$$
$$+ 0.0073\,u(t-1)\,u(t-3)^2 \tag{D.11}$$

For $\beta = 38.30$

$$y(t) \cdot 10^{-5} = +0.0226\,u(t-2)\,u(t-3) - 0.0196\,u(t-2)^2 - 0.0059\,u(t-3)^2$$
$$+ 0.0946\,u(t-2)\,u(t-3)^2 + 0.0000\,u(t-3)$$
$$- 4.5942\,u(t-2)^3\,u(t-3) + 0.3743\,u(t-3)^4$$
$$+ 0.1188\,u(t-2)^3 - 2.2016\,u(t-2)\,u(t-3)^3$$
$$+ 4.7441\,u(t-2)^2\,u(t-3)^2 - 0.0020\,u(t-1)^2$$
$$- 0.0122\,u(t-1)\,u(t-3) + 2.3552\,u(t-1)\,u(t-2)^2\,u(t-3)$$
$$- 1.1387\,u(t-1)\,u(t-2)^3 - 0.1825\,u(t-2)^2\,u(t-3)$$
$$+ 0.0256\,u(t-1)^2\,u(t-2)^2 + 0.0172\,u(t-1)\,u(t-2)$$

$$+\,0.0065\,u(t-1)^3\,u(t-2) + 1.6944\,u(t-2)^4$$

$$+\,0.0022\,u(t-1)^4 + 0.4947\,u(t-1)\,u(t-3)^3$$

$$-\,0.0369\,u(t-1)\,u(t-3)^2 + 0.0965\,u(t-1)^2\,u(t-2)\,u(t-3)$$

$$-\,0.0000\,u(t-2) - 1.7380\,u(t-1)\,u(t-2)\,u(t-3)^2$$

$$+\,0.0601\,u(t-1)^2\,u(t-2) + 0.0000\,u(t-1)$$

$$-\,0.1492\,u(t-1)\,u(t-2)^2 - 0.0314\,u(t-1)^2\,u(t-3)$$

$$-\,0.0030\,u(t-1)^3\,u(t-3) - 0.0169\,u(t-3)^3$$

$$-\,0.0069\,u(t-1)^3 - 0.1186\,u(t-1)^2\,u(t-3)^2$$

$$+\,0.1503\,u(t-1)\,u(t-2)\,u(t-3) \tag{D.12}$$

Appendix E

PLS score prediction for case study 2

The PLS feature extraction applied to case study 2 offers an additional result, which is an estimate of the class scores based or the partition matrix (5.33). These predictions are computed as a simple affine function of the original NOFRF features. The predictions are shown in Table E.1. The numbers in bold represent the highest score for each case.

Table E.1 shows class score predictions, which can be used as classification criteria, although it is not as efficient as the region analysis presented in Section 5.5. This is due to the simplicity of the PLS linear formulation and the small number of fault cases.

In order to use the predicted scores as a classification criterion, a maximum score principle can be applied, in which each point is assigned to the class for which the score is highest. For example, the first case (row) $\beta = 20.92$ fits into cluster 2, since the highest score is the second one. This approach avoids problems related to interpreting the predicted scores, which are considerably different from the binary values of the partition matrix (5.33).

The cluster assignment according to this maximum principle is shown in the second

E. PLS SCORE PREDICTION FOR CASE STUDY 2

Table E.1: Predicted class scores (PLS)

β	Cluster 1	Cluster 2	Cluster 3	Max. principle	True cluster
20.9200	0.1373	**0.7350**	0.1277	2	2
22.1400	-0.1553	**1.1723**	-0.0171	2	2
24.3600	0.1886	**0.5243**	0.2872	2	2
24.5100	**0.5177**	0.5158	-0.0334	1	2
26.9600	**0.4515**	0.2271	0.3214	1	1
28.2200	**0.6072**	0.1937	0.1991	1	1
31.2400	**0.6349**	0.2674	0.0976	1	1
32.6900	0.1623	**0.4255**	0.4122	2	3
34.7200	0.3669	0.2092	**0.4239**	3	3
36.1900	-0.2769	0.0519	**1.2250**	3	3
38.3000	0.3658	-0.3222	**0.9564**	3	3
19.0100	-1.0974	**2.1173**	-0.0199	2	2

last column of Table E.1. In order to check these results, the assignments are compared to the original cluster configuration (established before carrying out PLS), which is shown in the last column of Table E.1. It can be seen that cases β = 24.51 and β = 32.69 were incorrectly assigned. Notice, however, that this error occurs by very small margins: the score error for β = 24.51 is only 0.0019, while for β = 32.69 the error is 0.0133. This can be considered as part of the limitations of such a simple classifier, which could be possibly amended by using more training cases or by designing a classifier with more degrees of freedom.